Ion adsorption modeling
as a tool to characterize metal (hydr)oxide behavior in soil

Promotor: Prof. dr. W. H. van Riemsdijk
Hoogleraar in de Bodemscheikunde en chemische bodemkwaliteit

Promotiecommissie

Prof. dr. A. Maes
Katholieke Universiteit Leuven, België

Dr. ir. L. K. Koopal
Wageningen Universiteit, Nederland

Prof. dr. A. A. Koelmans
Wageningen Universiteit, Nederland

Prof. dr. R. N. J. Comans
Energy Research Center of the Netherlands (ECN), Nederland

Dit onderzoek is uitgevoerd binnen de onderzoekschool SENSE

Rasoul Rahnemaie

Ion adsorption modeling
as a tool to characterize metal (hydr)oxide behavior in soil

Proefschrift
ter verkrijging van de graad van doctor
op gezag van de rector magnificus
van Wageningen Universiteit,
Prof.dr.ir. L. Speelman,
in het openbaar te verdedigen
op woensdag 18 mei 2005
des namiddags te 13:30 uur in de Aula

CIP gegevens Koninklijke bibliotheek, Den Haag

Rahnemaie, R.
Ion adsorption modeling as a tool to characterize metal (hydr)oxide behavior in soil.
/ Rasoul Rahnemaie
Thesis Wageningen UR, The Netherlands - with ref. - with summary in Dutch, 152 p.
ISBN 90-8504-188-0

Subject heading: ion / adsorption / modeling / goethite / metal (hydr)oxides

Abstract

Rahnemaie, R., 2005, **Ion adsorption modeling as a tool to characterize metal (hydr)oxide behavior in soil**, PhD thesis, Wageningen University, The Netherlands, ISBN 90-8504-188-0, 152 pages.

This study aims to provide a better basis for application of adsorption models for metal (hydr)oxides to natural multicomponent systems. Adsorption of any ion in the environment will be potentially influenced by the effect of other ions present like calcium, phosphate, carbonate etc. The study starts with a detailed study of the binding of ions as outersphere complexes. The CD model has been extended to use the charge distribution for ions that bind as outersphere surface complex. This indicates that neither innersphere nor outersphere surface complexes are treated as point charges anymore. The new approach was applied to describe the adsorption of various electrolyte ions, phosphate, and carbonate. Batch experiments were performed using goethite as an adsorbent to determine the adsorption behavior of electrolyte ions (Li^{+1}, Na^{+1}, K^{+1}, Cs^{+1}, Ca^{+2}, Mg^{+2}, Cl^{-1}, NO_3^{-1}), phosphate, and carbonate. The adsorption of phosphate and carbonate ions was studied in a 'single ion' system and their interaction in a competition system. The charge distribution value of innersphere surface complexes of phosphate and carbonate was calculated using the new approach. New is also the use of quantum chemical calculations to derive the CD value based on a calculated geometry of the surface complexes. The calculated geometries were interpreted with the Brown bond-valence model, resulting in a calculated CD of the surface complex. The calculated CD values were used as a constraint in the surface complexation modeling. The CD model for inner- and outersphere surface complexation successfully described the adsorption data of electrolyte ions, phosphate, and carbonate. For accommodation of adsorbed ions within the Stern layer, a Three Plane (TP) model was used as a framework. For outersphere surface complexes, it was shown that the minimum distance of approach of adsorbed ions depends on the finite size of ions and their degree of hydration, which determine their relative distances to the surface of minerals. It has been shown that the capacitance of the inner Stern layer is determined by the minimum distance of approach of the ion closest to the surface, while the capacitance of the outer layer is determined by the minimum distance of approach of the ion furthest away from the surface. Modeling of phosphate adsorption data revealed that phosphate adsorbed mainly as a bidentate surface complex. At low pH, protonated species of phosphate are a combination of monodentate and bidentate surface complexes. The new CD approach shows that phosphate interacts with sodium at the mineral surface, which could not be detected using previous approaches.

Carbonate adsorption data were successfully described using a bidentate surface complex. This complex interacts with sodium at high pH and high salt level. The new approach not only predicts the shift in the isoelectric point as a function of phosphate loading, but also the measured zeta potential is in quite good agreement with predictions based on the assumption that the zeta potential coincides with the potential of the head end of the DDL. Furthermore, it has been shown that the parameterized CD model can be used to determine the effective reactive surface area of metal (hydr)oxides and the total reversibly adsorbed phosphate fraction in soils.

Contents

1

General Introduction

Soils are complex systems that sustain a very large number of interconnected chemical reactions. The principal features of soil chemical behavior can be understood based on principles and methods for the description of reactions in aqueous systems, interaction on surfaces and dissolution/precipitation reactions. The complete set of chemical reactions, which take place in the soil solution and between species in solution and solid phases, are quite complicated. Well-defined relevant solid phases, like goethite, can be used to quantify and better understand the interactions between the solution phase and solid phases. Open systems like soils and sediments are quite dynamic. This leads to continuous chemical reactions among ions in solution and at the interface, such as adsorption, desorption, dissolution, precipitation, and immobilization.

Phosphorus is an important element for studying the interactions at the solid-solution interface of minerals. The behavior of phosphate can give insight in the chemistry of mineral surfaces; it is relevant for bioavailability for organisms, and for the sustainability of environmental systems. On surfaces, the chemical reactions become more complicated the more ions interact. Phosphate and (bi)carbonate are two anions that are simultaneously present in soils and sediments. It is known for quite a long time that ions like phosphate bind to oxide surfaces through a ligand exchange mechanism (Russell et al., 1974), (Parfitt, 1979), a reaction in which one or more surface ligands are replaced by one or more ligands of phosphate or carbonate. This indicates the existence of chemical reactions at the surface and competition between different ions for these surface functional groups.

The description of chemical reactions in solutions and on surfaces needs to be defined in a model. Surface complexation models (SCM) are used to describe ion binding to surfaces. In surface complexation modeling, it is assumed that the adsorbing ion forms a surface complex with the adsorbing site, similar to the formation of a complex in solution. This implies that the surface complexation models should take the surface structure of the mineral into account as well as the structure of surface complexes. These models are a big step forward compared to empirical adsorption isotherm equations like the Freundlich or Langmuir models, which simply connect the solution concentration to the adsorbed amount of ions. The modeling is complicated by the effect of the surface charge on the concentration of the ion at the reaction site. Several kinds of SCM have been used to describe accumulation of ions at the surface, i.e. adsorption, and the distribution of the ions around the charged surface.

A well-known model in surface complexation modeling of ion adsorption is the CD-MUSIC model (Hiemstra and VanRiemsdijk, 1996). A major advantage of this model is that it intends to use surface species that have been determined by spectroscopy rather than simply describing the data using a free choice of surface

complexes. The CD model has been widely used to describe the adsorption of those ions that accumulate at the surface as innersphere surface complexes (Geelhoed *et al.*, 1997), (Geelhoed *et al.*, 1998), (Venema *et al.*, 1996), (Venema *et al.*, 1997), (Rietra *et al.*, 1999), (Rietra *et al.*, 2001b), (Filius *et al.*, 1997), (Filius *et al.*, 2000), (Weerasooriya *et al.*, 2002), (Weerasooriya *et al.*, 2003), (Tadanier and Eick, 2002), (Boily *et al.*, 2000), (Hiemstra *et al.*, 2004, Ch 5).

The CD-MUSIC model is used throughout this research to describe the adsorption of phosphate, carbonate, and a series of electrolyte ions. To take into account the outersphere surface complexes in the CD model, a new surface structural approach has been developed. The new approach uses a spatial charge distribution for innersphere as well as outersphere surface complexes. It has been shown that the new approach can successfully describe the adsorption of various surface complexes as a function of pH, ion loading, and salt concentration.

The ultimate goal of using the surface complexation model in environmental sciences is describing the reactions in a very complicated system like soil. This is still very difficult and further developments are required. As a starting point, we used our model to interpret the extractable amount of phosphate from a soil. The model has been parameterized based on our findings in pure relatively simple systems containing well-crystallized goethite. For the application to the soil, we used an extensive data set published by Barrow and Shaw (Barrow and Shaw, 1976b), (Barrow and Shaw, 1976c), (Barrow and Shaw, 1976a). The results showed that the model can successfully describe the amount of phosphate extracted from soil with the effective reactive surface area of oxides as the only adjustable parameter. In fact by this methodology, one can estimate the effective reactive surface area of oxides for a given soil.

The major aim of this study was to provide a better basis for application of adsorption models for metal (hydr)oxides to natural multicomponent systems. Adsorption of any ion in the environment will be potentially influenced by the effect of other ions present like calcium, phosphate, carbonate, etc. This major aim has several aspects like illustrating the outersphere complexation of common electrolyte ions in natural systems; studying the interaction of ions currently available in environmental systems, in particular the adsorption of phosphate, carbonate, calcium, and magnesium; and using this information in systems with natural soil materials.

Outline of the thesis

Ions have a finite size both in a crystallographic structure and when present in hydrated form in solution. At the solid-solution interface of minerals, counter ions are

adsorbed by a combination of chemical and/or electrostatic interactions. Electrolyte ions have always been treated as point charges in the double layer structure, when attempts have been made to model the ion adsorption. The finite size of electrolyte ions is taken into account by the presence of a Stern layer. However, each ion differs in size leading to differences in the distance of closest approach. A new surface structural approach is introduced in *chapter 2* in order to take into account the finite size of outersphere surface complexes. The model is applied to an internally consistent set of titration data and the model parameters are derived by simultaneous optimization of all data.

It has been shown by spectroscopy and ion adsorption modeling that some ions like strontium, sulfate, and selenate are adsorbed as a combination of innersphere and outersphere surface complexes (Peak *et al.*, 1999), (Collins *et al.*, 1998), (Rietra *et al.*, 2001a). The ratio of inner- and outersphere complexes depends on the loading and pH range. Since calcium and magnesium have similar electronic properties to strontium, it is expected that these two ions show similar adsorption behavior. This is considered in *chapter 3* as a function of pH and loading on goethite.

Phosphate is an ion that is environmentally significant and of great practical interest. It is an important plant nutrient as well as a major stimulant of eutrophication in fresh waters. Since adsorption is an important process controlling availability and mobility of phosphorus, understanding the reactions occurring during the adsorption is of more than just theoretical interest. In *chapter 4*, the adsorption of phosphate in a 'single ion' system is studied as a function of pH, P loading, and salt concentration. To the best of our knowledge, quantum mechanical calculation has never been used as a tool to derive the charge distribution that can be used in ion adsorption modeling. In *chapter 4*, a new approach is presented to derive the CD values of adsorbed phosphate complexes and use them in the modeling of phosphate adsorption data. This constraint reduces the degrees of freedom in ion adsorption modeling, since only the affinity of adsorbed complexes will be optimized on the data.

Carbon dioxide and its dissolved forms are present in all ecosystems. It has been shown that dissolved carbonate species affect the adsorption behavior of trace elements (Villalobos *et al.*, 1999). Realistic descriptions of carbonate adsorption and its interaction with other ions require a correct molecular structure of adsorbed carbonate. In *chapter 5* the available in situ FTIR spectroscopic information is reevaluated and compared with the information from the charge distribution of adsorbed carbonate complexes and proton co-adsorption. The surface speciation of carbonate is applied to an adsorption data set of carbonate in a 'single ion' system.

Because of the simultaneous presence of phosphate and carbonate in natural systems, one may expect interaction in the adsorption process. Therefore, it is

interesting to study how important it might be and how relevant these interactions are in studying ion adsorption in natural systems. In *chapter 6*, the competitive adsorption of carbonate and phosphate is measured as a function of pH, phosphate and carbonate loading, and salt concentration.

The major ion interactions, which take place in soils and natural waters, have been studied in chapters 2 to 6. The derived model parameters are thus essential for the description of adsorption interactions with any ions of interest, be it arsenic, selenium, technetium, etc., in complicated systems like soils. All results are used to interpret data of total extractable phosphate from a soil with a sodium-bicarbonate solution adjusted to pH 8.5. The extraction procedure, named Olson's method, is a well-known method in soil science and is widely used in the evaluation of plant-available phosphate in soils. The methodology allows estimating the effective reactive oxide surface in soils and the fraction reversibly bound phosphate, as described in *chapter 7*.

References

Barrow, N. J., and T. C. Shaw (1976a). Sodium bicarbonate as an extractant for soil phosphate .3. Effects of buffering capacity of a soil for phosphate. *Geoderma* **16**(4): 273.

Barrow, N. J., and T. C. Shaw (1976b). Sodium bicarbonate as an extractant for soil phosphate. 1. Separation of the factors affecting the amount of phosphate displaced from soil from those affecting secondary adsorption. *Geoderma, Sept* **16**(2): 91.

Barrow, N. J., and T. C. Shaw (1976c). Sodium bicarbonate as an extractant for soil phosphate. 2. Effect of varying the conditions of extraction on the amount of phosphate initially displaced and on the secondary adsorption. *Geoderma, Sept* **16**(2): 109.

Boily, J. F., P. Persson, and S. Sjoberg (2000). Benzenecarboxylate surface complexation at the goethite (alpha- feooh)/water interface: Ii. Linking ir spectroscopic observations to mechanistic surface complexation models for phthalate, trimellitate, and pyromellitate. *Geochim. Cosmochim. Acta* **64**(20): 3453.

Collins, C. R., D. M. Sherman, and K. V. Ragnarsdottir (1998). The adsorption mechanism of sr2+ on the surface of goethite. *Radiochimica Acta* **81**(4): 201.

Filius, J. D., T. Hiemstra, and W. H. Van Riemsdijk (1997). Adsorption of small weak organic acids on goethite: Modeling of mechanisms. *J. Colloid Interface Sci.* **195**(2): 368.

Filius, J. D., D. G. Lumsdon, J. C. L. Meeussen, T. Hiemstra, and W. H. Van Riemsdijk (2000). Adsorption of fulvic acid on goethite. *Geochim. Cosmochim. Acta* **64**(1): 51.

Geelhoed, J. S., T. Hiemstra, and W. H. Van Riemsdijk (1998). Competitive interaction between phosphate and citrate on goethite. *Environ. Sci. Technol.* **32**(14): 2119.

Geelhoed, J. S., T. Hiemstra, and W. H. Vanriemsdijk (1997). Phosphate and sulfate adsorption on goethite: Single anion and competitive adsorption. *Geochim. Cosmochim. Acta* **61**(12): 2389.

Hiemstra, T., R. Rahnemaie, and W. H. Van Riemsdijk (2004, Ch 5). Surface complexation of carbonate on goethite: Ir spectroscopy, structure and charge distribution. *J. Colloid Interface Sci.* **278**(2): 282.

Hiemstra, T., and W. H. Vanriemsdijk (1996). A surface structural approach to ion adsorption: The charge distribution (cd) model. *J. Colloid Interface Sci.* **179**(2): 488.

Parfitt, R. L. (1979). Nature of the phosphate-goethite (alpha-feooh) complex formed with ca(h2po4)2 at different surface coverage. *Soil Sci. Soc. Am. J.* **43**(3): 623.

Peak, D., R. G. Ford, and D. L. Sparks (1999). An in situ atr-ftir investigation of sulfate bonding mechanisms on goethite. *J. Colloid Interface Sci.* **218**(1): 289.

Rietra, R., T. Hiemstra, and W. H. Van Riemsdijk (1999). Sulfate adsorption on goethite. *J. Colloid Interface Sci.* **218**(2): 511.

Rietra, R., T. Hiemstra, and W. H. Van Riemsdijk (2001a). Comparison of selenate and sulfate adsorption on goethite. *J. Colloid Interface Sci.* **240**(2): 384.

Rietra, R., T. Hiemstra, and W. H. Van Riemsdijk (2001b). Interaction between calcium and phosphate adsorption on goethite. *Environ. Sci. Technol.* **35**(16): 3369.

Russell, J. D., R. L. Parfitt, A. R. Fraser, and V. C. Farmer (1974). Surface-structures of gibbsite goethite and phosphated goethite. *Nature* **248**(5445): 220.

Tadanier, C. J., and M. J. Eick (2002). Formulating the charge-distribution multisite surface complexation model using fiteql. *Soil Sci. Soc. Am. J.* **66**(5): 1505.

Venema, P., T. Hiemstra, and W. H. Vanriemsdijk (1996). Multisite adsorption of cadmium on goethite. *J. Colloid Interface Sci.* **183**(2): 515.

Venema, P., T. Hiemstra, and W. H. Vanriemsdijk (1997). Interaction of cadmium with phosphate on goethite. *J. Colloid Interface Sci.* **192**(1): 94.

Villalobos, M., J. D. Ostergren, M. A. Trotz, and J. O. Leckie (1999). Carbonate effects on the surface complexation of cr(vi) and pb(ii) with goethite. *Abstr. Pap. Am. Chem. Soc.* **218**: 32.

Weerasooriya, R., H. J. Tobschall, H. Wijesekara, E. Arachchige, and K. A. S. Pathirathne (2003). On the mechanistic modeling of as(iii) adsorption on gibbsite. *Chemosphere* **51**(9): 1001.

Weerasooriya, R., H. Wijesekara, and A. Bandara (2002). Surface complexation modeling of cadmium adsorption on gibbsite. *Colloid Surf. A-Physicochem. Eng. Asp.* **207**(1-3): 13.

2

A New Surface Structural Approach to Ion Adsorption: Tracing the Location of Electrolyte Ions

Abstract

Ions differ in size leading to the possibility that the distance of closest approach to a charged surface differs for different ions. Especially ions bound as outersphere complexes have so far been treated as point charges. For innersphere complexes, it has been argued that it is necessary to distribute the charge of the adsorbed ion over the surface and the next electrostatic plane. This concept has led to the CD model. A new surface structural approach was developed in order to take into account the physical reality of the ion pair's size by applying the charge distribution concept also to ions adsorbed as outersphere complexes. In this approach, the CD model is extended to take into account outersphere surface complexes as having a spatial charge distribution within the Basic Stern layer of the solid-solution interface. This indicates that neither innersphere nor outersphere surface complexes are treated as point charges anymore. The new approach has been applied to describe simultaneously the adsorption of various monovalent electrolyte ions. It was shown that the concept can successfully describe the development of surface charge for various electrolytes as a function of pH and salt level and the shift in the isoelectric point (IEP) of the goethite. The new concept also sheds more light on the degree of hydration of the ions when present as outersphere complexes.

Keywords: Electrolyte ion, Diffuse double layer; Basic Stern; Three Plane model; Adsorption; Iron oxide; Goethite; CD model; MUSIC model.

Introduction

Usually, mineral surfaces are charged. Surface charge is compensated by counter ions of opposite charge outside a particle as suggested by Helmholtz in 1835 (Sparks, 1999). The combination of surface charge and counter charge is called the double layer. Without chemical interaction of ions with the mineral surface, electrolyte ions have a distribution pattern as derived almost a century ago by Gouy (Gouy, 1910) and Chapman (Chapman, 1913). This structure is known as the diffuse double layer (DDL) and it can be experimentally tested with Atomic Force Microscopy (Israelachvili, 1991).

Near the surface, electrolyte ions cannot be treated as point charges. Counter ions have a finite size, which implies that the ions have a minimum distance of approach to the surface. Stern (Stern, 1924) described the concept of minimum charge

separation in 1924. The compact part of DDL, between surface- and counter- charge, is called the Stern layer. In terms of electrostatics, the compact part of the double layer can be considered as a plate condenser with a certain capacitance. An important parameter relating layer thickness and capacitance is the dielectric constant of the medium in the condenser. The precise value of the macroscopic quantity when applied to interfaces is unknown.

Electrolyte ions may in addition to electrostatic forces also be attracted by the surface due to specific weak interactions, (Grahame, 1947), (Yates *et al.*, 1974), (Yates, 1975), (Davis *et al.*, 1978). This phenomenon is called ion pair formation and the complexes are named outersphere complexes. In some cases, a simple electrolyte ion like Rb^{+1} may form an innersphere complex as shown recently by Fenter et al. (Fenter *et al.*, 2000). In such surface complexes, one or more ligands of the adsorbed ion are common with the metal ions of the solid.

Metal oxide surfaces have a variable charge, which is related to the relative adsorption of protons by surface oxygens. The proton binding is pH dependent. An important factor in the H binding is the electrostatic potential, which is created by the accumulation of charge at the surface. In principle, charge and electric field are localized. For surfaces, the local interaction can be described very well with a smeared out approach as was shown by Borkovec (Borkovec, 1997). This mean field approach is generally applied in surface complexation models.

Many models have been proposed to describe the relation between the solution composition and the charge properties of colloids. These surface complexation models are a combination of chemical equilibria and a chosen electrostatic model. From the perspective of physical reality, a minimum prerequisite to account for the variable influence of the electrolyte concentration is the use of a diffuse double layer in the model. According to Stern, the model should have a minimum distance of approach of the electrolyte ions. The combination is called the Basic Stern (BS) model. It can be considered as the simplest model for the description of the variable proton charge of metal oxide surfaces (Lutzenkirchen, 1998). Moreover, the BS model accounts for physical realistic features. If necessary, ion pair formation can be implemented within the BS concept, locating these outersphere complexes at the minimum distance of approach.

The BS approach can be extended with an additional layer to change the double layer profile. A known representative of this class of models is the Triple Layer (TL) model (Davis *et al.*, 1978). In the classical TL model, the distance of minimum approach of the electrolyte ions in the diffuse double layer is strongly enlarged by the choice of a very low capacitance for the second layer. This results in a much smaller interaction between ions in the DDL and proton charge at the surface. Due to this

constraint, ion pair formation is *a priori* needed in order to get sufficient surface charge in this model approach.

Increase of the electrolyte ion affinity in case of ion pair formation will lead to more surface charge at the metal oxide surface due to an improved screening of the electrostatic field. Generally, electrolyte ion affinities have been derived from the analysis of the charging behavior of oxides with a surface complexation model (e.g. (Sahai and Sverjensky, 1997)). A systematic analysis for the charging behavior of Ti-oxides with the BS model (Bourikas *et al.*, 2001), has shown that the affinity constants for electrolyte cations are generally larger than those for anions. A higher affinity of cations over anions will lead to an upward shift of the isoelectric point (IEP), in particular at high electrolyte concentrations (Breeuwsma and Lyklema, 1973). This phenomenon can be observed with electro-acoustic-phoresis, as has been shown for gibbsite, (Rowlands *et al.*, 1997) zirconia and rutile (Kosmulski and Rosenholm, 1996), anatase (Gustafsson *et al.*, 2000) and silica (Kosmulski and Matijevic, 1992). It indicates that the larger affinity of electrolyte cations *versus* anions is a general phenomenon. For goethite, the variation in affinity for various electrolyte anions has been derived from the interpretation of a consistent set of titration data (Rietra *et al.*, 2000) with the BS model. The authors measured the goethite charge in $NaClO_4$, $NaNO_3$, and NaCl. In their analysis, the arbitrary decision has been made to set the affinity of the surface for Na^{+1} and NO_3^{-1} equal. No attempt has been made to pinpoint the binding constant of Na^{+1} in detail.

In the present study, we will analyze the affinity of electrolyte cations and anions using new surface charge data for goethite, in a series of monovalent electrolyte ions ($LiNO_3$, LiCl, $NaNO_3$, NaCl, KNO_3, and $CsNO_3$). Preliminary modeling indicated that any difference in electrolyte affinity is most markedly observed at high pH and relatively high electrolyte concentrations. Such conditions were applied in our experiments. In a second paper (Rahnemaie *et al.*, Ch 3), we will describe the binding of divalent electrolyte ions (Ca^{+2}, Mg^{+2}, and SO_4^{-2}). The binding of these ions may be a combination of innersphere and outersphere complexation.

The compact part of the double layer is crucial in interface chemistry since changes in potential are most profound there. From this perspective, the location of the electrolyte ions is an important issue. It determines the electrostatic contribution (ΔG_{elec}) to the overall affinity ($\Delta G_{overall}$) of the electrolyte ions, i.e. $\Delta G_{overall} = \Delta G_{intr} + \Delta G_{elec}$. In most model approaches, the electrolyte cations and anions are located at the same position, i.e. they experience the same electrostatic field strength.

The question arises to what extent macroscopic data can reveal information on the location of the electrolyte ions in the double layer profile. In the present study, we will analyze primary charging behavior of a metal oxide in detail. In order to find both

capacitances and the individual ion pair formation constants, the experimental data will be analyzed simultaneously and the results will be interpreted in terms of the double layer structure.

MUSIC model

Reactive groups

In the lattice of goethite (α-FeOOH) two different types of triply coordinated oxygens exist, one non-protonated (Fe_3O) and one protonated (Fe_3OH) oxygen. The difference in proton affinity of both triply coordinated oxygens is linked to a difference in the distances between the oxygen and the coordinating Fe-ions. Both types of oxygens are also found at the surface of the dominant 110 face and the 100 face, (Hiemstra and Van Riemsdijk, 2000), (Weidler *et al.*, 1996), (Weidler *et al.*, 1998). The triply coordinated surface groups of type I are non-protonated over a wide pH range, i.e. present as $\equiv Fe_3O_I$. The other type of triply coordinated surface group (type II) has a higher proton affinity and can be present as $\equiv Fe_3O_{II}H$. Charge can be attributed to these surface groups applying the Pauling bond valence concept (Hiemstra *et al.*, 1989b), (Hiemstra *et al.*, 1996). Based on the concept of equal charge distribution (Pauling, 1929), the triply coordinated oxygen can be represented as $\equiv Fe_3O_I^{-1/2}$ and the triply coordinated hydroxyl as $\equiv Fe_3O_{II}H^{+1/2}$.

The triply coordinated oxygens and hydroxyls of the mineral bulk can also be found at the surface. In addition, the interface of goethite has surface groups with a lower Fe coordination. The doubly coordinated oxygens will have a high affinity for protons, because the $\equiv Fe_2O^{-1}$ is highly undersaturated in terms of charge (Hiemstra *et al.*, 1996). It leads to the formation of a stable and uncharged surface species $\equiv Fe_2OH^o$, which does not easily accept a second proton. Singly coordinated surface oxygens ($\equiv FeO^{-3/2}$) are highly unstable and are always transformed into $\equiv FeOH^{-1/2}$ in aqueous systems, (Hiemstra *et al.*, 1989b), (Rustad *et al.*, 1996). Depending on the pH, the hydroxyl ($\equiv FeOH^{-1/2}$) may accept a second proton forming a surface water group ($\equiv FeOH_2^{+1/2}$).

Surface structure and site density

At the 110 and 100 faces, one row of singly coordinated surface groups (≡FeOH(H)) is found on a unit cell basis, which is equivalent to a site density N_s of 3 nm^{-2} at the 110 face (Barron and Torrent, 1996). In addition, one row of non H-reactive doubly coordinated groups ($\equiv Fe_2OH$) is present. At the 110 and 100 faces, one also has three rows of triply coordinated groups ($\equiv Fe_3O(H)$) , one row with the low

proton affinity (type I) and two rows with the high proton affinity (type II). The large difference in proton affinity of both types of triply coordinated surface groups leads to a lower effective site density for the proton reactive one, (Hiemstra and VanRiemsdijk, 1996), (Hiemstra *et al.*, 1996), since the charge of one row of $\equiv Fe_3O^{-1/2}$ (type I) cancels against one row of $\equiv Fe_3OH^{+1/2}$ (type II). The apparent site density of the proton reactive triply coordinated surface group (type II) therefore is 3 nm^{-2}. The affinity constant of type II is estimated to be relatively close to that of the singly coordinated group, i.e. $\Delta \log K \approx 4$ (Hiemstra *et al.*, 1996). To simplify, the affinity constants of the proton reactive groups ($\equiv FeOH^{-1/2}$ and $\equiv Fe_3O_{II}^{-1/2}$) are set equal in the modeling, (Hiemstra and VanRiemsdijk, 1996), (Hiemstra *et al.*, 1996). It can be shown that with this simplification the logarithm of the affinity constant is equal to the value of the PZC, in the absence of ion pair formation or in case of symmetrical ion pair formation.

Faces like the 021 and 001 faces terminate the goethite needles at the top ends of the crystals. These crystal faces have equal numbers of singly and doubly coordinated surface groups (N_s=7-8 nm^{-2}). In the modeling, the protonation constant of the singly coordinated surface group at these faces is taken equal to that of the 110 face.

The overall effective site density of goethite is calculated assuming 90% 110/100 face and 10 % 021/001 face leading to 2.7+0.75=3.45 nm^{-2} for the singly coordinated and 2.7 nm^{-2} of the triply coordinated surface group.

Primary protonation reactions

Based on the above analysis, the protonation of the crystal face can be represented by two protonation reactions:

$$\equiv FeOH^{-1/2} + H^+(aq) \Leftrightarrow \equiv FeOH_2^{+1/2} \qquad [1]$$

$$\equiv Fe_3O^{-1/2} + H^+(aq) \Leftrightarrow \equiv Fe_3OH^{+1/2} \qquad [2]$$

The proton reactive surface groups may interact with electrolyte ions, forming outersphere surface complexes, resulting formation of the ion pairs $FeOH^{-1/2}\cdots C^{+z}$, $FeOH_2^{+1/2}\cdots A^{-z}$ and $Fe_3O^{-1/2}\cdots C^{+z}$, $Fe_3OH^{+1/2}\cdots A^{-z}$, in which C^{+z} represents the electrolyte cation and A^{-z} the anion.

In the modeling, the proton affinity constants for singly and triply coordinated surface groups are set equal, $\log K_{H,\ FeOH} = \log K_{H,\ Fe3O}$. The same is done for the ion

pair formation constants for singly and triply coordinated surface groups (Hiemstra and VanRiemsdijk, 1996).

Locating the ion charge

In the simplest physically realistic double layer profile, the outersphere complexes of electrolyte ions are located at a position determined by the minimum distance of approach of ions to the surface. They do not have common ligands with surface groups. For simplicity, they may be treated as point charges and located in one common electrostatic plane. The model is known as the Basic Stern (BS) model (Westall and Hohl, 1980).

Many ions may form innersphere complexes with surface groups. In these surface complexes, one or more ligands of the adsorbed ion are common with the surface. The other ligands are orientated towards the solution present in the model at a distinct distance from the surface in the compact part of the double layer. According to the bond valence concept, this leads to a distribution of charge in the compact part of the double layer (Hiemstra and VanRiemsdijk, 1996). In the Charge Distribution (CD) model, part of the ion charge is attributed to a surface plane and the other part is attributed to a second electrostatic plane, at some distance from the surface. In the simplest picture, the second electrostatic plane may coincide with the plane of minimum distance of approach, i.e. the CD distribution model is combined with the BS option. It implies that the electrolyte ions may have a rather large interaction with innersphere complexes. The interaction can be reduced by locating the outer ligands of the innersphere complexes at a smaller distance from the surface in a separate electrostatic plane. This model has been proposed by Hiemstra & van Riemsdijk (Hiemstra and VanRiemsdijk, 1996) and is named the Three Plane (TP) model. Innersphere complexation for SO_4^{-2} adsorption has been best described with the BS approach (Rietra et al., 1999), while PO_4^{-3} innersphere complexation has been best described with the TP model (Hiemstra and VanRiemsdijk, 1996). To unify both descriptions in one concept, Rietra et al. (Rietra et al., 1999) suggested to locate the anion pairs at the 1-plane and the cation pairs at the 2-plane. In Figure 1, the corresponding TP model is schematically represented.

A new approach

Electrolyte ions differ in size. It implies that the double layer will accommodate these different ions at different distances from the surface. As a consequence, one has to define, in principle, for each ion an individual electrostatic plane. This idea is not

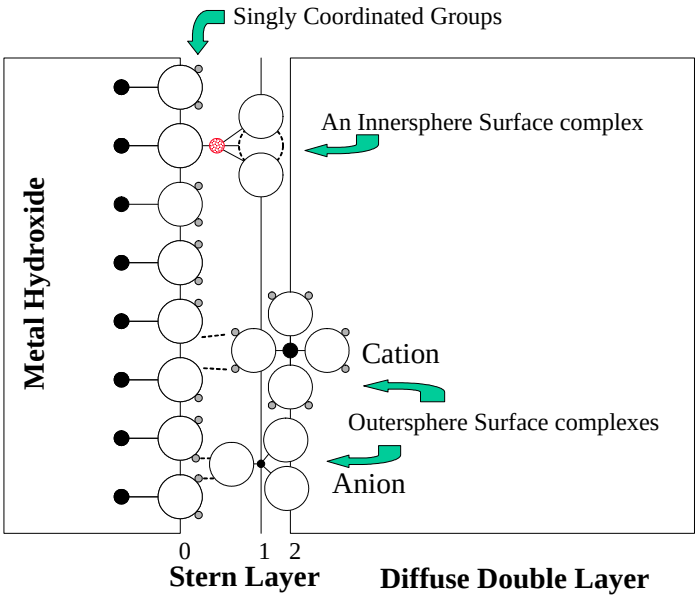

Figure 1. A schematic representation of the TP model at the goethite-water interface. In the TP model, there are three electrostatic planes at the surface. The common ligands of innersphere surface complexes with the surface groups are located at the 0-plane. The solution-oriented ligands of the innersphere complexes are located at the 1-plane. Electrolyte ions may be located at the 1- or 2-plane. The 2-plane coincides with the head end of the DDL.

very attractive, in particular in multi component systems. Therefore, electrolyte ions have often been located only at one electrostatic location. In case of the use of the above given Three Plane model (Figure 1), it is possible to accommodate the electrolyte ions in a second Stern layer, the layer between the 1 and 2-plane. Depending on the relative position of the electrolyte ions in the double layer profile, the charge of the electrolyte ion is divided over both electrostatic planes. Small ions will attribute more of their charge to the 1-plane. Large ions do the opposite. The relative locations of the electrolyte ions in the double layer can be found by determining the charge distribution coefficients from an accurate and internally calibrated data set.

The above-suggested model for outersphere complexes can be considered as an extension of the CD model. Actually, the charge distribution of the outersphere ions is related to the size of the ion, while the charge distribution of innersphere complexes can be related to the number of common ligands and the bound strength (Hiemstra and VanRiemsdijk, 1996), (Hiemstra and van Riemsdijk, 2002), (Hiemstra and van Riemsdijk, in preparation).

Material and methods

Synthesis and characterization of goethite

To avoid (bi)carbonate contamination, all chemicals (Merck p.a.) were made under a purified N_2 atmosphere. To be free of silica, these solutions were stored for a short period in polyethylene bottles. The acid solutions were stored in the glass bottles to avoid contamination by organic materials. Ultra pure water (≈0.018 dS/m) was used throughout the experiments. The ultra pure water has been pre-boiled to remove dissolved CO_2 before using in the experiments.

The preparation of goethite suspension was based on the method of Atkinson et al. (Atkinson *et al.*, 1967), which has been described in more detail by Hiemstra et al. (Hiemstra *et al.*, 1989a). A freshly prepared 0.5 M $Fe(NO_3)_3$ solution was slowly titrated with 2.5 M NaOH to pH 12.0. The prepared suspension was aged for 4 days at 60°C and subsequently dialyzed in ultra pure water. The BET(N_2) specific surface area of goethite equals 98.6 $m^2\ g^{-1}$.

Charging behavior of goethite

A salt-free suspension of goethite was acidified to pH 3.55 and continuously purged with purified N_2 to remove (bi)carbonate for 24 hours. Sub-samples of this stock suspension were used throughout the titration experiments. This assures that the starting condition for all the titrations is exactly identical.

Certain amounts of a specified salt solution were added to the series of individual batches of goethite suspension. This leads to a fixed concentration of goethite (16.52 g l^{-1}) for the series of titration in different background electrolyte ions. Each batch of goethite suspension, which contained a known amount of a specified salt, was titrated from its initial pH to a pH of about 10.5. This one-way titration makes it distinctive from the classical forward-backward titration. The initial pH of each batch was slightly different from the others, which is related to a different interaction of the added electrolyte ions with the surface.

Individual titrations were performed at different concentrations of different electrolyte ions, i.e. 0.04, 0.10, and 0.20 M LiCl, $LiNO_3$ and NaCl; 0.20 M $NaNO_3$, KNO_3, and $CsNO_3$. Each titration was started after equilibrium for half an hour and each data point was collected 15 minutes after an addition, when the drift was lower than 0.02 mV min^{-1}.

The goethite stock suspension was acidified with a small amount of 1 M HNO_3, and the titrations were done with 0.100 M NaOH. This procedure will introduce a

small amount of Na^{+1} and NO_3^{-1} ions in the background solution. Their concentration is actually negligible compared with the studied background electrolytes. Nevertheless, for each data point, the amount of both was taken into account during modeling. In addition, the change in the concentration of suspension components, i.e. the concentration of goethite and salt ions, due to addition of base during titration, was accounted using an appropriate bookkeeping.

In order to compare the one-way titration data with the more common forward-backward titrations, a sample of goethite suspension was titrated with 0.015, 0.05, and 0.2 M $NaNO_3$. The various electrolyte additions were done at low pH, followed by a forward and backward titration of the suspension.

A double-junction Ag-AgCl reference electrode and a glass electrode were used for the titration experiments. The outer junction of the reference electrode was filled with a solution of 0.125 M $NaNO_3$ and 0.875 M KNO_3. The mobility of the positive and the negative ions in this solution is about the same, i.e. the diffusion potential over the outer junction is independent of the salt concentration (McInnes, 1961). The titration was done using the Wallingford automatic computerized titrator (Kinniburgh *et al.*, 1995). The temperature was fixed at 20±0.1 °C using a thermostated reaction cell, while the whole equipment was present in a constant temperature room (22±1 °C).

Results and discussion

Treatment of goethite titration data

For each addition of base, a change in surface charge can be calculated relative to the starting point of the titration. Figure 2 illustrates an example of the relative surface charge of goethite in a 0.2 molar solution of a series of electrolyte ions. The data in Figure 2 show that for a given concentration of electrolyte ions, the proton desorption is affected by the type of cation as well as anion present. A close look to the data of Figure 2 reveals that the major difference in starting point is due to the specific type of anion, i.e. nitrate or chloride. The figure also shows that for a particular anion, the charging curve is strongly different for different cations. It points to a different interaction with the charged surface.

Symmetrical ion pair formation on goethite has often been assumed (Hiemstra and VanRiemsdijk, 1996), (Venema *et al.*, 1996), (Rietra *et al.*, 2000). This leads to the possibility to use the common intersection point (CIP) of the titration data as the pristine point of zero charge (PPZC), which is used to transform the relative surface

charge of goethite to an absolute scale. As a starting point, this idea was applied to the titration data of sodium nitrate and the affinity of sodium and nitrate was set equal to -1. Further modeling of the data revealed that the affinity of none of the ion pairs is equal. This means that the PPZC can no longer be experimentally obtained unequivocally with these electrolyte ions as background salts. The uncertainty in PZC increases proportional with the difference in the affinity between the cation and the anion of the background salt. Modeling of the titration data showed that the sodium and chloride ions have an affinity, which differ the least. This indicates that the CIP of titration data in NaCl is closer to the PPZC of the goethite surface than for other salts. Based on this perception, the goethite surface charge was scaled from the relative to the absolute charge by applying the corresponding CIP charge in NaCl (pH=9.0) to the overall titration data.

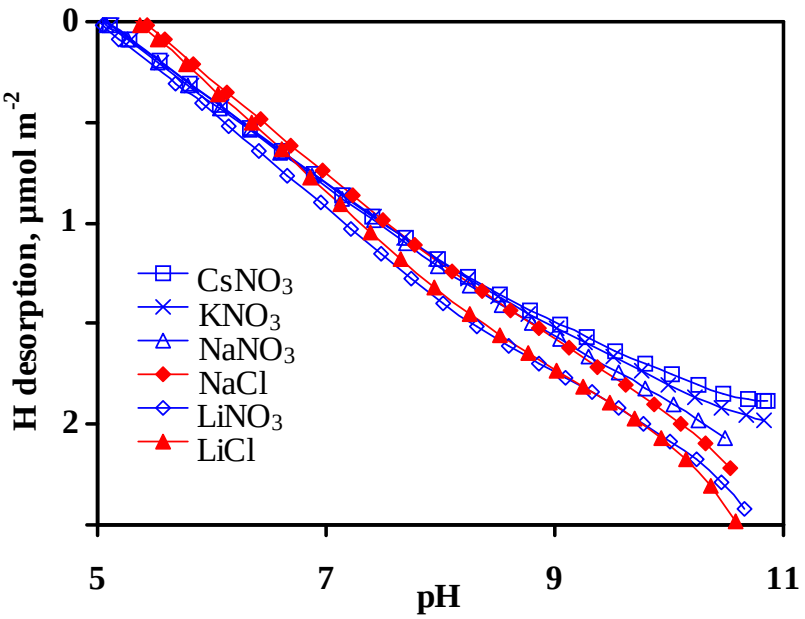

Figure 2. The relative surface charge of goethite as affected by the type of cation and anion of the background electrolytes. The concentration of added salts is 0.2 molar. The different symbols on the figure show the exact measured values and the lines are interpolation between the experimental data.

The affinity of monovalent electrolyte ions

Monovalent electrolyte ions are mainly adsorbed as outersphere surface complexes. The outersphere surface complexes do not share any ligand with the metal ion of the reactive surface groups. These ions are mainly adsorbed via electrostatic interactions with the surface. The following equations show the way that monovalent cations and anions were formulated in data processing. The equations are written only

using the singly coordinated surface groups. However, in the modeling the same treatment was applied to the triply coordinated surface groups.

$$\equiv \mathrm{FeOH}^{-1/2} + \mathrm{C}^{+1}(\mathrm{aq}) \Leftrightarrow \equiv \mathrm{FeOH}^{-1/2} \cdots \mathrm{C}^{+1} \qquad [3]$$

$$\equiv \mathrm{FeOH}^{+1/2} + \mathrm{A}^{-1}(\mathrm{aq}) \Leftrightarrow \equiv \mathrm{FeOH}_2^{+1/2} \cdots \mathrm{A}^{-1} \qquad [4]$$

where the **…** symbol emphasizes the weak chemical interaction between surface group and adsorbed ion. C and A characters represent the monovalent cations and anions respectively.

As mentioned above, the data of Figure 2 show that electrolyte cations and anions may have a different electrostatic interaction with the surface. This can be due to differences in intrinsic affinity constant of equation [3] and [4] and/or differences in electrostatic interaction. The latter can be interpreted in terms of difference in distance to the surface, which in the model can be implemented by locating the anions and cations between two different positions near the surface. The charge is allowed to be distributed between both electrostatic positions.

In the model approach, the charge distribution and the intrinsic electrolyte affinity constants are both derived from the data. The fitted charge distribution of the various outersphere complexes reflects the relative position of the ions. The capacitance of the inner and outer Stern layer was also fitted which is a measure of the absolute distance.

In the optimization, the charge distribution is restricted that the maximum attribution is equal to the maximum valence charge of the electrolyte ion. This restriction was necessary for Cl^{-1} on the 1-plane and for K^{+1} and Cs^{+1} on the 2-plane. The fitted parameters are given in Table 1 for monovalent electrolyte ions.

In Figure 3, the surface charge is given for goethite present in various electrolytes. Comparison of Figure 3a, 3b, 3c, 3d and 3e shows that in case of $LiNO_3$ the point of zero charge is lower than that in $NaNO_3$, KNO_3 and $CsNO_3$. This behavior can also be observed for goethite in LiCl and NaCl. This difference is due to the larger interaction of Li^{+1} with the protons at the surface, which is due a larger charge attribution to the 1-plane (Table 1) in combination with the higher affinity constant. Actually, Li^{+1} ions induces more proton co-adsorption than Na^{+1}, K^{+1} and Cs^{+1} ions due to a stronger interaction with the negatively charged groups of the surface.

Interaction of ClO_4^{-1}

Rietra et al. (Rietra *et al.*, 2000) have studied the proton adsorption in presence of chloride, nitrate, and perchlorate on goethite. The above model-derived parameters (capacitances, and affinity of Na^{+1}, Cl^{-1} and NO_3^{-1}) were applied to this data set, yielding a good description of the data. From the titration data in the Na perchlorate solution, the CD and adsorption affinity of ClO_4^{-1} was derived (Table 2). In this calculation, the proton affinity was set equal to the PZC (9.25) as given by Rietra et al (Rietra *et al.*, 2000). The difference in the PZC value of Rietra et al. with ours might be due to small differences in surface characteristics and uncertainty in determining the CIP.

Table 1. The affinity constants of interaction monovalent cations and anions with goethite as derived from modeling of the goethite titration data using the charge distribution model of the outersphere complexes over the 1- and 2-plane. The fitted capacitance for the first and second Stern layer are respectively C_1= 1.00 ± 0.01 and C_2= 0.89 ± 0.07 F m^{-2}

Ions	Δz_1	Δz_2	log K
Li^{+1}	0.41 ± 0.03	0.59 ± 0.03	0.51 ± 0.04
Na^{+1}	0.50 ± 0.07	0.50 ± 0.07	-0.27 ± 0.06
K^{+1}	0	1[a]	-0.41 ± 0.13
Cs^{+1}	0	1[a]	≤-1.5[b]
Cl^{-1}	-1[a]	0	-0.66 ± 0.03
NO_3^{-1}	-0.67 ± 0.02	-0.33 ± 0.02	-0.53 ± 0.03

a. The charge was placed by definition since the model showed that almost the total charge remains at this plane.
b. The log K value was not fitted but chosen, due to the low sensitivity of the data.

Table 2. The affinity constants of ClO_4^{-1} as derived from modeling of the goethite titration data (Rietra *et al.*, 2000). The modeling was done using CD model for outersphere complexes.

	Δz_0	Δz_1	log K
[†]ClO_4^{-1}	-0.59 ± 0.03	-0.41 ± 0.03	-0.95 ± 0.06

[†]The proton affinity was set on 9.25 as given by Rietra et al. (Rietra *et al.*, 2000). The capacitances and Na^{+1} and NO_3^{-1} affinities are taken from Table 1.

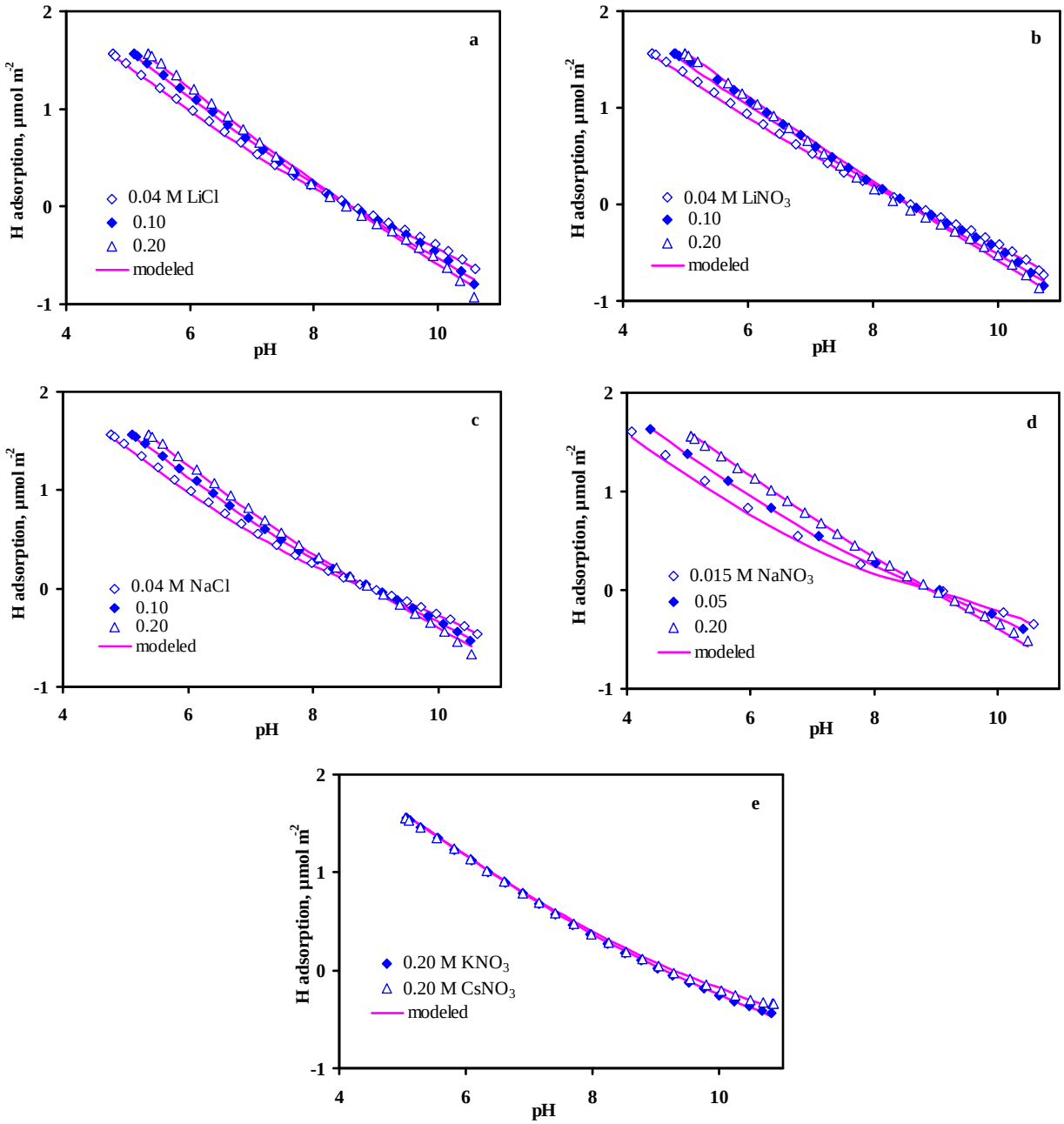

Figure 3. The experimental data and model description of the surface charge of goethite in different monovalent electrolytes as background salt. The CD model for outersphere complexation was used to describe the titration data.

The capacitance of the Stern layer

The capacitance of the Stern layer can be interpreted in terms of a distance, *d*, between the two electrostatic planes of the double layer (Bourikas *et al.*, 2001), according to:

$$C = \frac{\varepsilon_r \varepsilon_o}{d} \qquad [5]$$

in which ε_o and ε_r are respectively the absolute (8.85×10^{-12} $CV^{-1}m^{-1}$) and relative dielectric constant. Note that in case of two Stern layers we may write for the total distance $d=d_1+d_2$, i.e. $1/C = 1/C_1 + 1/C_2$.

In principle, the distance of approach of electrolyte ions may be different, leading to an ion dependent capacitance. It is preferable to make the capacitance a general characteristic of the solid/solution interface in case of application to multi-component systems. In the present approach, the Stern layer capacitance is taken as a constant and the effect of the position of the ion charge in the compact part of the double layer profile is taken into account via the charge distribution. In this approach, the capacitance of the inner Stern layer is determined by the minimum distance of approach of the ion closest to the surface (Cl^{-1}), while the capacitance of the second Stern layer is determined by the minimum distance of approach of the electrolyte ion that is the furthest away from the surface, in this study (K^{+1} and Cs^{+1}).

Distances

The fitted values of the capacitances are in the same order of magnitude ($C \approx 1$ F/m^2). It does not necessarily imply that both layers will have the same thickness, since the dielectric constant may change in the double layer profile. A point of concern is the use of a macroscopic quantity in the use of equation [5] and a precise interpretation on a micro-scale. Nevertheless, we will try to relate the capacitance to distances to sharpen our picture of the double layer. If water in the outer Stern layer has properties similar to that of water (ε_r=78), or slightly lower due to the presence of electrolytes, the capacitance C_2 of 0.9 F/m^2 leads to $d_2 \approx 7.7$ Å (7.7×10^{-10} m). The distance should be considered as a maximum.

If the dielectric properties of the inner Stern layer capacitance are similar to that of the outer Stern layer, the capacitance of 1 F/m^2 is equivalent with a distance $d_1 \leq \approx 6.9$ Å, being about ≤ 2-2.5 water molecules. In the modeling, the Cl^{-1} ion was found to determine the capacitance of the C_1 layer. The distance $d_1 \leq \approx 6.9$ Å would be lead to the picture in which Cl^{-1} is bound as a primary hydrated ion at the interface. However, if the value of the relative dielectric constant is half way between that of water (ε_r=78) and goethite (ε_r=11), the capacitance C_1 of 1 F/m^2 is equivalent with $d_1 \approx 4$ Å. In that case, the Cl^{-1} ion is directly coordinating to the surface groups. A distance of about 4 Å corresponds with the radius of Cl^{-1} (1.8 Å) plus the distance of half a water molecule.

This representation is given in Figure 4. The given representation gives more credit to the idea that considerable ion pair formation is stimulated by local electrostatic forces, which are larger when the opposite charges are as close as possible together. Recently, Predota et al. (Predota *et al.*, 2004) have simulated with molecular dynamics the binding of Cl^{-1} at the TiO_2 solid-solution interface. They found that the Cl^{-1} ions were directly coordinating with the surface groups.

The K^{+1} ion is found to determine the largest minimum distance of approach ($d= d_1+d_2$). This distance may relate to $d_1+d_2 \leq 4+7.7 \approx 12$ Å. The size of the second Stern layer ($d_2 \leq 7.7$ Å) might imply that the large electrolyte ions (K^{+1}, Rb^{+1}, Cs^{+1}) ions remain hydrated with a sheet of primary and secondary water molecules. The total distance can be explained as the sum of the ionic radius of the electrolyte ion (r = 1.33, 1.47, 1.67 Å) and the size of two water molecules (5.6 Å). The position is given in Figure 4.

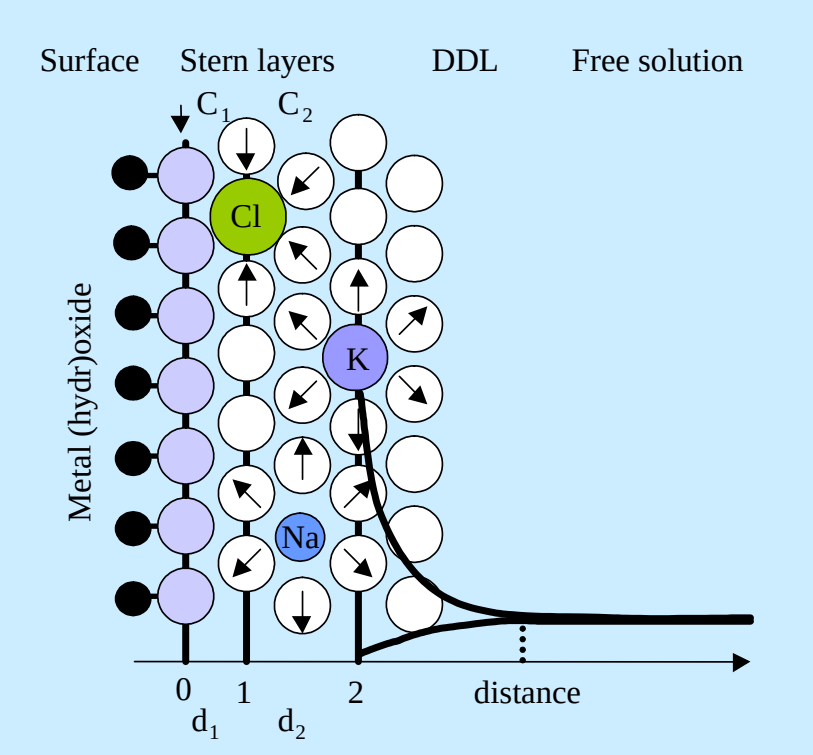

Figure 4. The double layer structure based on the interpretation of the CD of outersphere complexes (Cl^{-1}, K^{+1}, Na^{+1}) in the compact part of the double layer of metal (hydr)oxides in case the inner and outer Stern layer have a different dielectric constant.

The Na^{+1} and Li^{+1} ions were found to distribute their charge about equally over the 1- and 2-plane (Table 1). It indicates that both ions have a position that is intermediate between the Cl^{-1} ion and the K^{+1} ion. Interpretation of this conclusion

points to the presence of Na^{+1} and Li^{+1} in the double layer which is hydrated with primary water molecules, but stays at a larger distance of the surface than Cl^{-1}, due to the maintenance of a hydration shell of ions (Figure 4). The Cl^{-1} ion coordinates primarily in the above picture with the surface groups in contrast to Na^{+1}.

In this double layer picture, also the location of the anions can be indicated (Figure 5). For NO_3^{-1}, the charge distribution factor indicates that a considerable part of the charge (2/3) is in the 1-plane. This might imply that NO_3^{-1} partly penetrates into the layer where also the Cl^{-1} ion is bound. This might be with one or two ligands. We have also modeled the charge distribution of ClO_4^{-1}. Like Na^{+1}, this ion has a charge distribution in which the charge is about equally distributed over the 1- and 2-plane. This might be interpreted as a structure in which the bound ClO_4^{-1} keeps a layer of primary water molecules (Figure 5).

In the double layer picture of Figure 5, the maximum distance between surface and outersphere complexes is about 12 Å. The minimum distance between surface and outersphere complexes is 4 Å.

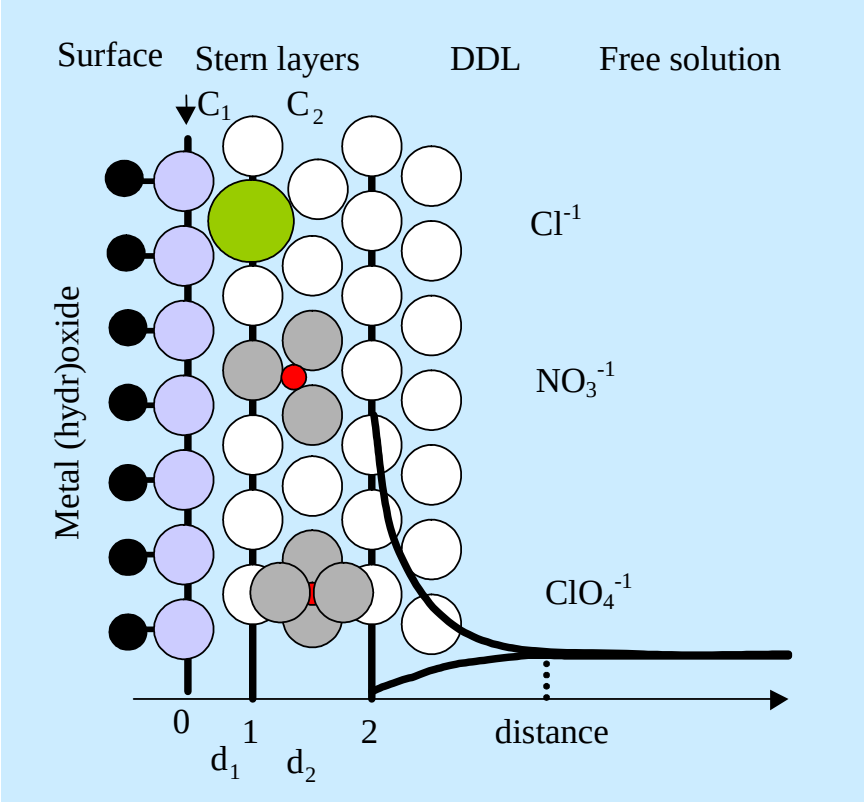

Figure 5. The double layer structure based on the interpretation of the CD of outersphere complexes of anions (Cl^{-1}, NO_3^{-1}, and ClO_4^{-1}) in the compact part of the double layer of metal (hydr)oxides.

Conclusions

- The minimum distance of approach of adsorbed ions depends on the finite size of ions and their degree of hydration, which determine their relative distances to the surface of minerals.
- The TP model can be used as a framework to accommodate the ion pairs within the Stern layer, while their charge is distributed spatially between two electrostatic planes. This indicates that ion pairs are not treated as point charges at the solid-solution interface of minerals anymore.
- The relative attribution of the charge of electrolyte ions to the 1-plane is proportional with their size; a smaller distance of closest approach leads to better screening of the surface charge affecting the pH dependent surface charging.
- The capacitance of inner Stern layer is determined by the minimum distance of approach of the ion closest to the surface, while the capacitance of the outer layer is determined by the minimum distance of approach of the ion furthest away from the surface.

Acknowledgments

The authors thank the Ministry of Science, Research, and Technology of Iran (MSRT) for financial support and Mr. A Korteweg (Laboratory of Physical and Colloid Chemistry) for the BET analysis.

References

Atkinson, R. J., P. A.M., and J. P. Quirk (1967). Adsorption of potential-determining ions at the ferric oxide-aqeous electrolyte interface. *J. Physic. Chem.* **71**: 550.

Barron, V., and J. Torrent (1996). Surface hydroxyl configuration of various crystal faces of hematite and goethite. *J. Colloid Interface Sci.* **177**(2): 407.

Borkovec, M. (1997). Origin of 1-pk and 2-pk models for ionizable water-solid interfaces. *Langmuir* **13**(10): 2608.

Bourikas, K., T. Hiemstra, and W. H. Van Riemsdijk (2001). Ion pair formation and primary charging behavior of titanium oxide (anatase and rutile). *Langmuir* **17**(3): 749.

Breeuwsma, A., and J. Lyklema (1973). Physical and chemical adsorption of ions in electrical double-layer on hematite (alpha-fe2o3). *J. Colloid Interface Sci.* **43**(2): 437.

Chapman, D. L. (1913). A contribution to the theory of electrocapillarity. *Philos. Mag.* **6**(25): 475.

Davis, J. A., R. O. James, and J. O. Leckie (1978). Surface ionization and complexation at the oxide/water interface. 1. Computation of electrical double layer properties in simple electrolytes. *J. Colloid Interface Sci.* **63**: 480.

Fenter, P., L. Cheng, S. Rihs, M. Machesky, M. J. Bedzyk, and N. C. Sturchio (2000). Electrical double-layer structure at the rutile-water interface as observed in situ with small-period x-ray standing waves. *J. Colloid Interface Sci.* **225**(1): 154.

Gouy, G. (1910). Sur la constitution de la charge electrique a la surface d'un electrolyte. *Ann. Phys. (Paris) Ser.* **4**(9): 457.

Grahame, D. C. (1947). The electrical double layer and the theory of electrocapillarity. *Chem. Rev.* **41**(3): 441.

Gustafsson, J., P. Mikkola, M. Jokinen, and J. B. Rosenholm (2000). The influence of ph and nacl on the zeta potential and rheology of anatase dispersions. *Colloid Surf. A-Physicochem. Eng. Asp.* **175**(3): 349.

Hiemstra, T., J. C. M. Dewit, and W. H. Vanriemsdijk (1989a). Multisite proton adsorption modeling at the solid-solution interface of (hydr)oxides - a new approach .2. Application to various important (hydr)oxides. *J. Colloid Interface Sci.* **133**(1): 105.

Hiemstra, T., and W. Van Riemsdijk (2002). Hydrolysis of surface complexes in relation to the microscopic surface structure of adsorbed ions. *Abstr. Pap. Am. Chem. Soc.* **223**: 097.

Hiemstra, T., and W. H. Van Riemsdijk (2000). Fluoride adsorption on goethite in relation to different types of surface sites. *J. Colloid Interface Sci.* **225**(1): 94.

Hiemstra, T., and W. H. Vanriemsdijk (1996). A surface structural approach to ion adsorption: The charge distribution (cd) model. *J. Colloid Interface Sci.* **179**(2): 488.

Hiemstra, T., W. H. Vanriemsdijk, and G. H. Bolt (1989b). Multisite proton adsorption modeling at the solid-solution interface of (hydr)oxides - a new approach .1. Model description and evaluation of intrinsic reaction constants. *J. Colloid Interface Sci.* **133**(1): 91.

Hiemstra, T., P. Venema, and W. H. Vanriemsdijk (1996). Intrinsic proton affinity of reactive surface groups of metal (hydr)oxides: The bond valence principle. *J. Colloid Interface Sci.* **184**(2): 680.

Israelachvili, J. N. (1991). Intermolecular and surface forces London [etc.] Academic Press

Kinniburgh, D. G., C. J. Milne, and P. Venema (1995). Design and construction of a personal-comupter-based automatic titrator. *Soil Sci. Soc. Am. J.* **59**(2): 417.

Kosmulski, M., and E. Matijevic (1992). Formation of the surface-charge on silica in mixed-solvents. *Colloid Polym. Sci.* **270**(10): 1046.

Kosmulski, M., and J. B. Rosenholm (1996). Electroacoustic study of adsorption of ions on anatase and zirconia from very concentrated electrolytes. *J. Phys. Chem.* **100**(28): 11681.

Lutzenkirchen, J. (1998). Comparison of 1-pk and 2-pk versions of surface complexation theory by the goodness of fit in describing surface charge data of (hydr)oxides. *Environ. Sci. Technol.* **32**(20): 3149.

Mcinnes, D. A. (1961). The principles of electrochemistry. New York, Dover publications Inc.

Pauling, L. (1929). The principles determining the structure of complex ionic crystals. *J. Am. Chem. Soc.* **51**: 1010.

Predota, M., A. V. Bandura, P. T. Cummings, J. D. Kubicki, D. J. Wesolowski, A. A. Chialvo, and M. L. Machesky (2004). Electric double layer at the rutile (110) surface. 1. Structure of surfaces and interfacial water from molecular dynamics by use of ab initio potentials. *J. Phys. Chem. B* **108**(32): 12049.

Rahnemaie, R., T. Hiemstra, and W. H. Van Riemsdijk (Ch 3). Inner- and outersphere complexation of ions at the goethite-solution interface.

Rietra, R., T. Hiemstra, and W. H. Van Riemsdijk (1999). Sulfate adsorption on goethite. *J. Colloid Interface Sci.* **218**(2): 511.

Rietra, R., T. Hiemstra, and W. H. Van Riemsdijk (2000). Electrolyte anion affinity and its effect on oxyanion adsorption on goethite. *J. Colloid Interface Sci.* **229**(1): 199.

Rowlands, W. N., R. W. Obrien, R. J. Hunter, and V. Patrick (1997). Surface properties of aluminum hydroxide at high salt concentration. *J. Colloid Interface Sci.* **188**(2): 325.

Rustad, J. R., A. R. Felmy, and B. P. Hay (1996). Molecular statics calculations of proton binding to goethite surfaces: A new approach to estimation of stability constants for multisite surface complexation models. *Geochim. Cosmochim. Acta* **60**(9): 1563.

Sahai, N., and D. A. Sverjensky (1997). Evaluation of internally consistent parameters for the triple-layer model by the systematic analysis of oxide surface titration data. *Geochim. Cosmochim. Acta* **61**(14): 2801.

Sparks, D. L. (1999). Soil physical chemistry Boca Raton [etc.] CRC Press

Stern, O. (1924). Zur theory der electrolytischen doppelschicht. *Z. Electrochem* **30**: 508.

Venema, P., T. Hiemstra, and W. H. Vanriemsdijk (1996). Multisite adsorption of cadmium on goethite. *J. Colloid Interface Sci.* **183**(2): 515.

Weidler, P. G., S. J. Hug, T. P. Wetche, and T. Hiemstra (1998). Determination of growth rates of (100) and (110) faces of synthetic goethite by scanning force microscopy. *Geochim. Cosmochim. Acta* **62**(21-22): 3407.

Weidler, P. G., T. Schwinn, and H. E. Gaub (1996). Vicinal faces on synthetic goethite observed by atomic force microscopy. *Clays Clay Miner.* **44**(4): 437.

Westall, J., and H. Hohl (1980). Comparison of electrostatic models for the oxide-solution interface. *Advances in Colloid and Interface Science* **12**(4): 265.

Yates, D. E. (1975). The structure of the oxide/aqueous electrolyte interface. Ph.D. Thesis,, University of Melbourne.

Yates, D. E., S. Levine, and T. W. Healy (1974). Site-binding model of the electric double layer at the oxide/water interface. *J. Chem. Soc. Faraday Trans.* **70**: 1807.

3

Inner- and Outersphere Complexation of Ions at the Goethite-Solution Interface

Abstract

Formation of inner- and outersphere complexes of environmentally important divalent ions on the goethite surface was examined applying the charge distribution CD model for inner- and outersphere complexation. The model assumed spatial charge distribution between the surface (0-plane) and the next electrostatic plane (1-plane) for innersphere complexation and between the 1-plane and the head end of diffuse double layer (2-plane) for the outersphere complexation. This approach has been used because the distance of closest approach to a charged surface differs for different ions. This new approach has been applied to describe the adsorption of magnesium, calcium, and sulfate. It has been shown that the concept can successfully describe the development of surface charge in the presence of these ions as a function of pH, loading, salt level, and also the shift in the isoelectric point (IEP) of goethite. This surface structural approach leads to the use of a Three Plane model for the compact part (Stern layer) of solid-solution interface, which is divided into two layers. The thickness of each layer depends on the capacitance and the local dielectric constant.

Keywords: Diffuse double layer; Basic Stern; Three Plane model; Adsorption; Electrolyte ions; Calcium; Magnesium; Sulfate; Iron oxide; Goethite; CD model; MUSIC model

Introduction

Mineral surfaces may be charged due to adsorption or desorption of protons by surface oxygens. Based on the principle of electroneutrality, the surface charge must be compensated by accumulation of counter-ion and depletion of co-ions in the solution near the surface. This structure is known as the diffuse double layer (DDL) (Gouy, 1910), (Chapman, 1913).

Electrolyte ions like Na^{+1}, K^{+1}, NO_3^{-1}, and Cl^{-1} may exhibit ion-specific weak interactions. This phenomenon is known as ion pair formation (Yates, 1975), (Davis *et al.*, 1978) and the complexes are named outersphere complexes. The affinity for various monovalent electrolyte cations and anions like Li^{+1}, Na^{+1}, K^{+1}, Cs^{+1}, Cl^{-1}, NO_3^{-1}, and ClO_4^{-1} can be derived using consistent sets of titration data (Rietra *et al.*, 2000), (Bourikas *et al.*, 2001), (Rahnemaie *et al.*, Ch 2).

In natural systems like soils, sediments, and fresh waters, dominant electrolyte ions may be Ca^{+2}, Mg^{+2} and SO_4^{-2}. These ions have a larger interaction with the mineral surfaces than monovalent ions (Breeuwsm and Lyklema, 1973), (Ridley *et al.*,

1999), (Pochard *et al.*, 2002), (Criscenti and Sverjensky, 1999). This can be due to the formation of innersphere complexes. For instance, it has been shown with in situ-FTIR analysis that sulfate may be adsorbed as innersphere surface complexes. However, under certain conditions, the same ions are also bound as outersphere surface complexes (Wijnja and Schulthess, 2000), (Peak *et al.*, 1999). For Sr^{+2}, a similar behavior is found. It has been shown with EXAFS (Collins *et al.*, 1998), (Sahai *et al.*, 2000) that this divalent ion may form innersphere complexes as well as outersphere complexes. It is possible that this behavior is also found for Ca^{+2} and Mg^{+2} ions. In the present study, we will analyze the interaction of $Mg(NO_3)_2$ and $Ca(NO_3)_2$ with goethite.

The compact part of the double layer is crucial in interface chemistry because there the potential changes strongly over small distances. Rahnemaie et al. (Rahnemaie *et al.*, Ch 2) have used a charge distribution model to derive the location of monovalent ion pairs. In the modeling, the charge of the ions has been allowed to be distributed between two electrostatic positions in the compact part of the double layer (Three plane approach). The derived charge distributions show that the Cl^{-1} ion is most closely located to the surface, followed by NO_3^{-1} at a slightly more outward position and ClO_4^{-1} ion, being located somewhere between both defined electrostatic planes. The Na^{+1} ion was also found at an intermediate position between these two electrostatic planes, while the large ions like K^{+1} and Cs^{+1} are found to be present at the largest distance.

In the present study, we will analyze the position of Mg^{+2} and Ca^{+2} ions in a similar way. However, for these ions we will also have to account for the possibility that these cations will form innersphere as well as outersphere complexes. Both adsorption phenomena will be treated with the charge distribution CD approach for inner- and outersphere surface complexation (Rahnemaie *et al.*, Ch 2). This model approach will also be applied to the binding of SO_4^{-2}, using data of Rietra et al. (Rietra *et al.*, 1999b). In the model approach, the surface charging is described with the MUSIC model approach (Hiemstra and VanRiemsdijk, 1996). Parameters and details have been described by Rahnemaie et al. (Rahnemaie *et al.*, Ch 2).

Material and methods

The experiments were done using a goethite suspension that was prepared based on the method of Atkinson et al. (Atkinson *et al.*, 1967), as described in detail by Hiemstra et al. (Hiemstra *et al.*, 1989). The BET(N_2) specific surface area of goethite was determined at 98.6 $m^2\ g^{-1}$.

The charging behavior of goethite in the presence of calcium and magnesium ions was measured using titration experiments. For an accurate interpretation of the data in various electrolytes, it is essential that all charging data are measured relatively to each other in a consistent manner. This was achieved by doing all titrations using an acidified salt-free stock suspension, from which sub-samples were taken for the various experiments. This assures that the initial surface charge of the goethite can serve as the reference charge point. The reference stock suspension was prepared by acidifying a salt-free suspension of goethite to pH 3.55 and purging it continuously with purified N_2 to remove (bi)carbonate.

Certain amounts of a specified salt solution were added to the series of individual batches of goethite suspension. This leads to a fixed concentration of goethite (16.52 g l^{-1}) for the series of titrations in different background electrolyte ions. Each batch of goethite suspension, which contained a known amount of a specified salt, was titrated from its initial pH to a pH of about 10.5. With this approach individual one way titrations were done for different concentrations of 0.05, 0.10 and 0.20 M $Mg(NO_3)_2$, and 0.10 and 0.20 M $Ca(NO_3)_2$. Each titration was started after equilibrium for half an hour and each data point was collected 15 minutes after an addition, when the drift was lower than 0.02 mV min^{-1}. It is important to note that the maximum pH range of titration in $Mg(NO_3)_2$ was smaller to prevent any precipitation of magnesium as magnesium hydroxide.

The goethite stock suspension was acidified with a small amount of 1 M HNO_3, and the titrations were done with 0.100 M NaOH. This procedure introduces small amounts of Na^{+1} and NO_3^{-1} ions. Actually, these concentrations are negligible when compared with the background electrolyte level of Ca^{+2} and Mg^{+2}. However, the amount of these two ions was calculated for each data point and taken into account in the modeling.

Results and discussion

Treatment of goethite titration data

For each addition of base, a change in surface charge can be calculated relatively to the starting point of the titration. Figure 1 illustrates as an example the relative surface charge of goethite in a 0.2 molar solutions of calcium and magnesium nitrate which are compared with data for other electrolyte ions (Rahnemaie *et al.*, Ch 2). The data in Figure 1 show that the charging curves are strongly different for

different cations. This is due to a different electrostatic interaction with the proton charge at the surface. The effect is stronger for the divalent cations like calcium and magnesium than monovalent ions. This stronger contribution to the surface charge is partly due to a better screening of the surface charge of divalent ions compare to monovalent ions. However, the large difference between Mg^{+2} and Ca^{+2} also points to specific chemical effects due to the formation of chemical bonds with surface groups, leading to outersphere and/or innersphere complexes for both divalent ions (to be discussed later).

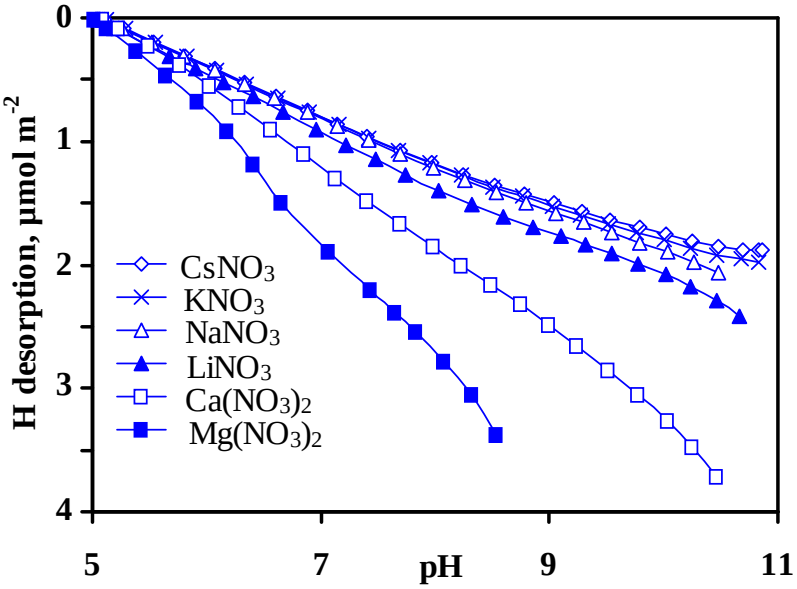

Figure 1. The relative surface charge of goethite as affected by the type of cations of the background electrolytes (0.2 M) used. The different symbols on the figure show the exact measured values and the lines are interpolation between the experimental data.

The above H^{+1} desorption is known on a relative adsorption scale. Classically, titration data are transformed to an absolute scale by using the common intersection point (CIP) of titrations at different electrolyte concentrations. In case of symmetrical ion pair formation or in absence of ion pair formation, the common intersection point (CIP) of the titration data coincides with the pristine point of zero charge (PPZC). This enables transformation of the relative surface charge of goethite to an absolute scale. The data of Figure 1 show that the affinity of ion pairs may be unequal. This implies that the PPZC can no longer be experimentally obtained unequivocally with these electrolyte ions as background salt. The uncertainty in PZC increases proportional with the difference in the affinity between the cation and the anion of the background salt. Preliminary analysis of the titration data in monovalent electrolytes (Rahnemaie *et al.*, Ch 2) shows that the affinity for sodium and chloride ions differed the least. Therefore,

the goethite surface charge was scaled from the relative to the absolute charge using the CIP charge in NaCl (Rahnemaie *et al.*, Ch 2).

Model approach

The titration data in calcium and magnesium nitrate was modeled allowing the formation of innersphere as well as outersphere complexes. We applied the charge distribution (CD) approach for inner- and outersphere surface complexation (Rahnemaie *et al.*, Ch 2). The charge for the innersphere complexes can be distributed between the surface and the first plane (Hiemstra and VanRiemsdijk, 1996). The charge of the outersphere complexes is distributed in the second Stern layer (Rahnemaie *et al.*, Ch 2).

The charge distribution of the innersphere complexes can be coupled to the structure of the complexes at the surface, in particular to the relative number of ligands that are involved in the chemical binding (Rietra *et al.*, 1999a). In case of hexa-coordination of calcium and magnesium ions and equal distribution of charge over the bonds, the Pauling bond valence is +0.33 v.u. It implies that the formation of a monodentate surface complex would have approximately a CD value of Δz_o=0.33 v.u. and Δz_1=1.67 v.u. In case of a bidentate complex the CD values are approximately Δz_0=0.67 v.u. and Δz_1=1.33 v.u. In this paper, the reactions will be formulated based on the CD value found in the modeling.

The fitted charge distribution of any calcium and magnesium outersphere complexes will reveal the relative position of these ions. The capacitance of the inner and outer Stern layer and the affinity constants were taken from Rahnemaie et al. (Rahnemaie *et al.*, Ch 2) as given in Table 1.

Table 1. The CD values and the affinity constants of adsorbed sodium and nitrate on goethite, and the capacitance of inner and outer Stern layer as derived from modeling of titration data using the CD model of outersphere complexation (Rahnemaie *et al.*, Ch 2).

Ions	Δz_0	Δz_1	Δz_2	log K
Na^{+1}	0	0.50	0.50	-0.27
NO_3^{-1}	0	-0.67	-0.33	-0.53
C_1 F m^{-2}	1.00			
C_2 F m^{-2}	0.89			

Interaction of Mg^{+2}

The adsorption mechanism of calcium and magnesium on goethite has not yet been studied by spectroscopy. However, the electronic properties of these two ions are related to strontium. Spectroscopic measurements for strontium has revealed that at high pH the Sr^{+2} ion is adsorbed as an innersphere surface complex and at a lower pH as an outersphere surface complex (Collins *et al.*, 1998), (Sahai *et al.*, 2000).

The data for the titration of goethite in magnesium nitrate solution are given in Figure 2. A very large interaction exists, which is typical for innersphere complexation. One may illustrate the importance in a semi-quantitative manner assuming an estimated proton co-desorption value of $\Delta\Gamma_H/\Delta\Gamma_{Mg}$=1-1.5 for the specific Mg binding. Based on this ratio, a measured $\Delta\Gamma_H$ of 3 μmol m^{-2} is equivalent with $\Delta\Gamma_{Mg}$ = 3-4.5 μmol m^{-2}. The calculation shows that in the system, the amount of specifically adsorbed Mg^{+2} (Γ_{Mg}) can be very high. This high specific adsorption is especially due to the high magnesium concentrations ($0.5\text{-}2\times10^{-1}$ M) used in the titrations. The high magnesium loading will increase the particle charge considerable. As a result, hydrolysis of the adsorbed Mg^{+2} ion is stimulated. We found indeed that the description of the titration was not possible without the assumption of formation of a hydrolyzed complex ($MgOH^{+1}$ adsorption). This complex is important at the highest pH values.

In the modeling, the magnesium adsorption reactions were formulated based on the formation of an innersphere and an outersphere complex. The CD values and log K values were fitted using the titration data. The results show that only innersphere complexation is needed to describe the data. The description of the data cannot be improved by the introduction of outersphere complexation. This indicates that under the current experimental conditions innersphere complexation is dominant. As will be discussed below, outersphere complexation may occur under other conditions. The absence of outersphere complexation under these conditions can be understood based on electrostatics. The introduction of much positive charge due to innersphere complexation of magnesium ions creates a relatively high change in the potential in the 1- and 2-plane. These potential changes will suppress the formation of outersphere complexes due to lower attraction or increased repulsion.

In Table 2, the parameters of the modeling are given. The modeling revealed the charge distribution of the innersphere magnesium complexes as Δz_o=0.6 v.u. and Δz_1=-1.4 v.u. This can be interpreted as formation of a bidentate surface complex, which in the most simple picture, as discussed before, is expected to result in Δz_0=0.67 v.u. and Δz_1=-1.33 v.u. As estimated above, the specific magnesium adsorption is very high, which implies that the description of the data is sensitive to the number of sites

involved. A good description was possible if we allowed the magnesium to form innersphere complexes with singly as well as triply coordinated surface groups. To minimize the number of parameters, we assumed the same affinity constant. The following reactions were formulated:

$$2 \equiv FeOH^{-1/2} + Mg^{+2}(OH_2)_x \Leftrightarrow \equiv (FeOH)_2^{-1+\Delta z_o} Mg(OH_2)_{x-2}^{\Delta z_1} + 2H_2O \quad [1]$$

$$2 \equiv FeOH^{-1/2} + Mg^{+2}(OH_2)_x \Leftrightarrow \equiv (FeOH)_2^{-1+\Delta z_o} MgOH(OH_2)_{x-3}^{\Delta z_1 - 1} + H^{+1} + 2H_2O \quad [2]$$

$$2 \equiv Fe_3O^{-1/2} + Mg^{+2}(OH_2)_x \Leftrightarrow \equiv (Fe_3O)_2^{-1+\Delta z_0} Mg(OH_2)_{x-2}^{\Delta z_1} + 2H_2O \quad [3]$$

$$2 \equiv Fe_3O^{-1/2} + Mg^{+2}(OH_2)_x \Leftrightarrow \equiv (Fe_3O)_2^{-1+\Delta z_o} MgOH(OH_2)_{x-3}^{\Delta z_1 - 1} + H^{+1} + 2H_2O \quad [4]$$

It is also possible that the magnesium bidentate complex is formed from the combination of a $FeOH^{-1/2}$ and a $Fe_3O^{-1/2}$ surface group. It is interesting to note that the adsorption of magnesium has shifted the IEP of the goethite to 5.4 (Figure 2).

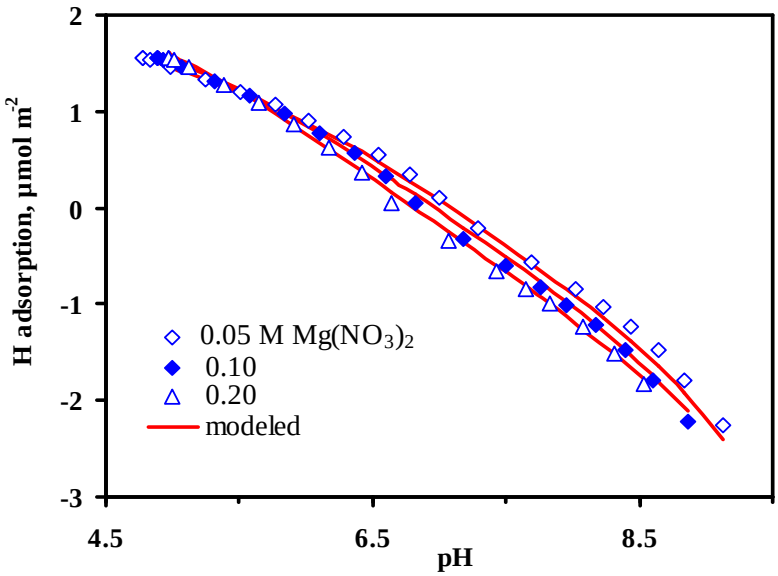

Figure 2. The experimental goethite titration data and model description in presence of $Mg(NO_3)_2$.

Based on the difference in log K values for the reactions [1] and [2] or [3] and [4], one can calculate the log K value for the protonation of the OH ligand in the hydrolyzed surface complex. The log K_H value is equal to 10.7. The value is rather close to the value found for the protonation of $MgOH^{+1}$(aq), which has a log K_H value of 11.5.

Table 2. The affinity constants of interaction of magnesium and calcium ions with goethite as derived from modeling of the goethite titration data using the charge distribution model of the outersphere complexes over the 1- and 2-plane.

Ions	Δz_0	Δz_1	Δz_2	log K
Mg^{+2}-is[a]	0.60 ± 0.02[b]	1.40 ± 0.02	0	4.39 ± 0.03
$MgOH^{+1}$-is	0.60 ± 0.02[b]	1.40-1± 0.02[c]	0	-6.37 ± 0.09
Mg^{+2}-os[a]	-	-	-	-
Ca^{+2}-is	0.22 ± 0.02[d]	1.78 ± 0.02	0	3.21 ± 0.07
$CaOH^{+1}$-is	0.22 ± 0.02[d]	1.78-1± 0.02[c]	0	-8.52 ± 0.16
Ca^{+2}-os	0	2[e]	0	3.15 ± 0.02

a. The suffixes is and os stand respectively for the innersphere and outersphere surface complex.
b. The charge of both magnesium surface species was set equal.
c. Hydrolysis of a water ligand (deprotonation) results in a release of 1 v.u.
d. The charge of both calcium surface species was set equal.
e. The charge was placed by definition since the model showed that almost the total charge remains at this plane.

Interaction of Ca^{+2}

In Figure 3, the titration data in 0.1 and 0.2 M calcium nitrate are given. The titration data in magnesium nitrate are also represented for comparison. It shows that the concentration dependency of surface charge for Ca^{+2} is significantly smaller than for Mg^{+2}. Probably, this is due to the lower affinity of Ca^{+2} in comparison with Mg^{+2}.

The above model approach for Mg^{+2} was also applied to Ca^{+2}. For Ca^{+2}, we came also to the conclusion that the data can be described using only innersphere complexes. For the conditions studied (0.1-0.2 M), the description of the data was not sensitive to the introduction of outersphere complexes.

The titration data in calcium nitrate can be described using only the adsorption of Ca^{+2}. However, the quality of the fit benefited from introduction of hydrolysis. The difference in the affinity constant of the reactions (Table 2) showed that the corresponding protonation reaction of the hydrolyzed calcium species was log K_H=11.6. The value is rather close to the value found for the protonation of $CaOH^{+1}$(aq), which has a log K_H value of 12.5.

A remarkable difference between Ca^{+2} and Mg^{+2} adsorption was the much lower CD value for Ca^{+2}. It may point to another binding mechanism. In Table 2, the parameters of the modeling are given. The charge distribution of the innersphere

calcium complexes are Δz_0=0.22 v.u. and Δz_1=-1.78 v.u. This can be interpreted as formation of a monodentate surface complex, which in the most simple picture is expected to result in Δz_0=0.33 v.u. and Δz_1=-1.67 v.u. The low CD value leads to the formulation of the following reactions:

$$\equiv FeOH^{-1/2} + Ca^{+2}(OH_2)_x \Leftrightarrow \equiv FeOH^{-1/2+\Delta z_0}Ca(OH_2)_{x-1}^{\Delta z_1} + H_2O \quad [5]$$

$$\equiv FeOH^{-1/2} + Ca^{+2}(OH_2)_x \Leftrightarrow \equiv FeOH^{-1/2+\Delta z_0}CaOH(OH_2)_{x-2}^{\Delta z_1 - 1} + H^{+1} + H_2O \quad [6]$$

$$\equiv Fe_3O^{-1/2} + Ca^{+2}(OH_2)_x \Leftrightarrow \equiv Fe_3O^{-1/2+\Delta z_0}Ca(OH_2)_{x-1}^{\Delta z_1} + H_2O \quad [7]$$

$$\equiv Fe_3O^{-1/2} + Ca^{+2}(OH_2)_x \Leftrightarrow \equiv Fe_3O^{-1/2+\Delta z_0}CaOH(OH_2)_{x-2}^{\Delta z_1 - 1} + H^{+1} + H_2O \quad [8]$$

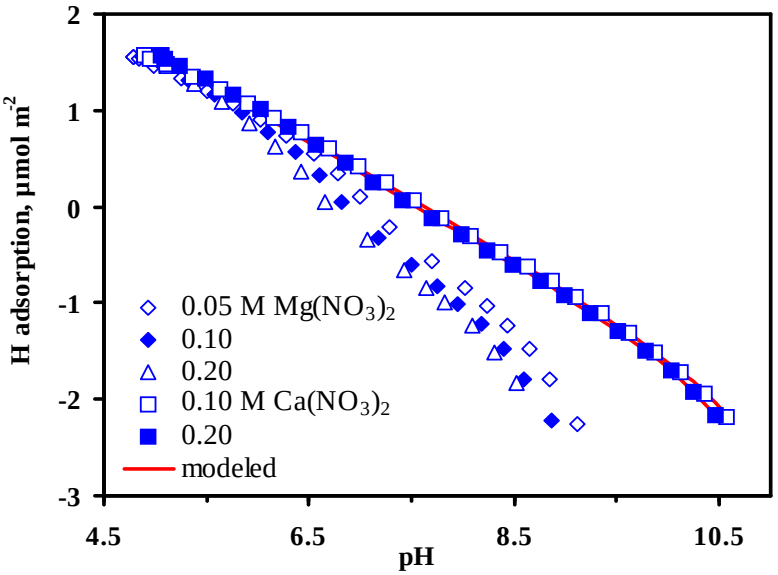

Figure 3. Goethite titration data in $Ca(NO_3)_2$ and model description as a function of pH and calcium concentration. The titration data in magnesium nitrate are included for comparison purpose.

It is important to stress that the absence of outersphere complexation in our experiments does not imply that this phenomenon does not exists for both ions. With calculations, it can be shown that outersphere complexation becomes relatively more important at a low loading. Since our concentrations are relatively extreme in comparison to concentration used in adsorption experiments (10^{-5}-10^{-3} M), another type of experiments is necessary to probe and parameterize this potential adsorption mechanism.

Outersphere Ca -adsorption

Rietra et al. (Rietra *et al.*, 2001b) have studied the adsorption edges of calcium on goethite in 0.01 and 0.1 M $NaNO_3$. Two different loadings of Ca^{+2} have been used. The equilibrium concentrations in these experiments are very low (Figure 4). Rietra et al. (Rietra *et al.*, 2001b) could model the adsorption data using either an innersphere monodentate surface complex or an innersphere bidentate surface complex alongside an outersphere monodentate. Monodentate complexation is not observed for Sr^{+2} with spectroscopy.

When applying our parameters for innersphere complexation, the data at the low Ca^{+2} level could not be described satisfactorily. However including an outersphere complex leads to a good description of the adsorption data (Figure 4). The fitted CD value for the calcium outersphere complex shows that all charge is situated at the 1-plane (Table 2). Using this result, the titration data in the presence of calcium nitrate (Figure 3) were remodeled. Addition of the outersphere complex, with the parameters found from modeling of the adsorption edge data (Figure 4), did not change the previous model description. It indicates that the titration data are fully dominated by the presence of the innersphere complex.

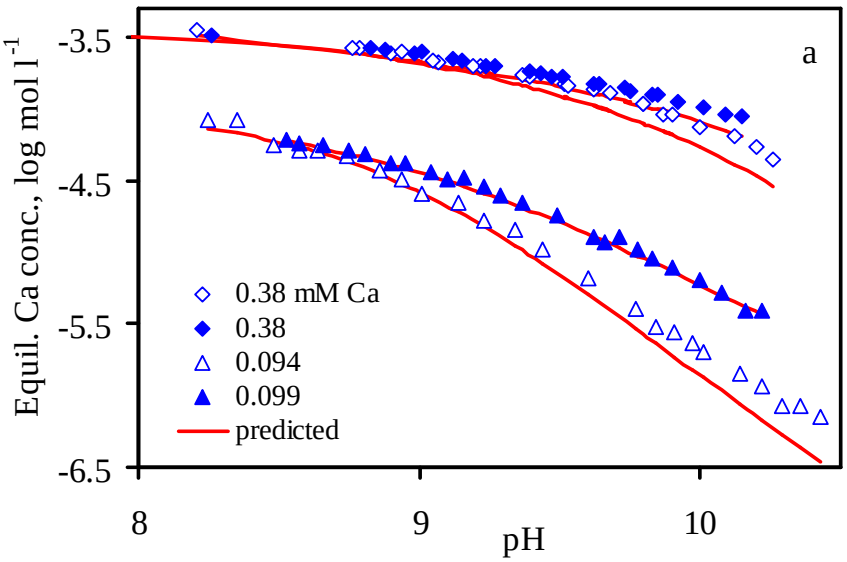

Figure 4. The calcium adsorption edges (Rietra *et al.*, 2001b) in 0.01 (open symbols) and 0.1 M (solid symbols) $NaNO_3$.

With the derived parameters, one can analyze the conditions at which inner- and outersphere complexation takes place. The CD parameters for Ca^{+2} complexes show that the charge for outersphere complexes is at a larger distance from the surface than for innersphere complexes. As pointed out by Rietra et al. (Rietra *et al.*, 2001a), it

implies that the proton co-desorption for innersphere complexes is larger than for outersphere complexes. Based on the thermodynamic principle of consistency, it indicates that the process of innersphere complexation has a stronger pH dependency. If both processes are simultaneously present, the innersphere complexation will become relatively more important when increasing the pH, since this process is most pH dependent. It implies that outersphere complexation will be found at relatively low pH values and is taken over by innersphere complexation at higher pH values.

Although the potential at 0-plane is hardly affected by the adsorption, however analysis of the effect of calcium loading indicates that the potentials in the 1- and 2-plane change strongly when the calcium loading increases lowering the total affinity for binding. Since outersphere complexation has the highest charge attribution to the outer parts of the Stern layer, it means that these complexes experience the largest decrease in total affinity with increasing loading. As a result, the outersphere complexation is suppressed relatively to the innersphere complexation. The change of the speciation with pH is given in Figure 5 for conditions, which normally found in natural systems like soils, i.e. 0.001 M magnesium and calcium in 0.1 M $NaNO_3$.

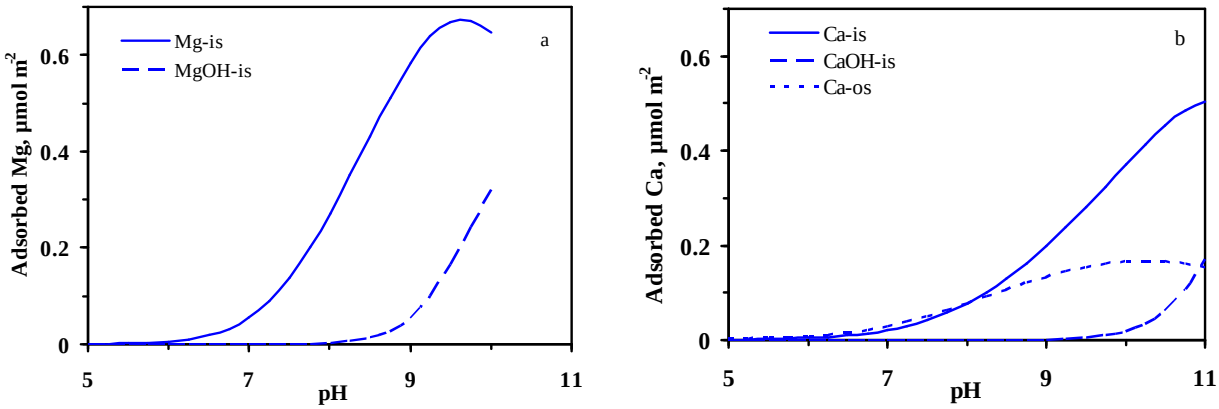

Figure 5. Simulation of (a) magnesium and (b) calcium surface speciation on the goethite using the CD values and affinity constants given in Table 2. The suffixes is and os stand respectively for innersphere and outersphere surface complex.

Interaction of SO_4^{-2}

Sulfate is an important anion in environmental ecosystems. Rietra et al. (Rietra *et al.*, 1999b), (Rietra *et al.*, 2001a) have studied sulfate adsorption on goethite. They concluded that sulfate adsorption can be modeled using either a monodentate innersphere surface complex or a monodentate innersphere alongside a monodentate

outersphere surface complex. The latter option is in agreement with the spectroscopic information (Wijnja and Schulthess, 2000), (Peak *et al.*, 1999). Spectroscopic information shows that sulfate is adsorbed as an innersphere surface complex at low pH. An outersphere surface complex dominates the sulfate adsorption at pH values above 6.

In the present approach, the sulfate adsorption data of Rietra et al. were modeled using the CD approach for inner- and outersphere complexation. The capacitances and ion pair formation constants for the background electrolytes were taken from Rahnemaie et al. (Rahnemaie *et al.*, Ch 2) as given in Table 1.

The model was able to describe sulfate adsorption satisfactorily. The sulfate adsorption affinity and its charge distribution based on this approach are given in Table 3.

The sulfate adsorption was formulated in the model based on the following equations.

$$\equiv FeOH_2^{+1/2} + SO_4^{-2}(aq) \Leftrightarrow \equiv FeO^{+1/2+\Delta z_o}SO_3^{\Delta z_1} + H_2O \qquad [9]$$

$$\equiv FeOH_2^{+1/2} + SO_4^{-2}(aq) \Leftrightarrow \equiv FeOH_2^{+1/2} \cdots {}^{\Delta z_1}SO_4^{\Delta z_2} \qquad [10]$$

in which the … expresses the weak bond in case of outersphere complexation.

Figure 6 presents a simulation of sulfate surface speciation using an innersphere and an outersphere surface complex based on parameters given in Table 3. The simulation is in agreement with spectroscopic information.

Table 3. The CD values and affinity constants of adsorbed sulfate on goethite as derived from modeling of adsorption edges and titration data of Rietra et al. (Rietra *et al.*, 1999b)

Ions	Δz_0	Δz_1	Δz_2	log K
SO_4^{-2}-is[a]	-0.40	-1.60	0	0.54 ± 0.03[c]
SO_4^{-2}-os[a]	0	-2[b]	0	1.45[c]

a. The suffixes is and os stand respectively for the innersphere and outersphere surface complex.
b. The charge was placed by definition since the model showed that almost the total charge remains at this plane.
c. The affinities of inner- and outersphere surface complexes of sulfate were optimized on the data in such a way that the ratio of these two species agrees with estimates based on FTIR analysis (see text).

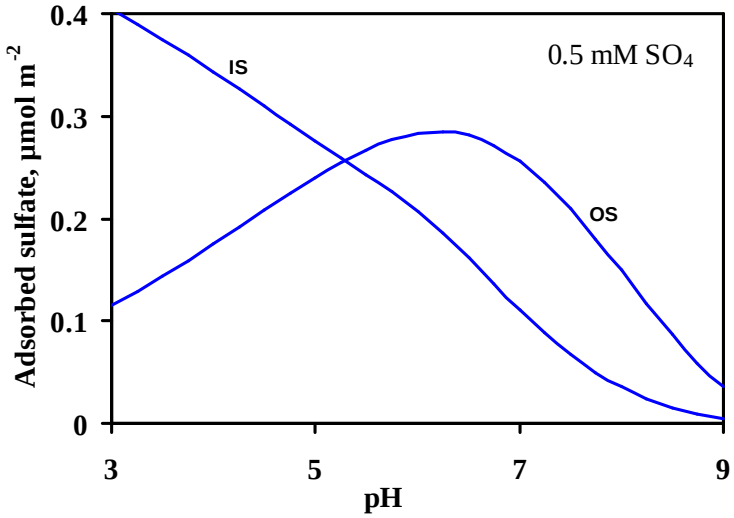

Figure 6. Simulation of sulfate surface speciation on the goethite taking into account a monodentate innersphere and a monodentate outersphere surface complexes. The calculation was done using derived parameters (Table 3) from modeling of sulfate adsorption data of Rietra et al. (Rietra *et al.*, 1999b). The modeling was performed by the CD model for inner- and outersphere complexation in 0.01 M $NaNO_3$.

Location of ions in the double layer profile

Modeling of the data with the CD model for inner- and outersphere complexation shows that the full charge of the outersphere complexes of calcium and sulfate are situated at the 1-plane, i.e. these ions are as close as possible to the surface for outersphere complexes, similar as found for Cl^{-1} ion (Rahnemaie *et al.*, Ch 2). Due to this behavior, the charge of the innersphere and outersphere complexes of Ca^{+2} and of SO_4^{-2} are predominantly present at the same electrostatic position, since the majority of the charge of the innersphere complexes is also present at the 1-plane (Table 2). This characteristic makes it difficult to derive the adsorption parameters unequivocally. For sulfate, the calculation was done in such a way that the model parameters describe satisfactorily the adsorption isotherm data and proton co-adsorption data in presence of sulfate, while ratio of inner- and outersphere surface complexes of sulfate are in accordance with IR spectroscopy information (Figure 6).

The relative location of the ions is indicated in Figure 7. In this picture, it is assumed that the inner Stern layer of the double layer has a lower dielectric constant, resulting in a thickness of about 4 Å. The thickness of the outer Stern layer is about double in size (8 Å). In this layer, outersphere complexes of ions Na^{+1}, NO_3^{-1}, ClO_4^{-1}, K^{+1} and Cs^{+1} are located. See discussion in (Rahnemaie *et al.*, Ch 2).

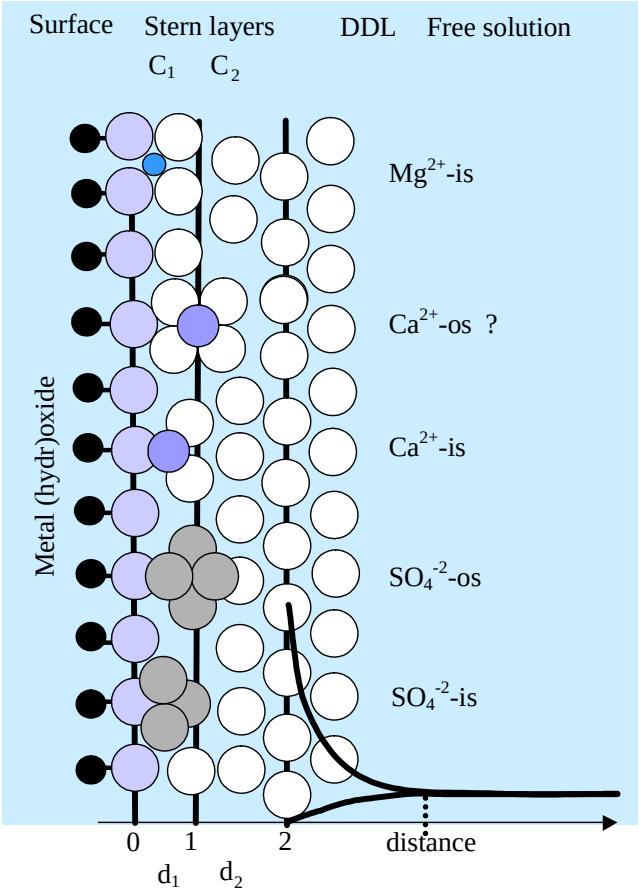

Figure 7. The double layer structure based on the interpretation of the CD of outersphere complexes of Ca^{+2} and SO_4^{-2} and innersphere complexes of Ca^{+2}, Mg^{+2} and SO_4^{-2}.

Conclusions

- The charge distribution model for inner- and outersphere complexation can successfully describe the adsorption of magnesium, calcium, and sulfate on goethite.
- Low ion concentrations and relatively low pH are favorable conditions for the formation of outersphere complexes of magnesium and calcium ions. The formation of outersphere complexes of sulfate ions is stimulated at relatively high pH.
- The minimum distance of approach of the outersphere complexes of calcium and sulfate is relatively close to the surface (1-plane). This makes it difficult to detect the outersphere complexes by ion adsorption modeling, and the spectroscopic information is required to get consistent results.

- High loading of magnesium and calcium on the charged surface favors the deprotonation of a water ligand of the cation.
- The charge distribution values of innersphere complexes of magnesium and calcium ions indicate that magnesium is dominantly adsorbed as a bidentate, while calcium adsorption is dominated by a monodentate surface complex.

Acknowledgments

The authors thank the Ministry of Science, Research, and Technology of Iran (MSRT) for financial support, Mr. A Korteweg (Laboratory of Physical and Colloid Chemistry) for the BET analysis and Mr. Peter Nobels (Soil Quality department) for ICP analysis.

References

Atkinson, R. J., P. A.M., and J. P. Quirk (1967). Adsorption of potential-determining ions at the ferric oxide-aqeous electrolyte interface. *J. Physic. Chem.* **71**: 550.

Bourikas, K., T. Hiemstra, and W. H. Van Riemsdijk (2001). Ion pair formation and primary charging behavior of titanium oxide (anatase and rutile). *Langmuir* **17**(3): 749.

Breeuwsm, A., and J. Lyklema (1973). Physical and chemical adsorption of ions in electrical double-layer on hematite (alpha-fe2o3). *Journal of Colloid and Interface Science* **43**(2): 437.

Chapman, D. L. (1913). A contribution to the theory of electrocapillarity. *Philos. Mag.* **6**(25): 475.

Collins, C. R., D. M. Sherman, and K. V. Ragnarsdottir (1998). The adsorption mechanism of sr2+ on the surface of goethite. *Radiochimica Acta* **81**(4): 201.

Criscenti, L. J., and D. A. Sverjensky (1999). The role of electrolyte anions (clo4-, no3-, and cl-) in divalent metal (m2+) adsorption on oxide and hydroxide surfaces in salt solutions. *Am. J. Sci.* **299**(10): 828.

Davis, J. A., R. O. James, and J. O. Leckie (1978). Surface ionization and complexation at the oxide/water interface. 1. Computation of electrical double layer properties in simple electrolytes. *J. Colloid Interface Sci.* **63**: 480.

Gouy, G. (1910). Sur la constitution de la charge electrique a la surface d'un electrolyte. *Ann. Phys. (Paris) Ser.* **4**(9): 457.

Hiemstra, T., J. C. M. Dewit, and W. H. Vanriemsdijk (1989). Multisite proton adsorption modeling at the solid-solution interface of (hydr)oxides - a new approach .2. Application to various important (hydr)oxides. *J. Colloid Interface Sci.* **133**(1): 105.

Hiemstra, T., and W. H. Vanriemsdijk (1996). A surface structural approach to ion adsorption: The charge distribution (cd) model. *J. Colloid Interface Sci.* **179**(2): 488.

Peak, D., R. G. Ford, and D. L. Sparks (1999). An in situ atr-ftir investigation of sulfate bonding mechanisms on goethite. *J. Colloid Interface Sci.* **218**(1): 289.

Pochard, I., R. Denoyel, P. Couchot, and A. Foissy (2002). Adsorption of barium and calcium chloride onto negatively charged alpha-fe2o3 particles. *J. Colloid Interface Sci.* **255**(1): 27.

Rahnemaie, R., T. Hiemstra, and W. H. Van Riemsdijk (Ch 2). A new surface structural approach to ion adsorption: Tracing the location of electrolyte ions.

Ridley, M. K., M. L. Machesky, D. J. Wesolowski, and D. A. Palmer (1999). Calcium adsorption at the rutile-water interface: A potentiometric study in nacl media to 250 degrees c. *Geochim. Cosmochim. Acta* **63**(19-20): 3087.

Rietra, R., T. Hiemstra, and W. H. Van Riemsdijk (1999a). The relationship between molecular structure and ion adsorption on variable charge minerals. *Geochim. Cosmochim. Acta* **63**(19-20): 3009.

Rietra, R., T. Hiemstra, and W. H. Van Riemsdijk (1999b). Sulfate adsorption on goethite. *J. Colloid Interface Sci.* **218**(2): 511.

Rietra, R., T. Hiemstra, and W. H. Van Riemsdijk (2000). Electrolyte anion affinity and its effect on oxyanion adsorption on goethite. *J. Colloid Interface Sci.* **229**(1): 199.

Rietra, R., T. Hiemstra, and W. H. Van Riemsdijk (2001a). Comparison of selenate and sulfate adsorption on goethite. *J. Colloid Interface Sci.* **240**(2): 384.

Rietra, R., T. Hiemstra, and W. H. Van Riemsdijk (2001b). Interaction between calcium and phosphate adsorption on goethite. *Environ. Sci. Technol.* **35**(16): 3369.

Sahai, N., S. A. Carroll, S. Roberts, and P. A. O'day (2000). X-ray absorption spectroscopy of strontium(ii) coordination - ii. Sorption and precipitation at kaolinite, amorphous silica, and goethite surfaces. *J. Colloid Interface Sci.* **222**(2): 198.

Wijnja, H., and C. P. Schulthess (2000). Vibrational spectroscopy study of selenate and sulfate adsorption mechanisms on fe and al (hydr)oxide surfaces. *J. Colloid Interface Sci.* **229**(1): 286.

Yates, D. E. (1975). The structure of the oxide/aqueous electrolyte interface. Ph.D. Thesis,, University of Melbourne.

4

Phosphate Adsorption on Goethite: Surface Speciation in relation to Charge Distribution

Abstract

Phosphate adsorption on goethite was extensively studied over a wide range of salt concentration, phosphate loading, and pH. The data were modeled using the CD model for inner- and outersphere surface complexation. The CD values were not fitted but were derived using quantum chemical calculation that determines the detailed geometry of phosphate surface complexes. These calculated CD values were relatively close to the values derived using Pauling bond valences, which assume a homogeneous distribution of charge over the ligands. The new approach is especially significant for the protonated bidentate species that shows about 0.2 v.u. charge transfer to the surface in comparison to the first application of the CD model that resulted in about 0.5 v.u. when the CD is fitted. Phosphate adsorption data can successfully be described using the CD model, when the charge distribution of phosphate complexes is constrained by quantum chemical information. However, more surface species are identified compare to a fitted procedure when the CD value is fitted. The new approach shows the presence of a singly and doubly protonated monodentate surface species and a protonated bidentate species in addition to non-protonated mono- and bidentate species. It has been shown that the new surface speciation is in reasonable agreement with FTIR spectroscopic information.

Keywords: Phosphate; Adsorption; Diffuse Double Layer; Basic Stern; Iron oxide; Goethite; CD model; MUSIC model; Surface speciation; Quantum chemistry; IR spectroscopy

Introduction

Metal (hydr)oxides are present in all mineral soils and sediments. The amount of these minerals may vary, but they can have an important effect on the chemical properties of these systems, in particular ion binding.

The surface charge of metal (hydr)oxides is compensated by the adsorbing ions. In natural systems, phosphate and organic acids will strongly interact with metal (hydr)oxides. Phosphate is important since it is a part of the life cycle. Phosphate binds strongly to metal (hydro)oxide surfaces. Therefore, it strongly influences the surface charge properties and colloidal stability. The total concentration of phosphate in solution is usually very low compared to other anions like chloride, sulfate, and bicarbonate. However, even at a very low concentration in the solution, the adsorbed amount of phosphorus on the surface is still relatively high. Therefore, it will always

play an important role at the surfaces of metal hydroxides in natural systems. It indicates that in any application of surface complexation models in natural systems, inclusion of phosphate in the description of data is a prerequisite.

Several surface complexation models have been proposed to describe the phosphate adsorption (Goldberg and Sposito, 1984), (Hawke *et al.*, 1989), (Dzombak and Morel, 1990), (Tadanier and Eick, 2002). Due to the thermodynamic character, in general these models are able to describe quite satisfactorily the macroscopic ion adsorption data in case of a free choice of types of surface species and types of sites. The chosen types of species and sites may not be realistic from the perspective of a spectroscopist. Even if models do describe adsorption data satisfactory, a large variation may exist in *prediction* of ion competition and cooperative adsorption with the various models. One of the main reasons is the very different treatment of the electrostatic interaction, which can be considered as a key factor for a correct description of ion-ion interactions.

A way to improve the quality of surface complexation models is to approach physical reality as far as possible by accounting for structural information. An important advantage of such a model approach is the possibility to validate the adsorption models using spectroscopic derived surface speciation and surface coordination rather than simply make a satisfactory description of macroscopic data. Hiemstra and van Riemsdijk (Hiemstra and VanRiemsdijk, 1996) developed the charge distribution (CD) model, in order to connect the microscopic surface speciation to macroscopic ion adsorption phenomena. In the CD model, an interfacial charge distribution of the adsorbed ions is assumed which is related to the structure of the surface complex as given by spectroscopic information.

Currently, the charge distribution values of various adsorbed ions have been derived from modeling of the adsorption data by considering it as a fitting parameter (Hiemstra and VanRiemsdijk, 1996), (Hiemstra and Van Riemsdijk, 1999), (Rietra *et al.*, 2001), (Hiemstra *et al.*, 2004), (Villalobos *et al.*, 2001), (Arai *et al.*, 2004).

For phosphate, the fitted CD of the non-protonated species ($\equiv Fe_2O_2PO_2$) is almost in agreement with the structural picture of bidentate species (Hiemstra and VanRiemsdijk, 1996). However, the fitted CD value of the protonated bidentate surface species ($\equiv Fe_2O_2POOH$) deviates considerably compare to the expected value based on the homogeneous charge distribution concept of Pauling. It has been interpreted as a shift of charge in the surface complex due to protonation. Based on the Brown bond valence approach (Brown, 2002), (Brown and Altermatt, 1985), such a shift will be connected with a change in the P-O bond length. In the present research, we will use quantum chemical calculations to derive the CD value based on a calculated geometry of the phosphate surface complexes. This geometry will be

interpreted with the Brown bond-valence model, resulting in a calculated charge distribution of the surface complex. The calculated CD values will be used as a constraint in the surface complexation modeling. It implies that only the affinity constants of adsorbed complexes will be optimized. The results will be compared with the situation in which charge distribution values are fitted on the adsorption data.

For the adsorption modeling, we will use a new approach for describing the location and binding of electrolyte ions in the compact part of the double layer (Rahnemaie *et al.*, Ch 2). As shown by Hiemstra and van Riemsdijk (1996), the position of electrolyte ions in the double layer profile is of strong influence on the salt dependency of the phosphate adsorption. Therefore, new PO_4^{-3} adsorption data as a function of pH, loading and electrolyte concentration will be presented. Moreover, the solution speciation of phosphate as a function of the $NaNO_3$ concentration will be critically evaluated.

The results of the CD modeling will be compared with spectroscopic information on PO_4^{-3} binding to iron oxides ((Russell *et al.*, 1974), (Parfitt, 1979), (Tejedor-Tejedor and Anderson, 1990), (Arai and Sparks, 2001)). Since arsenate and phosphate have a very similar behavior in terms of surface and solution chemistry, we will include a discussion on recent EXAFS data concerning the binding of arsenate to goethite (Sherman and Randall, 2003).

Material and methods

Preparation of reagents

To avoid (bi)carbonate contamination, all chemical solutions (Merck p.a.) were made under purified N_2 atmosphere. To be free of silica, these solutions were stored for a short time in polyethylene bottles. The acid solutions were stored in glass bottles, since it was found that the acid solutions can become polluted by release of organic materials in polyethylene bottles. A stock solution of NaOH was prepared CO_2-free from a highly concentrated 1:1 $NaOH/H_2O$. The mixture was centrifuged to remove any solid Na_2CO_3. The sub-sample of supernatant was pipetted into ultra pure water and stored in a desiccator, equipped with a CO_2 absorbing column.

All experiments were performed in polyethylene vessels under N_2 atmosphere. The ultra pure water (≈0.018 dS/m) was used throughout the experiments. It has been pre-boiled to remove dissolved CO_2 before using it in the experiments. The experiments were done in a constant temperature room (20-22 ^oC).

Preparation and characterization of the goethite

The goethite suspension was prepared based on the method of Atkinson et al. (Atkinson *et al.*, 1967), and described in detail by Hiemstra et al. (Hiemstra *et al.*, 1989). A freshly prepared 0.5 M $Fe(NO_3)_3$ was slowly titrated with 2.5 M NaOH to pH 12. The suspension was aged for 4 days at 60°C and subsequently dialyzed in ultra pure water. Before using it in the experiments, the goethite suspension was acidified (pH≈ 5) to desorb and remove the (bi)carbonate, by purging it continuously with N_2 for at least one day. The BET(N_2) specific surface area of goethite equals to 85 $m^2 g^{-1}$.

The surface charge of goethite was measured in $NaNO_3$ solutions. A sample of goethite was titrated forward and backward by base and acid within the pH range of almost 4 to 10.5. The temperature was fixed at 20±0.1 °C using a thermostated reaction cell. The details of the experimental setup and data handing is given elsewhere (Rahnemaie *et al.*, Ch 2).

Phosphate speciation in solution

The solution speciation of phosphate was measured by titration 0, 0.0001, 0.001, and 0.01 M NaH_2PO_4 concentrations in 0.05, 0.1, and 0.5 M $NaNO_3$ and 0.1 M NaH_2PO_4 in 0.5 M $NaNO_3$. The solutions were prepared under N_2 atmosphere. The experiments were done in a 100-ml thermostated reaction vessel at 20±0.1 ^oC under N_2 atmosphere. The titration was carried out in forward and backward pH cycles at fixed salt concentration. In the beginning of the titration, the pH of solution was kept at about 3 for half an hour while purging it with N_2 to remove CO_2.

Phosphate Adsorption edges

Adsorption experiments were performed in individual gas-tight 23.6 ml low-density polyethylene bottles with fixed amounts of salt, goethite, and phosphate at different pH values.

All solutions were added to the bottles under N_2 atmosphere to avoid carbonate contamination. A certain amount of HNO_3 or NaOH was added to the vessels, in order to obtain final pH values within the relevant pH range. $NaNO_3$ was used to fix the salt concentration of suspensions. The final volume of the suspensions was 20 ml. The bottles were equilibrated for 24 hours on the end-over-end shaker. After centrifugation, a sample of the supernatant was taken for phosphate analysis. Phosphate concentration was determined using an optimized molybdate blue method. The pH of suspensions was measured in the re-mixed suspensions under N_2

atmosphere. For each data point, the total concentrations of components of the system were calculated based on a book keeping of the concentrations of the added solutions.

The amount of adsorbed phosphate was calculated from difference between the total initial phosphate concentration and final equilibrium concentration.

Results

Quantum chemical geometry calculations

Fe- Octahedra

The quantum chemical calculations were done with the software of Wavefunction (Spartan'04). As a starting point, we defined a cluster with two Fe oxide octahedra with the appropriate multiplicity (m=11). This cluster served as a template to mimic the goethite mineral. The Fe coordination environment in goethite is asymmetrical and is characterized by two main Fe-O distances in the lattice (≈196 and ≈210 pm). In the calculations, the Fe-O distances and angles of the two octahedra were kept equal to the values found for goethite by Hazemann et al. (Hazemann *et al.*, 1991). The location of the protons in goethite can be derived from the isostructural mineral diaspor (α-AlOOH). It was used to construct the Fe-O octahedra. Additional protons were added to neutralize the structure. These OH bonds point in the direction of the H bridges found in a complete goethite structure. The O-H distances were set at 104 pm. The octahedron is completed with protons that form water molecules at the top and bottom of the octahedra resulting in the zero-charged cluster $Fe_2(OH)_6(OH_2)_4$ (z=0), which is given in Figure 1.

Complexes formation

A series of phosphate complexes were defined by exchanging PO_4^{-3} against one or two of the coordinated H_2O (d Fe-O=196 pm) ligands on top. These exchanged ligands (Figure 1) are equivalent with the singly coordinated surface groups at the 110 face of goethite. It resulted in the monodentate surface complexes $\equiv FeOPO_3$ (z=-3), $\equiv FeOPO_2OH$ (z=-2), and $\equiv FeOPO(OH)_2$ (z=-1), and the bidentate surface complexes $\equiv Fe_2O_2PO_2$ (z=-3) and $\equiv Fe_2O_2POOH$ (z=-2). Figure 2 shows a bidentate phosphate surface complex, which is formed through ligand exchange with the singly coordinated groups.

The lowest (PM3) energy configuration served as a starting point for the later geometry optimizations applying a model using density functional theory (DFT) for electron exchange-correlation. Pseudo potentials, defined in Spartan'04 as LACVP+**

(Los Alamos Core Valence Potentials) were used. This set comprises the 6-31+G** basis set for main group elements H-Ar. The final geometry was calculated with the Becket Perdue (BP86) model (Kong *et al.*, 2000).

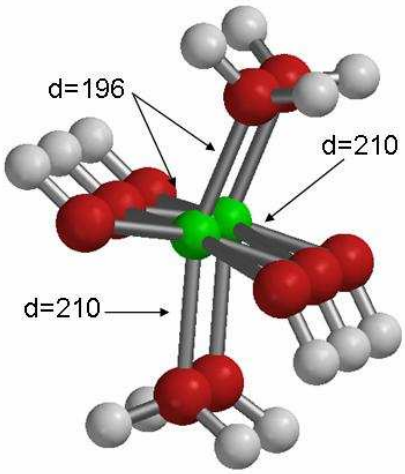

Figure 1. Two Fe(III)-O octahedra with Fe-O distances and angles as found in goethite (α-FeOOH). Big black spheres are oxygen, small white spheres are proton, and central gray spheres are iron.

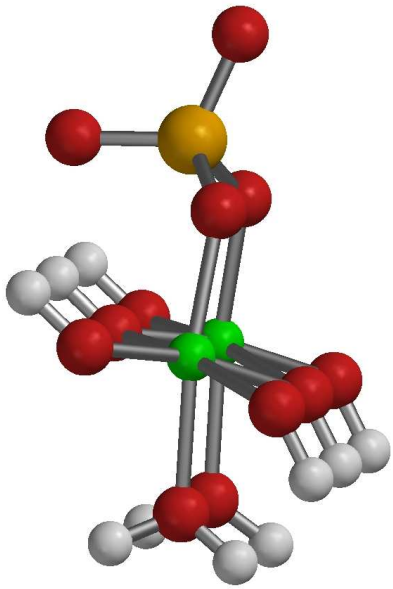

Figure 2. Two Fe(III)-O octahedra with a bidentate phosphate surface complex. The complex is formed by exchanging the PO_4^{-3} species with two coordinated H_2O that are equivalent with singly coordinated groups at the goethite interface.

Phosphate complexes

Two different situations were explored. In the first approach, the Fe octahedral structure was combined with only PO_4^{-3}. During the optimization of the geometry, the Fe-O distances were fixed to mimic the goethite bulk structure. Both upper oxygens were free to relax. The important characteristics of the calculated geometry of the different iron-phosphate complexes are given in Table 1. To explore the influence of hydration water, we added in the second approach additional water molecules, which were linked to the PO_4^{-3} moiety via hydrogen bonds. One H_2O was coordinated via one H bond to each common oxygen ligand of the Fe-O-P linkage. Both other oxygens of the PO_4^{-3} moiety were connected via H bonds to two water molecules. The results in case of a hydrated structure are given in Table 2.

In Table 1 and Table 2, the O-P distances refer to distance between the common O ligand and the P ion. The P-O and P-OH distances refer to the bond between the P ion and respectively the outer O or OH ligand(s). In addition, the Fe-O distance between the Fe ion and the common ligand has been given to judge the phenomenon of (surface) relaxation. The Fe-P value has been given since this value has been measured with EXAFS for small Fe-hydroxide-PO_4^{-3} clusters in the early stages of polymerization (Rose *et al.*, 1997). Rose et al. (Rose *et al.*, 1997) found Fe-P distances ranging from 339±7 to 305±7 pm with an average of 324±11. At the highest degree of neutralization of Fe (n=2) two Fe-P distances have been resolved, i.e. 327±4 pm and 310±5 pm. The first set of distances is close to our calculated values for mono and bidentate complex formation. The distances given in the tables are the average in case of two or three distances. The maximum variation is indicated with a ± symbol. The ± symbol in the last row with the experimental values refers to experimental uncertainty and/or variation.

Table 1. The calculated average and variation (±) in distances (pm) in the geometry of non-hydrated phosphate complexes optimized with the DFT-B86 model.

Species	O-P	P-O	P-OH	Fe-O	Fe-P	R_0
$FeOPO_3$	162.7	160.2 ± 0.08	-	205.5	330.0	170.2
$FeOPO_2OH$	160.5	155.4±0.5	170.3	203.4	321.1	168.2
$FeOPO(OH)_2$	158.3	152	164.3±1.7	206.7	313.5	167.6
$Fe_2O_2PO_2$	163.6±0.0	156.8±1.7	-	196.5±0.1	317.1±0.1	168.3
Fe_2O_2POOH	160.2±0.0	152.2	166.2	198.4±0.0	318.6±0.0	167.6
$Fe_2O_2P(OH)_2$	154.9±0.5	-	163.5±1.0	209.8±0.7	309.3±0.6	
Experimental	-	-		196 [a]	324±11 [b]	161.7 [c]

[a] Distance present in the goethite structure without relaxation.
[b] EXAES data (Rose *et al.*, 1997)
[c] Average R_0 for P in minerals (B=37 pm) (Brown and Altermatt, 1985)

Table 2. The calculated average and variation (±) in distances (pm) in the geometry of hydrated phosphate complexes optimized with the DFT-B86 model.

Species	O-P	P-O	P- OH	Fe-O	Fe-P	R_0
$FeOPO_3$	162.5	159.1±4.1	-	200.0	326.9	169.5
$FeOPO_2OH$	161.7	156.6±0.7	164.0	199.0	317.2	167.7
$FeOPO(OH)_2$	-	-	-	-	-	-
$Fe_2O_2PO_2$	161.6±0.2	157.4±1.8	-	200.2±1.8	325.5±1.1	167.7
Fe_2O_2POOH	157.1±1.4	155.1	164.9	203.8±2.0	320.3±1.3	167.6
$Fe_2O_2P(OH)_2$	-	-	-	-	-	-
Experimental		-		196 [a]	324±11 [b]	161.7 [c]

[a] Distance present in the goethite structure without relaxation.
[b] EXAFS data (Rose *et al.*, 1997)
[c] Average R_0 for P in minerals (B=37 pm) (Brown and Altermatt, 1985)

The geometries of Table 1 and 2 can be interpreted in terms of charge distribution using the Brown bond-valence concept. According to Brown (Brown and Altermatt, 1985), the bond valence **s** is related to the distance R as:

$$s = e^{-(R-R_0)/B} \qquad [1]$$

in which B is a constant and R_0 is the element specific parameter. The value of R_0 is chosen such that the sum of the bond valences around the P ion corresponds to the formal P valence (z=+5). These bond valences can be evaluated in terms of interfacial charge distribution values. Brown and Altermatt (Brown and Altermatt, 1985) used the value B=37 pm. More recently, it has been suggested that the B value is elements specific and coupled to the ionization potential. For P the value of B is 43.7. Using it in equation [1] will result soft bond valences. The calculated CD values are however almost not affected when the soft Bond valence is applied (B=43.7 pm). The CD values are given in Table 3 for the non-hydrated as well as hydrated options. The n_0 value is the charge of PO_4^{-3} attributed to the common ligand(s) and n_1 is the charge attributed to outer ligands. In case of protonation, the total charge on the outer ligands is increased with the formal charge of the proton(s), z_H.

Table 3 shows that the calculated CD values for the non-hydrated and hydrated structures are significantly different. In case of the presence of hydration water, more negative charge remains on the outer ligands of PO_4^{-3}. Actually, the charge is distributed more evenly over the ligands. This is due to the larger possibility for the outer ligands to be neutralized via H bridges formed by the water molecules. It may be expected that the calculated structures in case of hydration are closer to the situation in aqueous solutions. The CD values of the hydrated option were used in our further

model calculation with the CD model. It is interesting to notice that the calculated Fe-P distance in the hydrated structure (Table 2) fall within the range of distance observed with EXAFS for small Fe-hydroxide-PO_4 clusters (Rose *et al.*, 1997).

Table 3. CD values (n_0 and n_1; $n_0 + n_1 = -3$) calculated using the optimized geometries given in Table 1 and 2 using soft bond valences. The number z_H added to n_1 denotes the number of proton charges assigned to the outer ligands.

Species	Non-hydrated		Hydrated	
	n_0	n_1+z_H	n_0	n_1+z_H
$FeOPO_3$	-0.81	-2.18	-0.83	-2.17
$FeOPO_2OH$	-0.77	-2.23+1	-0.68	-2.32+1
$FeOPO(OH)_2$	-0.72	-2.28+2	-0.62	-2.38+2
$Fe_2O_2PO_2$	-1.70	-1.30	-1.63	-1.37
Fe_2O_2POOH	-1.55	-1.45+1	-1.42	-1.58+1
$Fe_2O_2PO(OH)_2$	-1.25	-1.75+2	-	-

The calculated CD values of Table 3 can be compared with CD values expected in case of a homogeneous distribution of the charge of P over the coordinating ligands, i.e. the use of Pauling Bond valences. Figure 3 shows a schematic representation of phosphate surface complexes in which the charge of the central ion, P, has been equally divided among the ligands based on the Pauling bond valence concept (Pauling, 1929). It shows that the CD values calculated using quantum chemistry technique are close to the values of Pauling bond valence, i.e. maximum deviation of 0.10±0.03 v.u. Comparison of both data sets illustrates that the presence of proton(s) on the solution-oriented ligands leads to a shift of some charge to the surface, i.e. a maximum shift of about 0.2 v.u. This shift is quite smaller than the value of 0.5 v.u. that follows from fitted CD values (Hiemstra and VanRiemsdijk, 1996).

Phosphate solution chemistry

Description of adsorption data is affected by the solution speciation of adsorbed ions as well as its surface speciation. In our experiments, a considerable part of the data refers to high ionic strength, where formation of ion pairs may occur in solution. To consider the possible presence and relative significance of these molecules, the acid base titrations were done in different phosphate solutions varying in background electrolyte concentrations. In the calculation, the affinities of protonated phosphate species were fixed to values given by Lindsay (Lindsay, 1979). For $NaHPO_4^{-1}$, the fitted affinity constant was equal to the log K reported by Turner et al. (Turner *et al.*, 1981). However, the modeling revealed a higher affinity for $NaPO_4^{-2}$ (log K=2.05)

compared to the previously reported value of log K=1.6 of Millero and Schreiber (Millero and Schreiber, 1982). The $NaPO_4^{-2}$ species is important at high pH. Table 4 presents the solution speciation of phosphate in $NaNO_3$ as used in the model calculation.

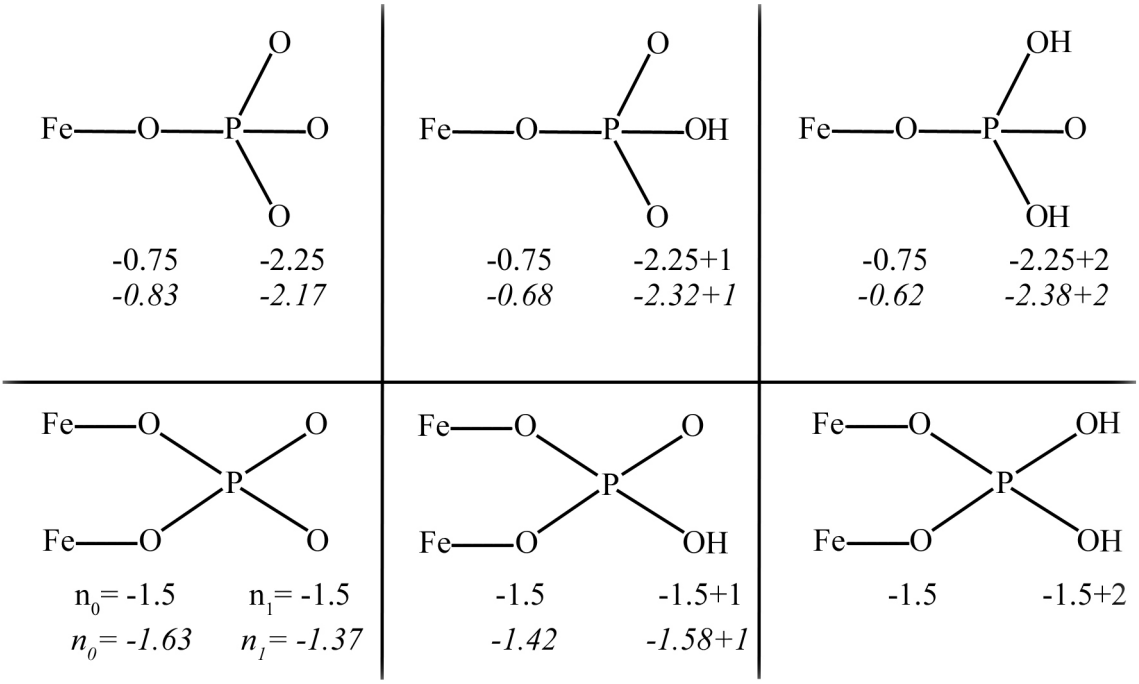

Figure 3. Charge allocation scheme of phosphate surface complexes at the interface of goethite based on the Pauling bond valence concept using a symmetrical distribution of the P^{+5} charge over four ligands, which leads to a υ=1.25, compare to the values derived from quantum chemical calculation (*italic values*).

Charging behavior

Rahnemaie et al. (Rahnemaie *et al.*, Ch 2) have measured and modeled the surface charge of goethite in different background electrolytes including sodium nitrate, using the CD model for inner- and outersphere surface complexation. The charge of the electrolyte ions is distributed over the outer electrostatic planes. We used their parameters (Table 5) to predict the surface charge of the goethite used in our experiments. Figure 4 shows the titration experimental data and the purely predicted surface charge.

Table 4. Phosphate aqueous speciation reactions and their equilibrium constant in the $NaNO_3$ medium

Species	Reaction	Log K
HPO_4^{-2}	$PO_4^{-3} + H^{+1} \Leftrightarrow HPO_4^{-2}$	12.35*
$H_2PO_4^{-1}$	$PO_4^{-3} + 2H^{+1} \Leftrightarrow H_2PO_4^{-1}$	19.55*
H_3PO_4	$PO_4^{-3} + 3H^{+1} \Leftrightarrow H_3PO_4$	21.70*
$NaHPO_4^{-1}$	$PO_4^{-3} + Na^{+1} + H^{+1} \Leftrightarrow NaHPO_4^{-1}$	13.40‡§
$NaPO_4^{-2}$	$PO_4^{-3} + Na^{+1} \Leftrightarrow NaPO_4^{-2}$	2.05§
H_2O	$H^{+1} + OH^{-1} \Leftrightarrow H_2O$	14.00*
$NaNO_3$	$Na^{+1} + NO_3^{-1} \Leftrightarrow NaNO_3$	-0.60†

From *Lindsay (Lindsay, 1979); †Smith et al. (Smith and Martell, 1981); ‡Turner et al.(Turner *et al.*, 1981), and § this study.

Table 5. Goethite interface parameters of Rahnemaie et al. (Rahnemaie *et al.*, Ch 2). The ion pair formation constants have been derived using the charge distribution model for outersphere complexes. The proton affinity constant for singly and triply coordinated surface groups is log K_H=9.0.

Ion	n_0	n_1	n_2	log K
Na^{+1}	0	0.50	0.50	-0.27
NO_3^{-1}	0	-0.67	-0.33	-0.53
C_1 F m^{-2}		1.00		
C_2 F m^{-2}			0.89	

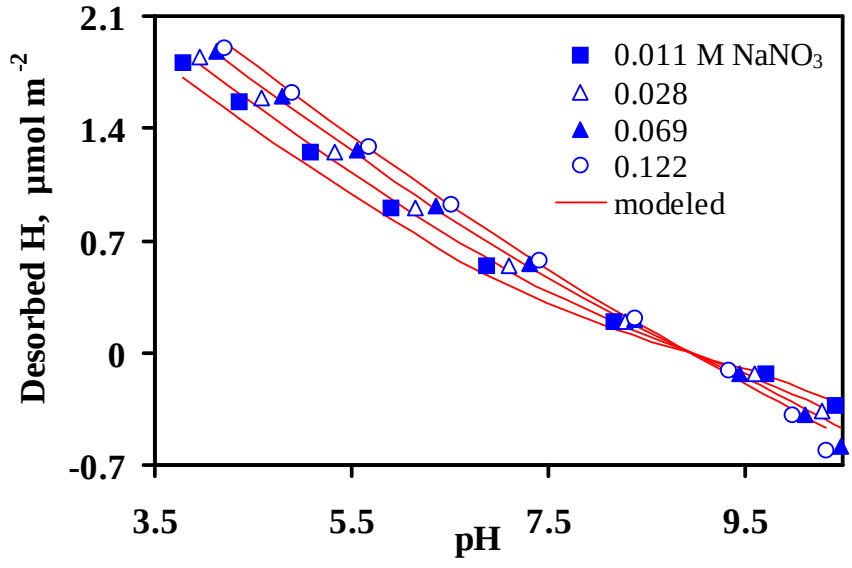

Figure 4. Experimental data and pure predicted surface charge of the goethite in presence of different levels of $NaNO_3$. The surface charge was predicted using the parameter values given in Table 5.

Phosphate adsorption edges

It has been shown (Russell *et al.*, 1974), (Parfitt *et al.*, 1975), (Sun and Doner, 1996) that oxyanions like phosphate only react with singly coordinated surface groups. The formation of phosphate complexes with these surface groups, which leads to either monodentate or bidentate species, are given in Table 6. The affinity of adsorbed surface complexes of phosphate were derived based on these reactions.

Table 6. Phosphate reactions with the singly coordinated groups on the goethite surface. The values of n_0 and n_1 represent the charge of PO_4^{-3} distributed between 0- and 1-plane.

Reaction	$\log K$
$\equiv FeOH^{-1/2} + H^{+1}(aq) + PO_4^{-3}(aq) \Leftrightarrow \equiv FeO^{n_0+1/2}PO_3^{n_1} + H_2O$	$\log K_{\equiv FeOPO_3}$
$\equiv FeOH^{-1/2} + 2H^{+1}(aq) + PO_4^{-3}(aq) \Leftrightarrow \equiv FeO^{n_0+1/2}PO_2(OH)^{n_1+1} + H_2O$	$\log K_{\equiv FeOPO_2OH}$
$\equiv FeOH^{-1/2} + 3H^{+1}(aq) + PO_4^{-3}(aq) \Leftrightarrow \equiv FeO^{n_0+1/2}PO(OH)_2^{n_1+2} + H_2O$	$\log K_{\equiv FeOPO(OH)_2}$
$\equiv 2FeOH^{-1/2} + 2H^{+1}(aq) + PO_4^{-3}(aq) \Leftrightarrow \equiv Fe_2O_2^{n_0+1}PO_2^{n_1} + 2H_2O$	$\log K_{\equiv Fe_2O_2PO_2}$
$\equiv 2FeOH^{-1/2} + 3H^{+1}(aq) + PO_4^{-3}(aq) \Leftrightarrow \equiv Fe_2O_2^{n_0+1}POOH^{n_1+1} + 2H_2O$	$\log K_{\equiv Fe_2O_2POOH}$
$\equiv FeOH^{-1/2} + 2H^{+1}(aq) + Na^{+1}(aq) + PO_4^{-3}(aq) \Leftrightarrow \equiv FeO^{n_0+1/2}PO_2(OH)^{n_1+1}Na^{+1} + H_2O$	$\log K_{\equiv FeOPO_2OHNa}$
$\equiv 2FeOH^{-1/2} + 2H^{+1}(aq) + Na^{+1}(aq) + PO_4^{-3}(aq) \Leftrightarrow \equiv Fe_2O_2^{n_0+1}PO_2^{n_1}Na^{+1} + 2H_2O$	$\log K_{\equiv Fe_2O_2PO_2Na}$

The effect of Ionic strength on the phosphate adsorption

Phosphate adsorption was determined as a function of pH, phosphate loading, and salt concentration. Ionic strength is an important factor in the ion adsorption process. For a phosphate-goethite system with an initial P loading of 0.4 mmol l^{-1}, which is equivalent to 1.57 μmol m^{-2}, the equilibrium PO_4^{-3} concentration is given in Figure 5. The experimental data show an intersection point, which is corresponding with the isoelectric point (IEP). Due to the introduction of negative charge of the PO_4^{-3}, the pristine IEP (PZC=9.0) has shifted to a lower value (IEP=5). On either side of the IEP, the salt effect is opposite. This effect of salt on ion adsorption can be explained by an increased screening of the surface charge (Strauss *et al.*, 1997). Increased salt effect lowers the electrostatic contribution to the binding, leading to decrease in binding below the IEP and increase in binding (lower repulsion) above the IEP.

The data in Figure 5 show that the salt effect is the biggest at the very low salt level. The salt concentration is below 0.001 M and not really constant for all data points. These data were excluded in the fitting procedure. Once the parameters were found, these data were predicted using the obtained constants of the known salt levels and resulted in an excellent prediction.

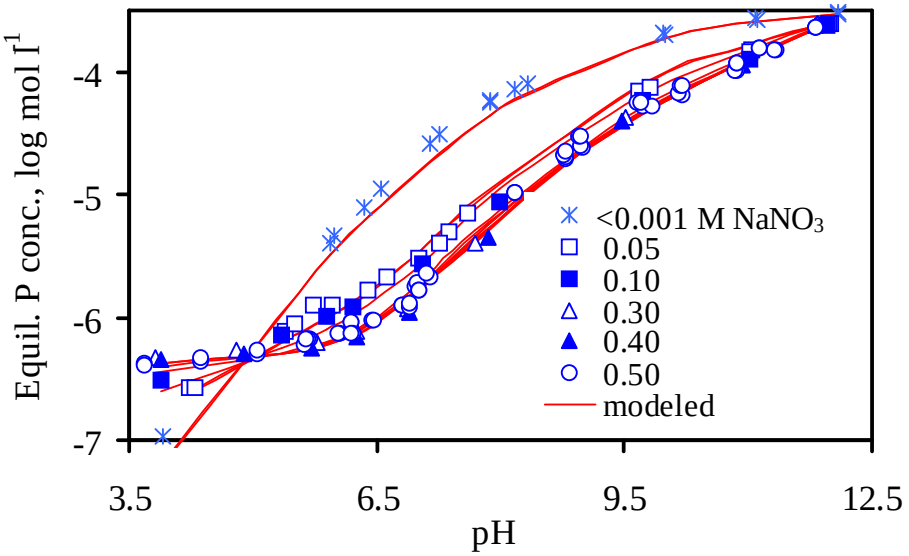

Figure 5. Experimental data and model description of salt-dependent phosphate adsorption edges as a function of pH. The data next to the symbols in the legend represent the concentration of background salt, i.e. $NaNO_3$. The adsorption data represent phosphate equilibrium concentration and the lines describe predicted adsorption edges based on the parameter values of Table 9. The experiments were done using 3 g l^{-1} goethite and 0.4 mmol l^{-1} phosphate.

The effect of loading on the phosphate adsorption

The adsorbate-adsorbent ratio is a key factor in the adsorption process. This is due to the number of available adsorption sites, which determine the adsorption maximum. Moreover, the change in the potential near the surface strongly affected by the amount and the speciation of the bound phosphate. This effect on the phosphate adsorption was studied applying different phosphate/goethite ratios in 0.5 M $NaNO_3$. Figure 6 illustrates the concentration-dependency of the PO_4^{-3} binding at various phosphate/goethite ratios. The corresponding adsorption is shown in Figure 7. At a certain P loading of the system, the highest adsorption is found at the low pH range. There, the adsorption is not very sensitive to pH. It is interesting to note that the theoretical adsorption maximum of the dominant 110 face is 2.85 µmol m^{-2} in case of bidentate binding, and double in case of monodentate binding.

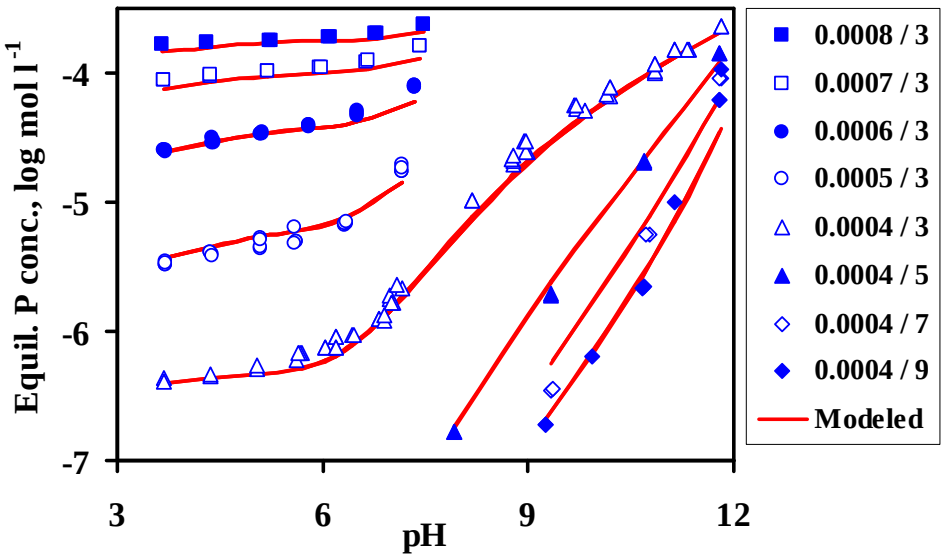

Figure 6. The effect of different phosphate loading on the phosphate adsorption edges. The data next to the symbols in the legend represent the ratio of phosphate concentration (mol l^{-1}) and goethite concentration (g l^{-1}) as applied in the experiments. The lines show the model description of data based on the parameter values of Table 9.

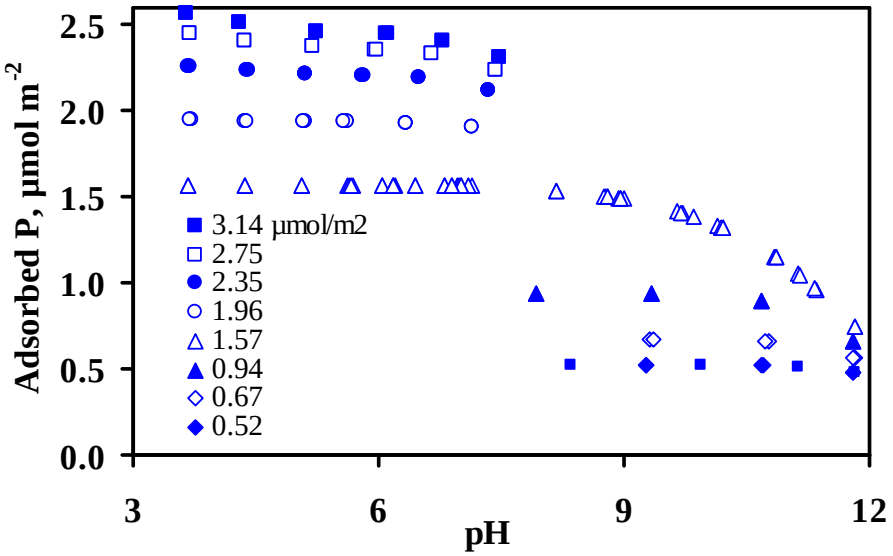

Figure 7. Phosphate adsorption on the goethite surfaces as a function of pH and different levels of phosphate loading. The symbols represent the corresponding adsorption of P measured as equilibrium concentrations (Figure 6), which were calculated by the CD model.

The CD modeling

The adsorption data were used to derive the relative importance of the various surface species of phosphate, constrained by the charge distribution values as derived from the quantum chemical calculations (Table 3). The formation constants of adsorbed complexes were calculated using the CD model. The log K values for the individual data sets (Figure 5, Figure 7) were optimized separately (Table 7, Table 8) and can be compared with the results for all data (Table 9). It is interesting to see that the constants fitted from the two completely different data sets correspond, within the uncertainty of the parameter values, very well. The only exception is the double protonated monodentate surface species, which is apparently not of relevance for the data where the salt effect was studied. This species may thus only be of relevance at a quite different loading of the system. This will be further addressed in the next section.

Table 7. The affinity constants of phosphate surface complexes as derived from modeling the data for different salt levels (Figure 5). The CD values were set equal to the values calculated using quantum chemistry technique for the hydrated ions.

Species	n_0	n_1	n_2	log K
$FeOPO_3$	-0.83	-2.17	0	20.46 ± 0.25
$FeOPO_2OH$	-0.68	-1.32	0	-
$FeOPO(OH)_2$	-0.62	-0.38	0	-
$Fe_2O_2PO_2$	-1.63	-1.37	0	29.47 ± 0.08
Fe_2O_2POOH	-1.42	-0.58	0	33.92 ± 0.04
$Fe_2O_2PO_2Na$	-1.42	-0.58	0	28.93 ± 0.02
$FeOPO_2OHNa$	-0.68	-1.32	1	27.90 ± 0.04

Table 8. The affinity constants of phosphate surface complexes as derived from modeling the data for different loading of phosphate (Figure 6). The CD values were set equal to the values calculated using quantum chemistry technique for the hydrated ions.

Species	n_0	n_1	n_2	log K
$FeOPO_3$	-0.83	-2.17	0	19.92 ± 0.09
$FeOPO_2OH$	-0.68	-1.32	0	-
$FeOPO(OH)_2$	-0.62	-0.38	0	29.59 ± 0.39
$Fe_2O_2PO_2$	-1.63	-1.37	0	29.59 ± 0.04
Fe_2O_2POOH	-1.42	-0.58	0	34.19 ± 0.06
$Fe_2O_2PO_2Na$	-1.42	-0.58	0	28.86 ± 0.03
$FeOPO_2OHNa$	-0.68	-1.32	1	27.82 ± 0.05

Table 9. The affinity constants of phosphate surface complexes as derived from modeling simultaneously the data for different salt levels and different phosphate loading (Figure 5 and Figure 6). The CD values were set equal to the values calculated using quantum chemistry technique for the hydrated ions.

Species	n_0	n_1	n_2	log K
$FeOPO_3$	-0.83	-2.17	0	20.14 ± 0.07
$FeOPO_2OH$	-0.68	-1.32	0	-
$FeOPO(OH)_2$	-0.62	-0.38	0	29.90 ± 0.19
$Fe_2O_2PO_2$	-1.63	-1.37	0	29.54 ± 0.03
Fe_2O_2POOH	-1.42	-0.58	0	34.02 ± 0.05
$Fe_2O_2PO_2Na$	-1.42	-0.58	0	28.95 ± 0.02
$FeOPO_2OHNa$	-0.68	-1.32	1	27.89 ± 0.04

Phosphate surface speciation

Figure 8 shows the mole fraction of the phosphate surface species as a function of pH, calculated for three PO_4^{-3} loadings, covering the low, intermediate, and high P loading of our experiments (see Figure 7). Calculation of surface speciation shows that the non-protonated bidentate complex is the major surface species for the studied pH range and phosphate loading. At low pH, the protonated bidentate species becomes important. Moreover, at low pH and only at high P loading the doubly protonated monodentate contribute to phosphate adsorption. The non-protonated monodentate species is formed at high pH, where the amount of bidentate complex decreases rapidly. The surface complexes of phosphate also interact with sodium and can form a sodium-phosphate surface complex, i.e. $Fe_2O_2PO_2Na$ and $FeOPO_2OHNa$. The singly protonated sodium phosphate surface complex interacts with surface groups at mid pH range, while the bidentate sodium phosphate complex is significant at the pH range above 6. These two complexes are especially necessary to describe the salt dependency data correctly.

Discussion

Experimental FTIR surface speciation

The calculated surface speciation can be compared with spectroscopic information. Tejedor-Tejedor and Anderson (Tejedor-Tejedor and Anderson, 1990) have studied the phosphate surface complexation on the goethite as a function of pH and P loading using CIR-FTIR. The non-protonated bidentate has been found to be the

main surface complex. At low pH, protonation of this complex has been claimed. At high pH (pH>8), a monodentate surface complex might be present. Recently, Arai and Sparks (Arai and Sparks, 2001) have studied the PO_4^{-3} speciation for HFO, using ATR-FTIR. As for goethite, the main surface species is the non-protonated bidentate surface complex. However, their work suggests that at low pH the speciation might be due to the presence of protonated bidentate as well as protonated monodentate complexes. This is in agreement with our calculated speciation using CD values derived from quantum chemistry. For this reason, we compared the model speciation (Table 9) quantitatively with the spectroscopic data of Tejedor-Tejedor and Anderson (Tejedor-Tejedor and Anderson, 1990). In the calculation, we assumed that the amount

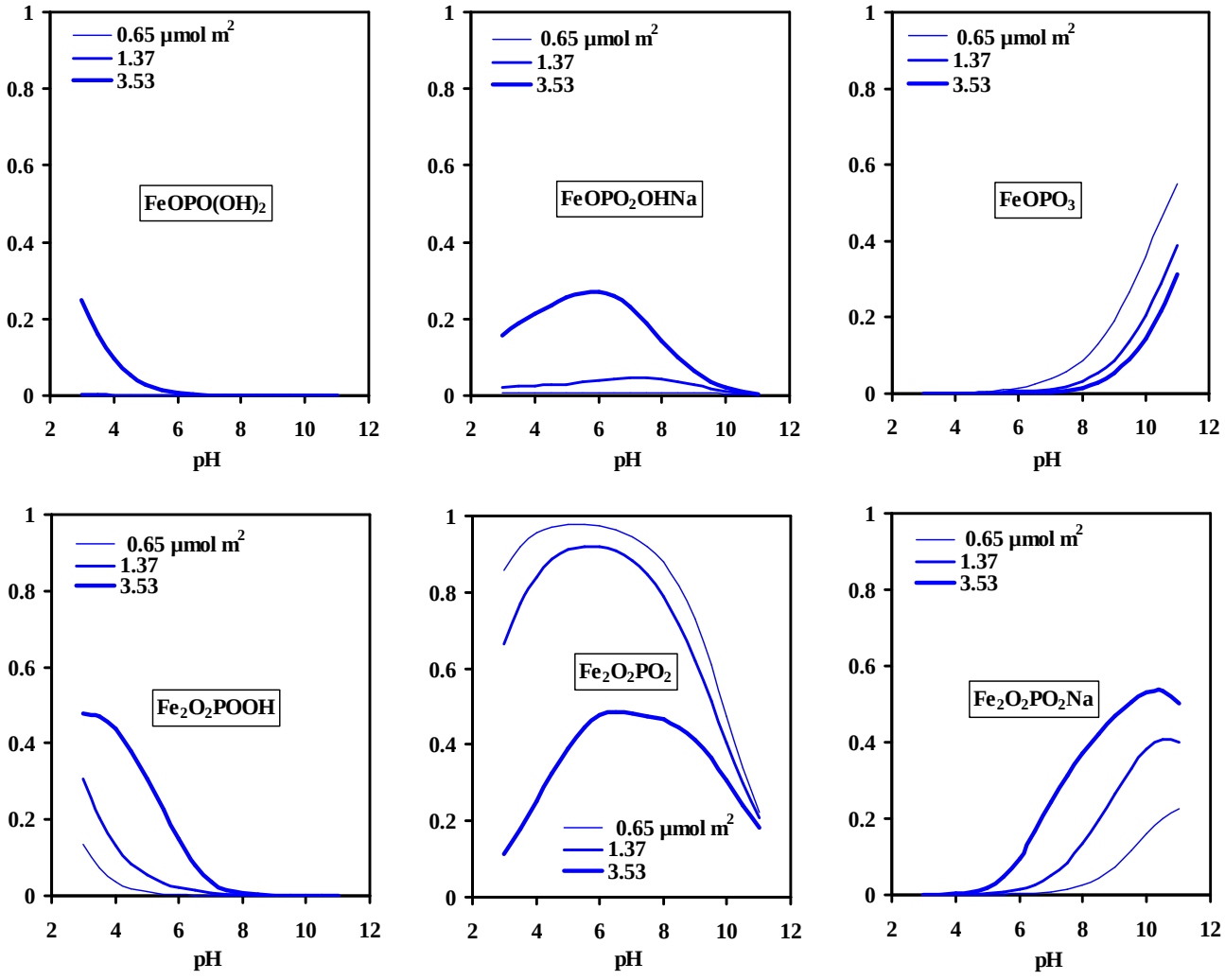

Figure 8. Calculated mole fraction of phosphate surface species on goethite as a function of pH and loading in 0.01 M $NaNO_3$. The calculation is based on the data of Table 9.

of protonated species can be summed, since only one set of frequencies has been identified by Tejedor-Tejedor and Anderson, and Arai and Sparks. We calculated the relative abundance of protonated species and the non-protonated species for the conditions in the CIR-FTIR experiments.

In Figure 9, the relative abundance of phosphate surface species is shown based on the spectroscopic data given by Tejedor-Tejedor et al. (Tejedor-Tejedor and Anderson, 1990). The figure shows two kinds of model description. In the first approach, it was assumed that the species have a similar molecular absorbance coefficient. The model cannot satisfactory describe the FTIR data (Figure 9, dash lines). It may denote that the species have different absorbance coefficients. Since

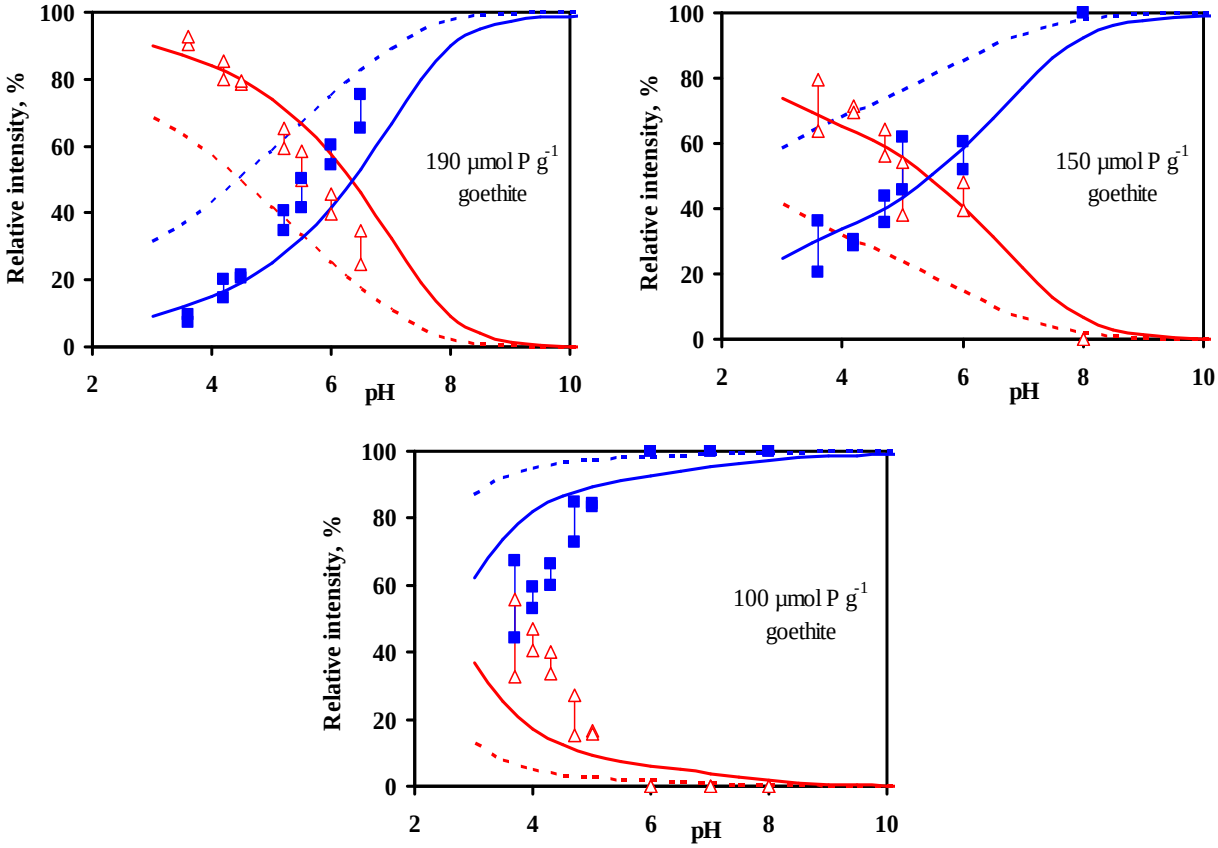

Figure 9. Relative intensity of IR spectroscopic data of phosphate adsorption on goethite (SA=81 m^2 g^{-1}) at three levels of loading and in 0.01 M NaCl (Tejedor-Tejedor and Anderson, 1990). The rectangular and triangular symbols represent the bidentate and protonated bidentate complexes respectively. The lines illustrate the pure model prediction using the surface speciation found in this study (Table 9) for two situations, assuming either similar molecular absorbance coefficient (dash lines) or different coefficient (solid lines).

these coefficients are not known, therefore a similar value was assumed for the protonated species vs. non-protonated species. The simulation showed that the ratio of coefficient might be in the order of 3-5. Figure 9 illustrates the model description (solid lines) when the coefficient has been set equal to 4. The figure shows that the model can describe spectroscopic data satisfactorily with this assumption.

Modeling of phosphate adsorption data by fitting the charge distribution parameter

In the previous section, the derivation of the charge distribution values from quantum chemical calculation was discussed. Previously, the PO_4^{-3} adsorption data have been described by optimizing the CD value by trial and error (Hiemstra and VanRiemsdijk, 1996), (Geelhoed *et al.*, 1998), or fitting (Rietra *et al.*, 2001), (Tadanier and Eick, 2002). For comparative purpose, we also modeled the new adsorption data of phosphate by choosing the charge distribution as a fitting parameter. The modeling was done for the salt dependency data and concentration dependency data separately and as a whole. The results are presented in Table 10. In this approach, the model excluded the monodentate species and its protonated forms from the calculation. The quality of the model description is comparable with the previous option.

The fitted CD value (n_o=-1.26) of the non-protonated bidentate species is reasonably close to the expected value based on a Pauling bond valence approach (n_o=-1.50) and to the value derived from quantum chemical calculation (n_o=-1.63). However, the fitted n_o value of the protonated bidentate (-0.85) is far from the expected value based on the Pauling bond valence approach (n_o=-1.50) and the value according to quantum chemistry (n_o=-1.42). This denotes the presence of much smaller negative charge at the surface. This might be due to formation of monodentate instead of bidentate.

Actually, the fitted value for the protonated species (n_o=-0.85) is between the values obtained from quantum chemical calculation for monodentate (n_o=-0.62 or -0.68) and bidentate (n_o=-1.42) complexes. Attempts to fit the data freely assuming simultaneously the presence of a singly protonated mono- and bidentate complex did not resolve both species. This can be done by allocating more charge at the surface (higher CD value) or by more species. The former is done when the CD is assumed as a fitting parameter while the latter denotes the presence of additional types of surface species.

Table 10. The affinity constants of adsorbed phosphate surface complexes as derived from modeling of phosphate adsorption data by fitting the charge distribution parameter. The modeling was done for salt and concentration dependency data separately and together.

Species	n_0	n_1	n_2	log K
	Salt dependency data			
$Fe_2O_2PO_2$	-1.35 ± 0.03	-1.65 ± 0.03	0	30.68 ± 0.05
Fe_2O_2POOH	-0.99 ± 0.12	-1.01 ± 0.012	0	35.89 ± 0.50
$Fe_2O_2PO_2Na$	-1.67 ± 0.03	-0.33 ± 0.03	0	28.68 ± 0.07
	Concentration dependency data			
$Fe_2O_2PO_2$	-1.30 ± 0.04	-1.70 ± 0.04	0	29.70 ± 0.12
Fe_2O_2POOH	-0.83 ± 0.04	-1.17 ± 0.04	0	36.50 ± 0.22
$Fe_2O_2PO_2Na$	-1.39 ± 0.03	-1.00 ± 0.03	0.39 ± 0.06	29.65 ± 0.14
	Both data sets			
$Fe_2O_2PO_2$	-1.26 ± 0.03	-1.74 ± 0.03	0	29.92 ± 0.07
Fe_2O_2POOH	-0.85 ± 0.04	-1.15 ± 0.04	0	36.37 ± 0.21
$Fe_2O_2PO_2Na$	-1.44 ± 0.03	-0.88 ± 0.03	0.32 ± 0.06	29.56 ± 0.14

Doubly protonated bidentate surface species

Arsenate is electronically comparable with phosphate. Hiemstra and van Riemsdijk (Hiemstra and Van Riemsdijk, 1999) noticed that As(V)-P competition data for goethite could only be described if similar surface species were used. It suggests a similarity in surface species for both elements. Recently, surface complexation of arsenate onto iron (hydr)oxides has been studied by EXAFS spectroscopy (Sherman and Randall, 2003). The authors studied the As binding on goethite at pH 3.9 at a As/Fe ratio of 3.5‰, equivalent with 1.16 μmol m^{-2}. For these conditions, they suggested the formation of a doubly protonated bidentate innersphere surface complex, i.e. $\equiv Fe_2O_2As(OH)_2$.

Based on CD modeling, we can exclude the formation of a doubly protonated bidentate surface species for phosphate ($\equiv Fe_2O_2P(OH)_2$). Dominance of this species at low pH would lead to a far too high positive particle charge, i.e. the measured shift of the IEP (Figure 5) would be far too small. Writing the overall adsorption reaction for a neutral goethite particle: $\equiv FeOH^{-1/2} + \equiv FeOH_2^{+1/2} + H_3PO_4 \Leftrightarrow \equiv Fe_2O_2P(OH)_2 + 2H_2O$ illustrates that no or little negative charge is introduced in the surface for this case. For phosphate, we calculate with the CD model at such a loading that the PO_4^{-3} surface species are a mixture of non-protonated and singly protonated *bidentate* complexes. Monodentate complexes are not important under these conditions of pH and loading (Figure 8), which agree with the conclusion of Sherman and Schreiber for arsenate.

Particle charge

From an electromobility point of view, the double layer may be considered to be consisting of two layers: an inner layer in which ions bind strongly to the surface and an outer layer in which the ion concentration decreases continuously toward the bulk solution. The potential in this region decays as the distance from the surface increases until it reaches the bulk solution value.

In an electric field a charged particle and its most closely associated ions will move. The boundary between the particle and the surrounding medium for a moving particle is known as the plane of shear or slipping plane and the potential of this plane is named the zeta potential ζ. The exact position of the slipping plane is unknown. Hiemstra and van Riemsdijk (Hiemstra and VanRiemsdijk, 1996) located the slipping plane in the diffuse double layer at a distance of about 0.8 nm from the head end of DDL (BS approach).

Tejedor-Tejedor and Anderson (Tejedor-Tejedor and Anderson, 1990) have measured the electromobility of goethite as a function of pH and phosphate loading. The mobility data have been transformed to the zeta potential (Figure 10). These data can be described with the CD model for inner- and outersphere surface complexation (Rahnemaie *et al.*, Ch 2). We assumed that the position of the slipping plane is identical with the head end of diffuse double layer, i.e. the 2-plane. The lines in Figure 10 show the calculated potential at the 2-plane in a system containing a series of different levels of phosphate in 0.01 M NaCl. The lines in the figure indicate that within the uncertainty the model can successfully predict the zeta potential and the IEP. This denotes that the position of the 2-plane in the present CD model (Rahnemaie *et al.*, Ch 2) is approximately identical with the slipping plane and the potential at this plane can be considered as the zeta potential. This is thus in contrast with the earlier version of the CD model, where it had to be assumed that the slipping plane is further away from the head end of the DDL.

The present CD approach leads to a lower potential at the solution side of the Stern layer due to the smaller capacitance of the outer Stern layer. This is equivalent with a larger distance, over which the potential decays before the DDL starts.

Conclusions

- Quantum chemical calculations show that protonation of PO_4^{-3} surface species leads to only a limited transfer of formal charge in the surface complex (<0.2 v.u.).

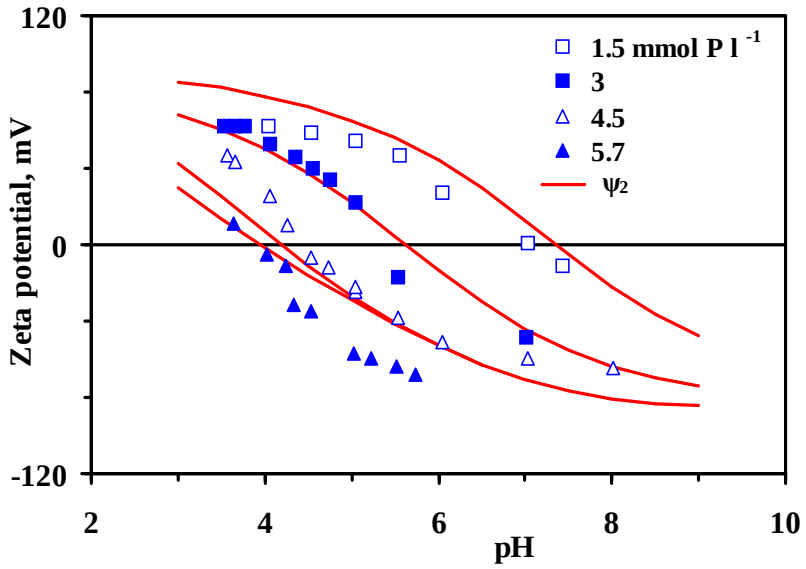

Figure 10. The zeta potential at the slipping plane based on the measured electromobility of a goethite suspension as a function of phosphate loading and pH in 0.01 M NaCl (Tejedor-Tejedor and Anderson, 1990). The lines present the calculated zeta potential with the CD model for inner- and outersphere surface complexation assuming that the position of slipping plane is identical with the head end of DDL (2-plane).

- Hydration of a surface complexes leads to a more equal distribution of the charge over the coordinating ligands.
- The PO_4^{-3} adsorption data can be described assuming the presence of only 3 surface species when the CD values are considered as unconstrained adjustable parameters
- The fitted surface charge attribution (n_o) of the dominant bidentate surface complex is reasonably close to the value found by quantum chemical optimization of the surface geometry of this complex ($\Delta n_o \leq 0.37$ v.u.). The fitted surface charge attribution (n_o=-0.85 v.u.) assuming a protonated bidentate is roughly average of the values calculated for a protonated monodentate complexes (n_o=-0.62-0.68) and protonated bidentate complex (n_o=-1.42) using quantum chemical calculations.
- The PO_4^{-3} adsorption data can be described using CD values constrained by quantum chemical optimized geometries of the surface complexes.
- The protonated species at low pH are a combination of *mono*- and *bi*dentate surface complexes.
- Doubly protonated bidentate species do not contribute to the PO_4^{-3} binding.
- The calculated surface speciation is in reasonable agreement with spectroscopic information.

- The CD model for inner- and outersphere surface complexation predicts correctly the zeta potential, considering it is identical with the potential at the head end of the DDL (2-plane).

Acknowledgments

The authors thank the Ministry of Science, Research, and Technology of Iran (MSRT) for financial support and Mr. A Korteweg (Laboratory of Physical and Colloid Chemistry) for the BET analysis.

References

Arai, Y., and D. L. Sparks (2001). Atr-ftir spectroscopic investigation on phosphate adsorption mechanisms at the ferrihydrite-water interface. *J. Colloid Interface Sci.* **241**(2): 317.

Arai, Y., D. L. Sparks, and J. A. Davis (2004). Effects of dissolved carbonate on arsenate adsorption and surface speciation at the hematite-water interface. *Environ. Sci. Technol.* **38**(3): 817.

Atkinson, R. J., P. A.M., and J. P. Quirk (1967). Adsorption of potential-determining ions at the ferric oxide-aqeous electrolyte interface. *J. Physic. Chem.* **71**: 550.

Brown, I. D. (2002). The chemical bond in inorganic chemistry: The bond valence model. Oxford, Oxford University Press.

Brown, I. D., and D. Altermatt (1985). Bond-valence parameters obtained from a systematic analysis of the inorganic crystal-structure database. *Acta Crystallographica Section B-Structural Science* **41**(AUG): 244.

Dzombak, D. A., and F. M. M. Morel (1990). Surface complexation modelling: Hydrous ferric oxide. New York, John Wiely & Sons.

Geelhoed, J. S., T. Hiemstra, and W. H. Van Riemsdijk (1998). Competitive interaction between phosphate and citrate on goethite. *Environ. Sci. Technol.* **32**(14): 2119.

Goldberg, S., and G. Sposito (1984). A chemical model of phosphate adsorption by soils: 1. Reference oxide minerals. *Soil Sci. Soc. Am. J.* **48**: 772.

Hawke, D., P. D. Carpenter, and K. A. Hunter (1989). Competitive adsorption of phosphate on goethite in marine electrolytes. *Environ. Sci. Technol.* **23**(2): 187.

Hazemann, J. L., J. F. Berar, and A. Manceau (1991). Rietveld studies of the aluminium-iron substituation in synthetic goethite. *Material Science Forum* **79**: 821.

Hiemstra, T., J. C. M. Dewit, and W. H. Vanriemsdijk (1989). Multisite proton adsorption modeling at the solid-solution interface of (hydr)oxides - a new approach .2. Application to various important (hydr)oxides. *J. Colloid Interface Sci.* **133**(1): 105.

Hiemstra, T., R. Rahnemaie, and W. H. Van Riemsdijk (2004). Surface complexation of carbonate on goethite: Ir spectroscopy, structure and charge distribution. *J. Colloid Interface Sci.* **278**(2): 282.

Hiemstra, T., and W. H. Van Riemsdijk (1999). Surface structural ion adsorption modeling of competitive binding of oxyanions by metal (hydr)oxides. *J. Colloid Interface Sci.* **210**(1): 182.

Hiemstra, T., and W. H. Vanriemsdijk (1996). A surface structural approach to ion adsorption: The charge distribution (cd) model. *J. Colloid Interface Sci.* **179**(2): 488.

Kong, J., C. A. White, A. I. Krylov, D. Sherrill, R. D. Adamson, T. R. Furlani, M. S. Lee, A. M. Lee, S. R. Gwaltney, T. R. Adams, et al. (2000). Q-chem 2.0: A high-performance ab initio electronic structure program package. *Journal of Computational Chemistry* **21**(16): 1532.

Lindsay, W. L. (1979). Chemical equilibria in soils, John Wiley & Sons.

Millero, F. J., and D. R. Schreiber (1982). Use of the ion-pairing model to estimate activity-coefficients of the ionic components of natural-waters. *Am. J. Sci.* **282**(9): 1508.

Parfitt, R. L. (1979). Nature of the phosphate-goethite (alpha-feooh) complex formed with ca(h2po4)2 at different surface coverage. *Soil Sci. Soc. Am. J.* **43**(3): 623.

Parfitt, R. L., R. J. Atkinson, and R. S. C. Smart (1975). Mechanism of phosphate fixation by iron oxides. *Soil Sci. Soc. Am. J.* **39**(5): 837.

Pauling, L. (1929). The principles determining the structure of complex ionic crystals. *J. Am. Chem. Soc.* **51**: 1010.

Rahnemaie, R., T. Hiemstra, and W. H. Van Riemsdijk (Ch 2). A new surface structural approach to ion adsorption: Tracing the location of electrolyte ions.

Rietra, R., T. Hiemstra, and W. H. Van Riemsdijk (2001). Interaction between calcium and phosphate adsorption on goethite. *Environ. Sci. Technol.* **35**(16): 3369.

Rose, J., A. M. Flank, A. Masion, J. Y. Bottero, and P. Elmerich (1997). Nucleation and growth mechanisms of fe oxyhydroxide in the presence of po4 ions .2. P k-edge exafs study. *Langmuir* **13**(6): 1827.

Russell, J. D., R. L. Parfitt, A. R. Fraser, and V. C. Farmer (1974). Surface-structures of gibbsite goethite and phosphated goethite. *Nature* **248**(5445): 220.

Sherman, D. M., and S. R. Randall (2003). Surface complexation of arsenie(v) to iron(iii) (hydr)oxides: Structural mechanism from ab initio molecular geometries and exafs spectroscopy. *Geochim. Cosmochim. Acta* **67**(22): 4223.

Smith, R. M., and A. E. Martell (1981). Critical stability constants. New York, Plenum.

Strauss, R., G. W. Brummer, and N. J. Barrow (1997). Effects of crystallinity of goethite .1. Preparation and properties of goethites of differing crystallinity. *Eur. J. Soil Sci.* **48**(1): 87.

Sun, X. H., and H. E. Doner (1996). An investigation of arsenate and arsenite bonding structures on goethite by ftir. *Soil Sci.* **161**(12): 865.

Tadanier, C. J., and M. J. Eick (2002). Formulating the charge-distribution multisite surface complexation model using fiteql. *Soil Sci. Soc. Am. J.* **66**(5): 1505.

Tejedor-Tejedor, M. I., and M. A. Anderson (1990). Protonation of phosphate on the surface of goethite as studied by cir-ftir and electrophoretic mobility. *Langmuir* **6**(3): 602.

Turner, D. R., M. Whitfield, and A. G. Dickson (1981). The equilibrium speciation of dissolved components in fresh-water and seawater at 25-degrees-c and 1 atm pressure. *Geochim. Cosmochim. Acta* **45**(6): 855.

Villalobos, M., M. A. Trotz, and J. O. Leckie (2001). Surface complexation modeling of carbonate effects on the adsorption of cr(vi), pb(ii), and u(vi) on goethite. *Environ. Sci. Technol.* **35**(19): 3849.

5

Surface Complexation of Carbonate on Goethite: IR Spectroscopy, Structure, and Charge Distribution

Abstract

The adsorption of carbonate on goethite has been evaluated, focusing on the relation between the structure of the surface complex and corresponding adsorption characteristics, like pH dependency and proton co-adsorption. The surface structure of adsorbed CO_3^{-2} has been assessed with 1) a reinterpretation of IR spectroscopy data, 2) determination of the charge distribution within the carbonate complex using surface complexation modeling and 3) evaluation of the proton co-adsorption of various oxyanions, including carbonate, in relation with structural differences. Carbonate adsorption leads to a degeneration of the ν_3 IR vibration. Currently, the magnitude of the $\Delta\nu_3$ band splitting is used as a criterion for metal coordination. However, the interpretation is not unambiguous, since the magnitude of $\Delta\nu_3$ is influenced by polarization and additional field effects, due to e.g. H bonding. Our evaluation shows that for goethite the magnitude of band splitting $\Delta\nu_3$ falls within the range of values that is representative for bidentate complex formation, despite contrarily assignments made in literature. Determination of the charge distribution (CD), derived by modeling available carbonate adsorption data, shows that a very large part (2/3) of the carbonate charge resides in the surface. Interpretation of this result with a bond valence and a ligand charge analysis strongly favors the bidentate surface complexation option for adsorbed carbonate. This option is also supported by the proton co-adsorption of carbonate. The H co-adsorption is very high, which corresponds closely to an oxyanion surface complex in which 2/3 of the ligands are common with the surface. The high H co-adsorption is in conflict with the monodentate option for adsorbed CO_3^{-2}. The study shows that the H co-adsorption of CO_3^{-2} is almost equal to the experimental H co-adsorption obtained for SeO_3^{-2} adsorption, which can be rationalized supposing for both XO_3^{-2} complexes the same ligand distribution in the interface, i.e. bidentate complex formation.

Key words: carbonate, sulfate, selenite, chromate, proton, adsorption, co-adsorption, goethite, hematite, iron, aluminum, oxide, IR, ATR, FTIR, DRIFT, EXAFS, spectroscopy, CD model, charge distribution, SCM, MUSIC, monodentate, bidentate, surface, charge.

Introduction

Infrared (IR) and Raman spectroscopy can be used to study the structure of surface complexes. Currently, in-situ approaches are used (ATR-FTIR, DRIFT). The identification of the binding mode with IR spectroscopy is not an easy task as is

illustrated in the history of the identification of the SO4 and SeO4 surface complex structure on goethite, bouncing between bidentate, monodentate and outersphere complexation (Parfitt and Smart, 1978), (Persson and Lovgren, 1996), (Hug, 1997), (Rietra *et al.*, 1999), (Peak *et al.*, 1999), (Wijnja and Schulthess, 2000), (Ostergren *et al.*, 2000a)).

The surface structure of adsorbed carbonate has been studied recently with in-situ IR spectroscopy for goethite (Wijnja and Schulthess, 2001), (Villalobos and Leckie, 2000), (Villalobos and Leckie, 2001), (Bargar *et al.*, 1999), (Ostergren *et al.*, 2000b) and Al-(hydr)oxide (Wijnja and Schulthess, 1999). Based on the splitting of the CO_3 stretching frequency due to metal coordination, the surface complex of CO_3 on these metal (hydr)oxides has been categorized as a monodentate innersphere complex.

As will be argued, the issue of monodentate and bidentate complex formation is particularly of interest for understanding the pH dependency of ion adsorption. In case of monodentate formation, the interaction of carbonate ions with the surface is rather limited since only one out of three ligands is incorporated in the surface and the other two ligands remain at some distance. In contrast, bidentate surface complexation will lead to a large interaction with the surface because in that case 2/3 of the ligands with corresponding negative charge is present in the surface plane. The interaction of the negatively charged CO3-2 ion with the surface will lead to additional adsorption of protons, i.e. H co-adsorption. In case of monodentate complex formation, co-adsorption of H+ will be smaller than in case of bidentate formation as has been demonstrated by Rietra et al. (Rietra *et al.*, 1999). This is a very important observation because Perona and Leckie (Perona and Leckie, 1985) have shown, on a thermodynamic basis, that H^+ co-adsorption is linked to the pH dependency of the adsorption of the ion. The combination of both issues shows that a distinct relation will exist between the macroscopic pH dependency of adsorption and the microscopic structure of the surface complex.

The key factor in the relationship between *pH dependency & structure of surface complexes* resides in the electrostatics of charged surfaces. The double layer potential near the surface varies very strongly with distance. Fokkink et al. (Fokkink *et al.*, 1987) have shown that the pH dependency of ion adsorption is tightly connected to the exact location of the ion charge in this electrostatic double layer profile. Therefore, location of charge is a key factor in understanding pH dependency. The Surface Complexation Models (SCM) of the first generation locate the charge of the innersphere complexes at one electrostatic position (surface), treating an ion as a single point charge. It is clear from the structure of innersphere complexes that only part of the adsorbing ion and the corresponding charge is incorporated in the surface, while the other part is located at a some distance from the surface. The latter part has fewer interactions with the protons at the surface, i.e. a lower co-adsorption of H. The large differences in structure of

innersphere surface complexes and corresponding location of charge cannot be easily introduced in single point charge models. This has lead to the development of the charge distribution (CD) model (Hiemstra and VanRiemsdijk, 1996). In the CD model, the charge of an adsorbed ion is distributed over its ligands. In turn, these ligands are distributed over the electrostatic interface locations, depending on the structure of the surface complex. This concept will be used here to study the relation between pH dependency of carbonate adsorption and the structure of the carbonate surface complex.

In the neutral pH range, the carbonate ion is protonated in solution (HCO_3^{-1}), whereas it is non-protonated at the surface (Wijnja and Schulthess (Wijnja and Schulthess, 2001) according to IR analysis. The proton-carbonate adsorption ratio for goethite has been established experimentally. Wijnja and Schulthess (Wijnja and Schulthess, 2001) reported a value of 1.54 and Villalobos and Leckie (Villalobos and Leckie, 2000) found 1.5±0.2 in a series of experiments (CO_3^{-2} used as reference species). As noticed by Wijnja and Schulthess (Wijnja and Schulthess, 2001), these values are high for monodentate complex formation. We consider the high proton-carbonate adsorption ratio for goethite as representative of bidentate formation (Rietra *et al.*, 1999), (Hiemstra and Van Riemsdijk, 2002). In the present study, this issue will be addressed.

Our contribution will start with a critical evaluation of the current criteria used in IR spectroscopy for the distinction between monodentate and bidentate coordination of CO_3^{-2}. The outcome of the semi-quantitative approach will be used to pinpoint the structure of the carbonate surface complexes. The surface complex structure will also be assessed from the determination of the charge distribution in the interface using SCM (CD model). In addition, proton co-adsorption of CO_3^{-2} will be evaluated and compared with other oxyanions. In the modeling, the excellent data set of Villalobos and Leckie for carbonate adsorption on goethite (Villalobos and Leckie, 2000), (Villalobos and Leckie, 2001) will be used.

Infrared spectroscopy

In several studies, the binding of carbonate on goethite has been examined with in situ IR spectroscopy (Wijnja and Schulthess, 2001), (Villalobos and Leckie, 2001), (Bargar *et al.*, 1999), (Ostergren *et al.*, 2000b), (Russell *et al.*, 1975), (Zeltner and Anderson, 1988), (Su and Suarez, 1997). A non-coordinated CO3-2 in vacuum has a calculated symmetric stretching frequency ν1 at 1010 cm-1 and two asymmetric OCO frequencies ν3 at 1447 cm-1 (quantum chemical calculation LMP2 model using the cc-pVTZ basis set). In an aqueous solution, the CO3-2 (aq) ion has an experimental

asymmetric OCO stretching ν3 at 1390 cm-1 (Wijnja and Schulthess, 1999). A similar value (1370-1390 cm-1) is found for the non-coordinated CO3-2 ion in crystalline Co(III)(NH3)6 Cl CO3 (Nakamoto *et al.*, 1957).

In case of metal coordination, the symmetry of the carbonate ion may change. This leads to a split of the ν_3 band, as shown experimentally (Nakamoto *et al.*, 1957) for a series of cobalt-ammine-carbonates. The degree of splitting, given as Δν3, depends on the type of coordination. For monodentate (M) cobalt-ammine-carbonate complexes (Figure 1) a relatively small Δν3 (80-120 cm-1) is found (Nakamoto *et al.*, 1957), (Goldsmit and Ross, 1968) while formation of a mononuclear bidentate (MB) Co(III) carbonate complex results in a large split (300-340 cm^{-1}). This observation is widely used for identification of the type of carbonate complexes.

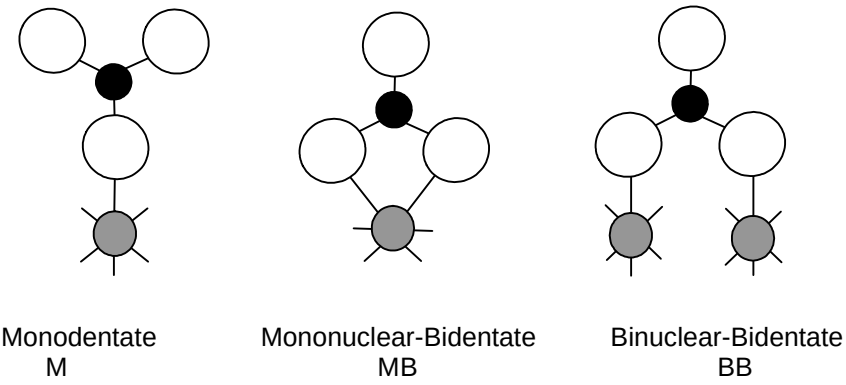

Figure 1. The structure of a monodentate, a mono- and a bi-nuclear bidentate XO_3 complex

The $\Delta\nu_3$ value of bidentate Cu(II) carbonate complexes in crystalline $Na_2Cu(CO_3)_2$ (138 cm^{-1}) and $Na_2Cu(CO_3)_2{\cdot}3H_2O$ (140-195 cm^{-1}) is considerably lower compared to the bidentate carbonate complexes of Co(III) (Jolivet *et al.*, 1982). The lower Δν3 value can be related to the polarization power of the coordinating metal ion(s), generating an interacting electrostatic field. The field strength ε of a point charge is proportional with $z/r2$, where z is ion charge and r the distance from the point charge. The influence of polarization of metal ions on the band splitting Δν3 was shown by Jolivet et al. (Jolivet *et al.*, 1982) for a series of solid carbonate complexes with a known complex structure (MB complexes). This correlation is shown in Figure 2 (open diamonds). The triangles in Figure 2 are the $\Delta\nu_3$ values for monodentate Co(III)-ammine-carbonates (M).

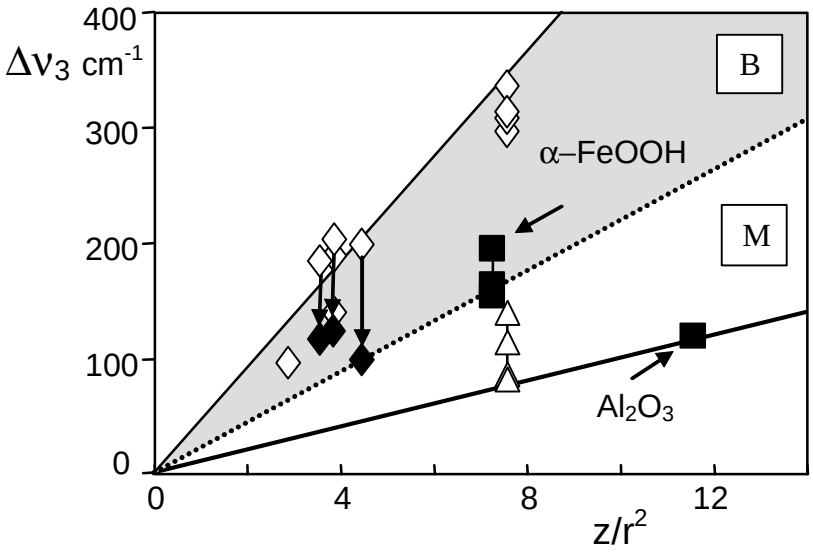

Figure 2. The relation between the $\Delta\nu_3$ band splitting of CO_3^{-2} and the field strength of the coordinating metal ions. All diamonds refer to mononuclear bidentate (MB) complexes. The order of the ions with increasing field strength is: La(III), Ce(IV), Th(IV)/Cu(II), Sc(III), Co(III). The black diamonds are related to MB-carbonate complexes that are influenced by hydrogen bond formation (Th(IV), Ce(III), Sc(III)). In the latter case, a strong reduction in band splitting occurs. The series of triangles indicate monodentate (M) complexes in crystalline Co(III)-penta-ammine-carbonates. The dark area indicates the field where bidentate complexes can be found. The series of black squares indicate the $\Delta\nu_3$ values of carbonate surface complexes measured in goethite suspensions and an aged Al-oxide suspension. The position of these $\Delta\nu_3$ suggests that the CO_3 complex at the goethite surface might be a bidentate complex and that the complex at aged Al_2O_3 might be a monodentate surface complex.

Three important observations were reported by Jolivet et al. (Jolivet *et al.*, 1982). First of all, they showed that the band splitting for carbonates of Ce^{4+} and Th^{4+} ($Na_6[Ce(CO_3)_5].12H_2O$ and $Na_6[Th(CO_3)_5].12H_2O$) strongly decreased (vertical arrows in Figure 2) from respectively 185 and 189 (open diamonds) to respectively 117 and 124 cm^{-1} (dark diamonds) if the Na^+ ions in the solids were replaced by $C(NH_2)_3^+$, while maintaining the bidentate structure for the carbonate ion. The difference in splitting is attributed to the presence of additional field effects counteracting the polarization of the metal ion. Jolivet et al. (Jolivet *et al.*, 1982) suggested that this might be due to formation of hydrogen bonds. These H bonds are required for the neutralization of the oxygens of CO_3 in case of the removal of the Na^+ charge.

A second important observation of Jolivet et al. (Jolivet *et al.*, 1982) was related to the $Sc(CO_3)_4^{5-}$ moiety in which carbonate is bound as a mononuclear bidentate complex. The structural unit can be found in the crystalline state as well as in solution.

The band splitting is however very different. In solution, where it may form H-bonds, the band splitting is only 100 cm^{-1} (dark diamond) while in the crystalline state 200 cm^{-1} is found (open diamond). Both mentioned observations suggest that H bond formation may lead to a considerable reduction of the band splitting $\Delta\nu3$. The reduction is indicated in Figure 2 with vertical arrows. The dotted line in Figure 2 gives the estimated lower limit of the $\Delta\nu3$ values for mononuclear bidentate complexes.

The third point is the difference between mono- and bi-nuclear bidentate complexes (MB and BB in Figure 1b,c). In crystalline $Na_2Cu(CO_3)_2.3H_2O$ both types of bidentate complexes are found (Jolivet *et al.*, 1982). The $\Delta\nu3$ values of this compound are 140, 170 and 190 cm-1. In crystalline $Na_2Cu(CO_3)_2$ only binuclear bidentate complexes are found (Healy and White, 1972). The $\Delta\nu3$ value for this compound is 138 cm-1, which coincides with the lower value of $Na_2Cu(CO_3)_2.3H_2O$. It illustrates that BB complexes may have a lower $\Delta\nu3$ than MB complexes, in contrast to suggestions made in some general $\Delta\nu3$ classification schemes. The lower $\Delta\nu3$ value for crystalline $Na_2Cu(CO_3)_2$ falls in the dark $\Delta\nu3$ area for bidentate complexes in Figure 2. In conclusion, in the mentioned $\Delta\nu3$ area of Figure 2, bidentate complex formation is plausible.

We are now ready to introduce the carbonate band splitting for α-FeOOH (goethite) and Al_2O_3. Wijnja and Schulthess (Wijnja and Schulthess, 2001) found for adsorbed CO_3 in a goethite suspension $\Delta\nu3$ =195 cm^{-1}. The most frequently reported band splitting is however 155 ± 10 cm^{-1} (Villalobos and Leckie, 2001), (Bargar *et al.*, 1999), (Ostergren *et al.*, 2000b), (Zeltner and Anderson, 1988). For aged Al_2O_3 a $\Delta\nu3$ of 120 cm^{-1} is found (Wijnja and Schulthess, 1999). This value is close to the lower line in Figure 2. Apparently, the $\Delta\nu3$ values for the Fe and Al (hydr)oxides are not too different. However, the polarization power of Fe and Al differs strongly. The $\Delta\nu_3$ values for the surface complexes are plotted in Figure 2 (squares). The position of the $\Delta\nu_3$ values suggests that the CO_3 complex at the goethite surface might be a bidentate and that the complex at Al_2O_3 might be a monodentate surface complex. In this interpretation, the aqueous surface complexes of FeOOH and Al_2O_3 are in the lower parts of the $\Delta\nu_3$ area of respectively bidentate (B) and monodentate (M) complexes (Figure 2).

Surface Complexation modeling

Villalobos and Leckie (Villalobos and Leckie, 2000), (Villalobos and Leckie, 2001) have provided an extensive data set for carbonate adsorption on goethite. The adsorption of carbonate has been measured in two types of systems, i.e. gas closed and open systems. In the closed systems, a known amount of carbonate is added. The

experimental CO_2 pressure results from the speciation processes in solution, the binding of carbonate at the surface and the gas/water volume ratio V_g/V_l. In the open systems, the CO_2 pressure is kept constant. The total amount of carbonate in the system will vary depending on the speciation in solution and the extent of surface complexation. The pH dependent carbonate adsorption has been measured as function of the ionic strength (0.01 and 0.1 M) and the type of electrolyte (NaCl, $NaNO_3$).

Primary charge

The primary charging behavior of goethite is due to protonation of singly (≡FeOH(H)) and triply coordinated (≡Fe_3O(H)) surface groups as found at the dominant 110 face, each having a site density N_s of 3 s/nm^2 (Hiemstra *et al.*, 1996). The 001 and 021 faces at the top end of goethite needles have singly coordinated surface groups (N_s = 7-8 nm^{-2}). In case of a 90 % contribution of the 110 face, the overall mean site densities are 0.75+2.7 and 2.7 s/nm^2 for respectively the ≡FeOH(H) and ≡Fe_3O(H) groups. The protonation constants for both types of surface groups are set equal to the value of the PZC. The ion pair formation reactions with corresponding constants for Na^+, Cl^-, NO_3^{-1} and ClO_4^{-1} are taken from Rietra et al. (Rietra *et al.*, 2000) (Table 1). We used a capacitance of 0.9 F/m2 (Basic Stern model) as obtained for well-crystallized goethites (Hiemstra *et al.*, 1989), (Hiemstra and VanRiemsdijk, 1996), (Rietra *et al.*, 2000), (Boily *et al.*, 2001). All calculations have been done with the ECOSAT software (Keizer and van Riemsdijk, 1998) in combination with FIT (Kinniburgh, 1993).

Table 1. Primary charging reactions of goethite

Reaction	
$\equiv FeOH^{-1/2} + H^{+1} \Leftrightarrow FeOH_2^{+1/2}$	$\log K_{FeOH_2}$
$\equiv FeOH^{-1/2} + Na^{+1} \Leftrightarrow FeOH^{-1/2}\cdots Na^{+1}$	$\log K_{FeOHNa}$
$\equiv FeOH^{-1/2} + H^{+1} + NO_3^{-1} \Leftrightarrow FeOH_2^{+1/2}\cdots NO_3^{-1}$	$\log K_{FeOH_2NO_3}$
$\equiv FeOH^{-1/2} + H^{+1} + Cl^{-1} \Leftrightarrow FeOH_2^{+1/2}\cdots Cl^{-1}$	$\log K_{FeOH_2Cl}$
$\equiv FeOH^{-1/2} + H^{+1} + ClO_4^{-1} \Leftrightarrow FeOH_2^{+1/2}\cdots ClO_4^{-1}$	$\log K_{FeOH_2ClO_4}$
$\equiv Fe_3O^{-1/2} + H^{+1} \Leftrightarrow Fe_3OH^{+1/2}$	$\log K_{Fe_3OH}$
$\equiv Fe_3O^{-1/2} + Na^{+1} \Leftrightarrow Fe_3O^{-1/2}\cdots Na^{+1}$	$\log K_{Fe_3ONa}$
$\equiv Fe_3O^{-1/2} + H^{+1} + NO_3^{-1} \Leftrightarrow Fe_3OH^{+1/2}\cdots NO_3^{-1}$	$\log K_{Fe_3OHNO_3}$
$\equiv Fe_3O^{-1/2} + H^{+1} + Cl^{-1} \Leftrightarrow Fe_3OH^{+1/2}\cdots Cl^{-1}$	$\log K_{Fe_3OHCl}$
$\equiv Fe_3O^{-1/2} + H^{+1} + ClO_4^{-1} \Leftrightarrow Fe_3OH^{+1/2}\cdots ClO_4^{-1}$	$\log K_{Fe_3OHClO_4}$

Log K_H = 9.2, log K_{Na}= -1, log K_{NO3}= -1, log K_{Cl}= -0.5, log K_{ClO4}=-1.7, C=0.9 F/m^2 (BS), N_s(FeOH)=3.45 nm^{-2}, N_s(Fe_3O)=2.7 nm^{-2}

Carbonate adsorption on goethite

Based on the above evaluation of the IR spectroscopy data, one may define a binuclear bidentate adsorption reaction as:

$$2 \equiv FeOH_2^{+1/2} + CO_3^{-2} \Leftrightarrow \equiv Fe_2O_2{}^pCO^q + 2H_2O \qquad [1]$$

in which $p+q= -1$, the total charge of the surface species.

In this paper, the interfacial charge distribution (CD) of the CO_3^{-2} ion will be expressed in the valences $n0$ and $n1$. These values are defined as the partial charges of the CO3-2 ion which are attributed to respectively the 0- and 1-plane in the BS approach ($n0+n1= -2$). Note that the n values are equal to the Boltzmann coefficients if the reactions are defined with FeOH2+1/2 as reference group (eq.[1]). If FeOH-1/2 is used as reference, the Boltzmann coefficients $z0$ and $z1$ are $z0 = n0 + n$H and $z1 = n1$, in which nH equals the total number of protons adsorbing at the ≡FeOH surface groups (nH=2, in case of $2 \equiv FeOH^{-1/2} + 2\ H^+ + CO_3^{-2} <=> \equiv Fe_2O_2CO + 2\ H_2O$).

The data sets for the open and closed CO_2 systems have first been fitted separately. The formation constants used for aqueous $NaCO_3^{-1}$(aq) and $NaHCO_3^{0}$ (aq) are respectively $logK^o=1.02$ and $logK^o= -0.19$ (Millero and Schreiber, 1982). All singly coordinated surface sites are assumed to be reactive with respect to carbonate (Ns=3.45 nm-2). For the open systems one finds $n0 = -1.35\pm0.02$ and $n1 =-0.65\pm0.02$ with logKCO3 = 4.02±0.04 (R2=0.974). For the closed systems one gets $n0 = -1.31\pm0.02$ and $n1 = -0.69\pm0.02$ with logKCO3=3.85±0.03 (R2=0.978). The fitting shows the charge distribution values are very similar for both data sets. The mean CD value can be given as $n0 = -1.33$ and $n1 = -0.67$. The corresponding affinity constant is logK=3.90. With the CD values obtained, we are also able to describe the CO3-2 adsorption data sets of van Geen et al. (Vangeen *et al.*, 1994) measured in 0.1 M NaClO4 (R2=0.99, logK=4.3) and of Villalobos et al. (Villalobos *et al.*, 2001) measured in 0.01 M $NaNO_3$ (R^2=0.98, logK=3.7).

The description of the adsorption data of Villalobos and Leckie (Villalobos and Leckie, 2000), (Villalobos and Leckie, 2001) might be improved assuming also the presence of a Na-carbonate interaction, i.e. the formation of ≡Fe_2O_2CO-Na:

$$2 \equiv FeOH_2^{+1/2} + CO_3^{-2} + Na^+ \Leftrightarrow \equiv Fe_2O_2{}^pCO - Na^{q+1} + 2H_2O \qquad [2]$$

In the calculations, the charge of the Na^+ ion is attributed to the 1-plane (BS model). In case of the simultaneous presence of both surface species (reaction [1] and [2]), the fitted CD values (R^2=0.976) for the CO_3^{-2} ion are $n0 = -1.37\pm0.02$ and $n1 =-$

0.63±0.02 and the corresponding affinity constants are logKCO3=3.75±0.02 and logKCO3Na=4.47±0.17 (open systems). For the closed systems one obtains $n0$=-1.33±0.01 and n_1=-0.67±0.01 with $\log K_{CO3}$=3.90±0.02 and $\log K_{CO3Na}$=5.06±0.05 (R^2=0.988). Note that the correlation coefficient is slightly higher when the $\equiv Fe_2O_2CO$-Na species is introduced. Only calculated lines for the simplest option are shown in Figure 3, i.e. the presence of only one surface species.

For further analysis, we have also determined the CD values in case the adsorption would not be due to the formation $\equiv Fe_2O_2CO$ but to other surface complexes. The formation of the surface species $\equiv Fe_2O_2COH$ (protonated bidentate), $\equiv FeOCO_2$ (non-protonated monodentate) and $\equiv FeOCO_2H$ (protonated monodentate) can be defined respectively with the reactions:

$$2 \equiv FeOH_2^{+1/2} + HCO_3^{-1} \Leftrightarrow \equiv Fe_2O_2^pCOH^q + 2H_2O \quad [3a]$$

$$1 \equiv FeOH_2^{+1/2} + CO_3^{-2} \Leftrightarrow \equiv FeO^pCO_2{}^q + 1H_2O \quad [3b]$$

$$1 \equiv FeOH_2^{+1/2} + HCO_3^{-1} \Leftrightarrow \equiv FeO^pCOOH^q + 1H_2O \quad [3c]$$

The results of the modeling process with each species individually are given in Table 2. The fitted charge distribution values of the carbonate ion (n) in Table 2 refer to the net charge introduced in the interface, i.e. $n0+n1$=-2 for CO3-2 or $n0+n1$=-1 in case of the formation of a protonated carbonate surface complex. It is striking to see that the fitted value in Table 2 for the charge attribution to the 1-plane ($n1$) remains almost constant, independent of the formulation of the reaction (protonated versus non-protonated surface complex). In contrast, the corresponding $n0$ values increase strongly if a protonated surface complex is defined, i.e. the proton charge is apparently redirected towards the surface plane. The steadiness of $n1$ shows that the charge attribution to the 1-plane is the most essential parameter needed in the description of the adsorption behavior. This is due to electrostatics. At a given pH, the charge attribution $n1$ regulates predominantly the electrostatic potential in the 1-plane ($\psi 1$). Therefore, the potential will change rapidly with increasing ion adsorption, which will strongly affect the overall affinity of the adsorption reaction. This phenomenon is also extremely important in ion competition as has been discussed previously in more detail (Hiemstra and Van Riemsdijk, 1999). The potential of the surface plane (ψo) is less strongly influenced by the charge attribution $n0$. The main reason for this phenomenon is the buffering of the surface charge by the presence of proton reactive surface groups, enabling H co-adsorption. If one defines in an adsorption reaction the involvement of more protons (e.g. eq.[3c] instead of [3b]), that proton charge is invariably pushed to the surface plane in the fitting procedure. The surface will react via a smaller co-adsorption of protons on the

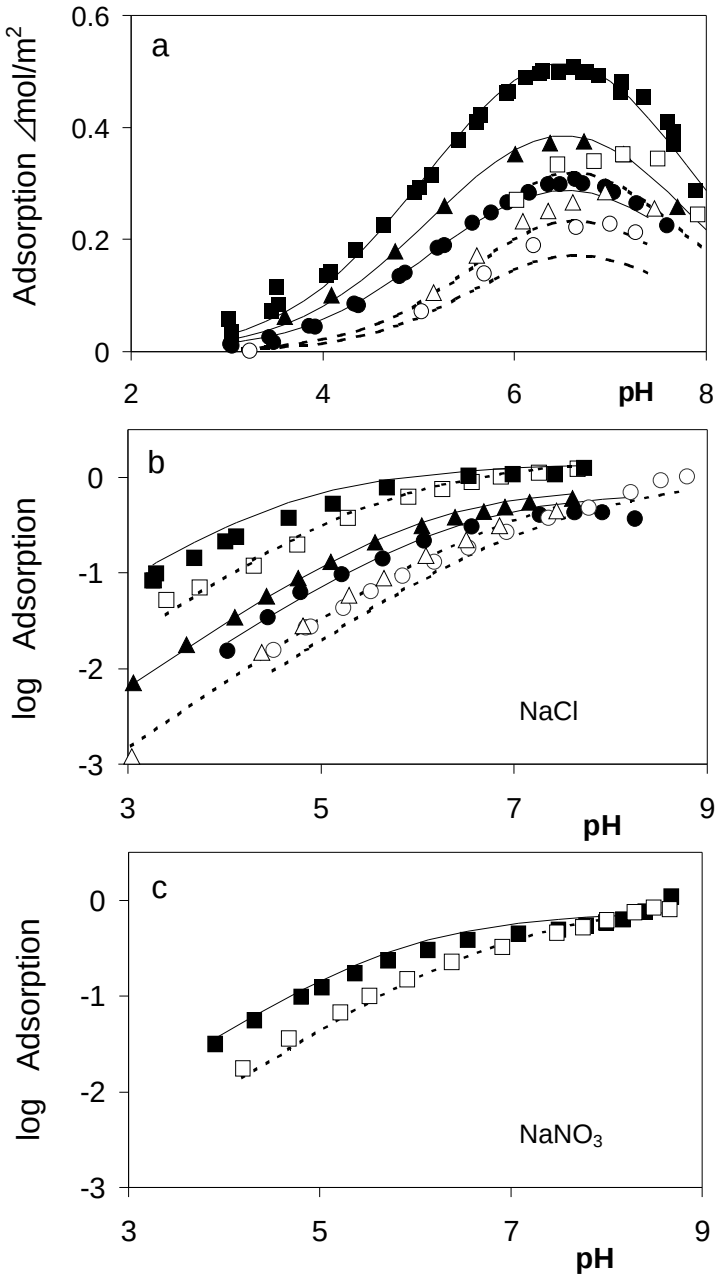

Figure 3. The adsorption of carbonate on goethite in CO_2 closed (3a) and open (3b,c) systems in 0.01 M (dark symbols) and in 0.1 M NaCl (open symbols) at various levels total carbonate (3a) or P-CO_2 (3b,c). The data are from Villalobos and Leckie (Villalobos and Leckie, 2000), (Villalobos and Leckie, 2001). The gas volume /water volume ratio in Figure 3a was set at V_g/V_l=0.77 l/l. The lines are calculated with the CD-model using the charge distribution in ≡Fe2O2CO of n_0= -1.33 and n_1= -0.67 (n_0+n_1= -2). In Figure 3a the total carbonate is 133 μmol/l (squares), 90 μmol/l (triangles) and 63 μmol/l (circles). In Figure 3b the partial CO_2 pressures and solid concentrations are P-CO_2= 5.59 mbar and ρ=14.7 g/l (squares), P-CO_2= 240 μbar and ρ=10 g/l (triangles), P-CO_2= 413 μbar and ρ=2 g/l (circles). The P-CO_2= 331 μbar and ρ=9.4 g/l (squares) in Figure 3c.

Table 2. Four options with individually fitted charge distributions of bidentate and monodentate $(H)CO_3$ surface species. The sum of the charge allocation to the 0- and 1-plane (n_0+n_1) is equal to -2 in case of adsorption of CO_3^{-2} (eq.[1,3b]) and equals -1 (eq.[3a,c]) in case of protonation of the carbonate complex ($z_{CO3}+ z_H = -2+1 = -1$). The quality of the fits is characterized with the correlation coefficient R^2.

Species	n_0	n_1	n_0+n_1	R^2
$\equiv Fe_2O_2CO$	-1.33	-0.67	-2	0.975
$\equiv Fe_2O_2COH$	-0.25	-0.75	-1	0.973
$\equiv FeOCO_2$	-1.35	-0.65	-2	0.973
$\equiv FeOCOOH$	-0.29	-0.71	-1	0.950

proton reactive surface groups. However, the total proton co-adsorption (H in the surface complex reaction plus the H+ co-adsorbed on other surface groups) remains almost constant. This is necessary for a good description of the pH dependency of the adsorption, because the total proton co-adsorption and pH dependency of ion adsorption are thermodynamically linked (Perona and Leckie, 1985), (Hiemstra and Van Riemsdijk, 2002).

Villalobos and Leckie (Villalobos and Leckie, 2001) have fitted the carbonate data using the CD concept in a hybrid combination with the 2-pK model. They derived for the monodentate and bidentate surface complex similar values for n1 (n1 ≈ -0.7-0.8) at the same quality of fit. As in our case (Table 2, R2), the quality of fits was in all cases acceptable. It illustrates that quality of fit is not of much help in discriminating between different options. Interpretation of the fitted CD values in relation to surface and complex structure with the bond valence concept can be very useful tool (Rietra *et al.*, 1999). This approach will be discussed in the next section.

Discussion

Charge distribution

The above data analysis revealed that the main part of the CO3-2 charge (≈ -1.3 v.u.) is present in the surface plane. The charge in the 1-plane is relatively small (≈ -0.7 v.u.). This can also be concluded from the modeling work of Villalobos and Leckie (Villalobos and Leckie, 2001).

The fitted CD values can be compared with the results of a simple model calculation in which one combines the interfacial ligand distribution of the surface complex with the Pauling bond valence concept (Pauling, 1929). An equal distribution of

the divalent carbonate charge over the three oxygen ligands, leads to a mean oxygen charge of -0.67 v.u. In case of bidentate formation, two oxygen ligands are present in the surface, yielding a Pauling valence of $n0 = -1.33$ (= 2 -0.67) v.u., and one oxygen ligand is present in the 1-plane, yielding $n1$=-0.67 v.u.. These calculated n values are equal to the values obtained by fitting ($n0$= -1.33±0.04, $n1$= -0.67±0.04 v.u.). This similarity is not found for the other surface complex options presented in Table 2. For instance, using the same approach, one calculates for the monodentate complex the charge distribution coefficients $n0$ = -0.67 and n_1 = -1.33, which are very different from the fitted CD coefficients (Table 2). The analysis advocates that a bidentate structure is more likely than a monodentate structure.

The fitted n values, obtained for the four different surface complexes of Table 2 (≡Fe2O2CO, ≡Fe2O2COH and ≡FeOCO2, ≡FeOCO2H), can be interpreted in more detail by calculating the corresponding charge on the ligands of the various complexes. This is shown in Figure 4. For each option, the sum of the charges on the outer ligand(s) is equal to the corresponding $n1$ value in Table 2. The charge at the common surface ligands (coordinated to C and Fe simultaneously) can be calculated using $n0$ and the bond valence contribution s of the Fe-O bond(s). For the singly coordinated groups on the 110 face of goethite the Brown bond valence s equals +0.6 v.u. (Hiemstra *et al.*, 1996). It should be noted that the Brown bond valence value s is different from the classical Pauling bond valence ν used in the formulation of the charging reaction. The Pauling bond valence is merely used as an overall charge book keeping tool, while the Brown bond valence traces the local formal charge in the surface complex. The calculation with the Brown bondvalence approach shows that formation of the non-protonated bidentate complex (Figure 4.a) leads to a rather acceptable charge on the common surface ligands, which is close to zero. In the other three cases, the common oxygen(s) is/are strongly over-saturated (4b,d) or strongly under-saturated (4c).

A second feature that can be resolved from the above ligand charge calculation is the symmetry in the charge distribution within the CO3 moiety. In the bidentate complex option (Figure 4a), one finds an equal charge distribution of C over the three coordinated oxygens (s=1.33 v.u.). This is equivalent with equal C-O distances (Brown, 1977), (Brown, 1978), (Brown and Altermatt, 1985). However, if the adsorption has to be explained exclusively by protonated bidentate complexes (option 4b), the actual bond valence s of the C-OH bond would be only s=0.25 v.u.. The value for both other C-O bonds, directed to the surface, is in this option s=1.87 v.u. The first value is extremely low, the latter one is very high. It would imply respectively very long and very short C-O distances, making the protonated bidentate option unlikely.

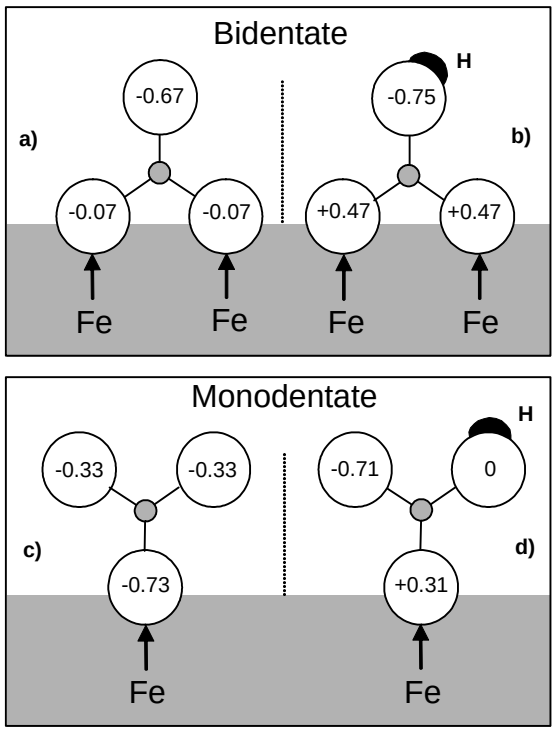

Figure 4. The ligand (O or OH) charge in non-protonated and protonated bidentate and monodentate carbonate surface complexes, calculated on the basis of the fitted charge distribution. The ligand charge at the common ligands is in three cases strongly under-saturated (c) or over-saturated (b, d). The charge distribution in $\equiv Fe_2O_2CO$ (a) is most likely since I) the carbon charge is well distributed over the three oxygens of CO_3 (Pauling distribution) and since II) the common surface ligands of the $\equiv Fe_2O_2CO$ are all most completely neutralized. The charge attribution coming from the Fe ion is set equal to 0.6 v.u. in the calculations.

A bond valence analysis of the C-O distances in crystalline carbonates such as Na2CO3, CaCO3, MgCO3, PbCO3, Na2Cu(CO3).3H2O, Cu2(OH)2CO3 etc. (Anonymous, 1995) shows that the difference in bond valence charge (Δs) of the C-O bonds is generally low, in the range of Δs=0-0.2 v.u. It means that the carbon charge is rather symmetrically distributed. For bicarbonates like crystalline NaHCO3 and KHCO3, the asymmetry in the CO3 moiety is larger, i.e. the difference in bond valence is larger (Δs=0.2-0.3 v.u.). In some particular cases like in crystalline cobalt(III)-ammine-carbonates (e.g. Co(NH3)4BrCO3, (Co(NH3)4NO3CO3)2.H2O and Co(NH3)5BrCO3.H2O), exceptionally large differences are found, being between Δs=0.3 and Δs=0.4 v.u. The Δs values in crystalline materials can be compared with those required in both monodentate surface complex options (Figure 4 c, d). The required Δs values in these surface complexes are much larger (Δs=0.6-1 v.u.), i.e. a rather unlikely high asymmetry would exist.

Summarizing, the ligand charge analysis as well as and the analysis of the charge distribution in the adsorbed CO3 favor the bidentate surface complexation option.

It has been suggested that H bond formation between particular surface groups and the carbonate surface complex may lead to redistribution of charge in the complex (Russell et al., 1975), (Wijnja and Schulthess, 2001). The question arises whether this suggestion can explain the low charge in the 1-plane in combination with monodentate surface complexation. Indeed, additional OH stretching frequencies are observed in the IR spectrum. However, the OH stretching bands are found in the range 3700-3400 cm-1 (Wijnja and Schulthess, 2001). It can be shown (unpublished results) that the H bonds formed in this range are quite ordinary H bonds with an O-H.....O charge distribution close to the value for H bonds in water. It implies that one type of H bond is replaced by an almost similar type during the formation of the surface complex. Therefore, no considerable redistribution of charge via H bonds is expected in the interface.

Proton co-adsorption

A high negative charge attribution to the surface will lead to a high proton coadsorption (Rietra *et al.*, 1999), (Hiemstra and Van Riemsdijk, 2002). Figure 5 shows the calculated proton co-adsorption (lines) for the experiments of Villalobos and Leckie (Villalobos and Leckie, 2000) in NaCl and $NaNO_3$. The predicted H co-adsorption is in line with the experimental data.

The H co-adsorption due to carbonate binding can be compared with the H co-adsorption found for other oxyanions. Usually, the proton co-adsorption is determined at constant pH. In the experiments of Villalobos and Leckie the pH varied. Therefore, we will rely for carbonate on the calculated proton co-adsorption in order to compare it with other experimental data sets where the H co-adsorption has been measured at constant pH. The calculated proton - carbonate interaction is based on the above-derived parameter set.

In Figure 6, the experimental H co-adsorption is given for a series oxyanions (SeO3-2, CrO4-2, SO4-2). The proton co-adsorption has been determined by Rietra et al. (Rietra *et al.*, 1999) with pH-stat ion titrations at a relatively high solid/solution ratio. This technique allows a simple but accurate determination of the H co-adsorption for these ions. The ions considered are all divalent and form, at the conditions studied, innersphere complexes (Hug, 1997), (Peak *et al.*, 1999), (Wijnja and Schulthess, 2000), (Hayes *et al.*, 1987), (Fendorf *et al.*, 1997). Selenite (Hayes *et al.*, 1987) and chromate ions (Fendorf *et al.*, 1997) form bidentate surface complexes. Sulfate is bound as a monodentate complex (Hug, 1997), (Peak *et al.*, 1999), (Wijnja and Schulthess, 2000), (Rietra *et al.*, 2001).

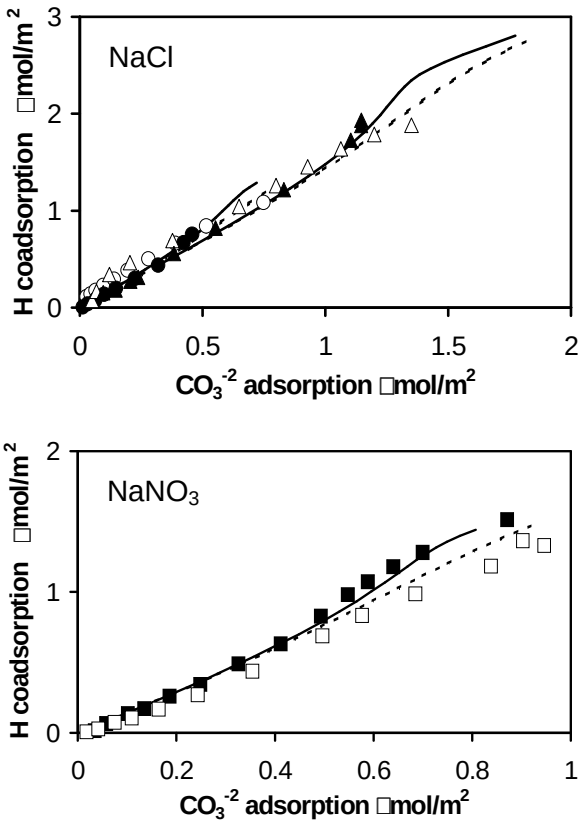

Figure 5. The H co-adsorption in the CO_3 -adsorption experiments of Villalobos and Leckie (Villalobos and Leckie, 2000). The full lines and dark symbols refer to 0.01 M. The dashed lines and open symbols are for 0.1 M. The CO_2 pressure and solid concentrations (ρ) are respectively: P-CO_2= 5.59 mbar, ρ=14.7 g/l (triangles), P-CO_2= 240 μbar, ρ=10.0 g/l (circles) and P-CO_2= 331 μbar, ρ=9.4 g/l (squares).

The SeO_3 ion has, on a relative basis, the highest number of oxygens common with the surface (2/3). It therefore has the highest negative charge attribution to the surface, which results in the strongest interaction in terms of the uptake of additional protons, i.e. the highest proton co-adsorption. The chromate ions have the same number of oxygen ligands common with the surface. However, adsorbed chromate ions have, in contrast to adsorbed SeO_3^{-2}, two oxygens in the 1-plane. In other words, proportionally a smaller part (2/4) of the divalent charge is attributed to the surface, leading to a lower H co-adsorption. The sulfate ions have the lowest number of oxygens common with the surface. Three quarters of the ligands are present in the 1-plane. It means that a relatively small portion of the -2 v.u. charge is directly interacting with the surface, i.e. one expects the lowest H /ion ratio.

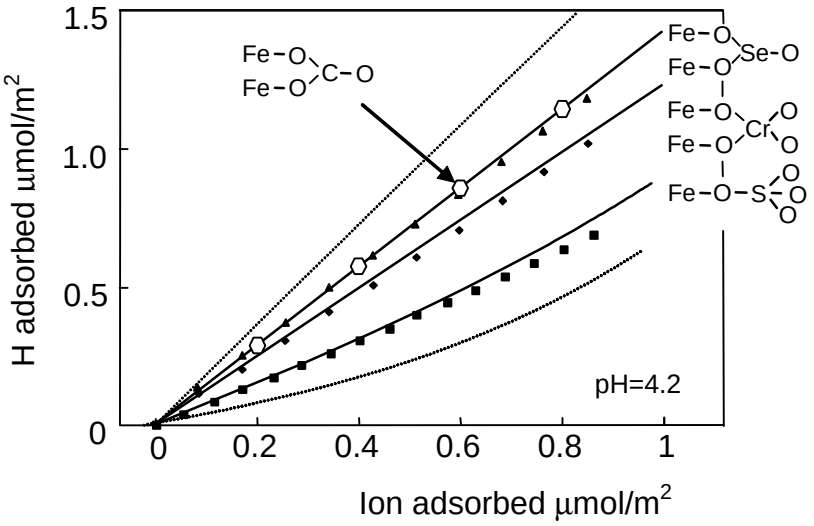

Figure 6. The H co-adsorption of protons due to the binding of CO_3^{-2}, SeO_3^{-2}, CrO_4^{-2} and SO_4^{-2} on goethite in 0.01 M $NaNO_3$ at pH=4.2. The dashed lines indicate the expected co-adsorption in case all ion charge (-2) is present or in the surface plane or in the 1-plane (BS approach), yielding respectively a very high or a low H co-adsorption. The full lines are calculated assuming a Pauling distribution of charge of the central ion over the coordinating ligands, leading to a surface charge attribution of respectively 2/3, 2/3, 2/4 and 1/4 of the anion charge (-2). Data for SeO_3^{-2}, CrO_4^{-2} and SO_4^{-2} (dark symbols) are from Rietra et al. (Rietra *et al.*, 2000). The points for CO_3^{-2} (open symbols) are generated using the parameter set derived in this study, which is based on the work of Villalobos and Leckie (Villalobos and Leckie, 2000).

Figure 6 shows that for the conditions given, the H co-adsorption due to carbonate adsorption is almost equal to that for selenite adsorption. For the H co-adsorption at pH 6.2 (Rietra *et al.*, 1999) the same conclusion can be drawn (not shown). The similarity in H co-adsorption can be understood assuming that both complexes have the same ligand and corresponding charge distribution in the interface. Selenite ions form bidentate complexes (Hayes *et al.*, 1987), i.e. the striking similarity of the H co-adsorption of CO3-2 and SeO3-2 strongly suggests that carbonate is also bound as a bidentate surface complex.

The lines in Figure 6 have been calculated for different charge distributions. The charge distribution can vary between two extreme cases (dotted lines in Figure 6). The highest dashed line in Figure 6 refers to the H co-adsorption in case all divalent charge is located in the surface plane. The lower dotted line represents the situation in which all charge is present in the 1-plane at the head end of the DDL. These two lines set the upper and lower limit of H co-adsorption for the specific adsorption of divalent ions (BS approach). The full lines in Figure 6 are calculated *predictions* based on the known

structures of the various surface complexes involved, assuming a Pauling distribution of charge within the adsorbed ions, i.e. the lines are not fitted (Rietra *et al.*, 1999). The calculations show that even without any adjustment of the CD value, the results give acceptable predictions of the H co-adsorption. It also illustrates that a quantitative relation exists between the interfacial ligand distribution and proton co-adsorption. A comparable Figure is discussed in more detail by Hiemstra and Van Riemsdijk (Hiemstra and Van Riemsdijk, 2002).

Summarizing, one observes a striking similarity between the H co-adsorption of SeO_3^{-2} and CO_3^{-2}. The proton co-adsorption of both ions is high, which points to a high attribution of negative charge to the surface. This agrees with the formation of bidentate innersphere complexes, as determined for selenite by EXAFS (Hayes *et al.*, 1987). The similarity in co-adsorption of SeO_3^{-2} and CO_3^{-2} supports the hypothesis that carbonate ions form bidentate surface complexes.

Conclusions

Our evaluation of carbonate adsorption by goethite can be summarized as follows:

- Carbonate ions may show a degeneration of the ν_3 (CO) IR vibration, which not only varies with the metal coordination and the field strength ε generated by the coordinating metal ion(s), but varies also due to additional field effects in relation to H-bonding. The experimental band splitting $\Delta\nu_3$ for goethite (155-195 cm^{-1}) is relatively high. The magnitude of the $\Delta\nu_3$ values falls within the range of values that are representative for bidentate complex formation, despite contrarily assignments made in literature.
- Description of the pH dependent carbonate adsorption data of Villalobos and Leckie (Villalobos and Leckie, 2000), (Villalobos and Leckie, 2001) with the CD model leads to derivation of the charge distribution in the carbonate surface complex. About 2/3 of the divalent carbonate charge is present in the electrostatic surface plane, 1/3 is present in the 1-plane (BS model).
- A bond valence and ligand charge analysis of the surface complex, based on the fitted charge distribution, favors the bidentate surface complexation option for carbonate.
- The proton co-adsorption due to anion binding is related to the structure of a surface complex. For homovalent oxyanions, the H co-adsorption is determined by the relative number of oxygen ligands that are common

with the surface, i.e. the ligand distribution. The proton co-adsorption of carbonate is high and almost equal to the H co-adsorption found for the bidentate innersphere complex formation of SeO_3^{-2}. This similarity in H co-adsorption of both XO_3^{-2} ions also strongly advocates the bidentate complexation option for carbonate.

References

Anonymous (1995). Inorganic crystal structure database, Fachinformationszentrum FIZ Max-Planck_Society.

Bargar, J. R., R. Reitmeyer, and J. A. Davis (1999). Spectroscopic confirmation of uranium(vi)-carbonato adsorption complexes on hematite. *Environ. Sci. Technol.* **33**(14): 2481.

Boily, J. F., J. Lutzenkirchen, O. Balmes, J. Beattie, and S. Sjoberg (2001). Modeling proton binding at the goethite (alpha-feooh)-water interface. *Colloid Surf. A-Physicochem. Eng. Asp.* **179**(1): 11.

Brown, I. D. (1977). Predicting bond lengths in inorganic crystals. *Acta Crystallographica Section B-Structural Science* **33**(MAY13): 1305.

Brown, I. D. (1978). Bond valences - simple structural model for inorganic-chemistry. *Chemical Society Reviews* **7**(3): 359.

Brown, I. D., and D. Altermatt (1985). Bond-valence parameters obtained from a systematic analysis of the inorganic crystal-structure database. *Acta Crystallographica Section B-Structural Science* **41**(AUG): 244.

Fendorf, S., M. J. Eick, P. Grossl, and D. L. Sparks (1997). Arsenate and chromate retention mechanisms on goethite .1. Surface structure. *Environ. Sci. Technol.* **31**(2): 315.

Fokkink, L. G. J., A. Dekeizer, and J. Lyklema (1987). Specific ion adsorption on oxides - surface-charge adjustment and proton stoichiometry. *J. Colloid Interface Sci.* **118**(2): 454.

Goldsmit, J. A., and S. D. Ross (1968). Factors affecting infra-red spectra of planar anions with d3h symmetry .4. Vibrational spectra of some complex carbonates in region 4000-400 cm-1. *Spectrochimica Acta Part a-Molecular Spectroscopy* **A 24**(8): 993.

Hayes, K. F., A. L. Roe, G. E. Brown, K. O. Hodgson, J. O. Leckie, and G. A. Parks (1987). Insitu x-ray absorption study of surface complexes - selenium oxyanions on alpha-feooh. *Science* **238**(4828): 783.

Healy, P. C., and A. H. White (1972). Crystal-structure and physical properties of anhydrous sodium copper carbonate. *Journal of the Chemical Society-Dalton Transactions*(17): 1913.

Hiemstra, T., J. C. M. Dewit, and W. H. Vanriemsdijk (1989). Multisite proton adsorption modeling at the solid-solution interface of (hydr)oxides - a new approach .2. Application to various important (hydr)oxides. *J. Colloid Interface Sci.* **133**(1): 105.

Hiemstra, T., and W. H. Van Riemsdijk (1999). Surface structural ion adsorption modeling of competitive binding of oxyanions by metal (hydr)oxides. *J. Colloid Interface Sci.* **210**(1): 182.

Hiemstra, T., and W. H. Van Riemsdijk (2002). On the relationship between surface structure and ion complexation of oxide–solution interfaces. Encyclopedia of surface and colloid science. A. T. Hubbard. New York, Marcel Dekker, Inc. **1**.

Hiemstra, T., and W. H. Vanriemsdijk (1996). A surface structural approach to ion adsorption: The charge distribution (cd) model. *J. Colloid Interface Sci.* **179**(2): 488.

Hiemstra, T., P. Venema, and W. H. Vanriemsdijk (1996). Intrinsic proton affinity of reactive surface groups of metal (hydr)oxides: The bond valence principle. *J. Colloid Interface Sci.* **184**(2): 680.

Hug, S. J. (1997). In situ fourier transform infrared measurements of sulfate adsorption on hematite in aqueous solutions. *J. Colloid Interface Sci.* **188**(2): 415.

Jolivet, J. P., Y. Thomas, B. Taravel, V. Lorenzelli, and G. Busca (1982). Infrared-spectra of cerium and thorium penta-carbonate complexes. *Journal of Molecular Structure* **79**(1-4): 403.

Keizer, M. G., and W. H. Van Riemsdijk (1998). Ecosat, technical report. Wageningen, Department of Soil Science, Wageningen Agricultural University.

Kinniburgh, D. G. (1993). Fit, technical report, British geological survey.

Millero, F. J., and D. R. Schreiber (1982). Use of the ion-pairing model to estimate activity-coefficients of the ionic components of natural-waters. *Am. J. Sci.* **282**(9): 1508.

Nakamoto, K., J. Fujita, S. Tanaka, and M. Kobayashi (1957). Infrared spectra of metallic complexes .4. Comparison of the infrared spectra of unidentate and bidentate metallic complexes. *Journal of the American Chemical Society* **79**(18): 4904.

Ostergren, J. D., G. E. Brown, G. A. Parks, and P. Persson (2000a). Inorganic ligand effects on pb(ii) sorption to goethite (alpha-feooh) - ii. Sulfate. *J. Colloid Interface Sci.* **225**(2): 483.

Ostergren, J. D., T. P. Trainor, J. R. Bargar, G. E. Brown, and G. A. Parks (2000b). Inorganic ligand effects on pb(ii) sorption to goethite (alpha-feooh) - i. Carbonate. *J. Colloid Interface Sci.* **225**(2): 466.

Parfitt, R. L., and R. S. C. Smart (1978). Mechanism of sulfate adsorption on iron-oxides. *Soil Sci. Soc. Am. J.* **42**(1): 48.

Pauling, L. (1929). The principles determining the structure of complex ionic crystals. *J. Am. Chem. Soc.* **51**: 1010.

Peak, D., R. G. Ford, and D. L. Sparks (1999). An in situ atr-ftir investigation of sulfate bonding mechanisms on goethite. *J. Colloid Interface Sci.* **218**(1): 289.

Perona, M. J., and J. O. Leckie (1985). Proton stoichiometry for the adsorption of cations on oxide surfaces. *J. Colloid Interface Sci.* **106**(1): 64.

Persson, P., and L. Lovgren (1996). Potentiometric and spectroscopic studies of sulfate complexation at the goethite-water interface. *Geochim. Cosmochim. Acta* **60**(15): 2789.

Rietra, R., T. Hiemstra, and W. H. Van Riemsdijk (1999). The relationship between molecular structure and ion adsorption on variable charge minerals. *Geochim. Cosmochim. Acta* **63**(19-20): 3009.

Rietra, R., T. Hiemstra, and W. H. Van Riemsdijk (2000). Electrolyte anion affinity and its effect on oxyanion adsorption on goethite. *J. Colloid Interface Sci.* **229**(1): 199.

Rietra, R., T. Hiemstra, and W. H. Van Riemsdijk (2001). Comparison of selenate and sulfate adsorption on goethite. *J. Colloid Interface Sci.* **240**(2): 384.

Russell, J. D., E. Paterson, A. R. Fraser, and V. C. Farmer (1975). Adsorption of carbon-dioxide on goethite (alpha-feooh) surfaces, and its implications for anion adsorption. *Journal of the Chemical Society-Faraday Transactions I* **71**(7): 1623.

Su, C., and D. L. Suarez (1997). In situ infrared speciation of adsorbed carbonate on aluminum and iron oxides. *Clays and Clay Minerals* **45**(6): 814.

Vangeen, A., A. P. Robertson, and J. O. Leckie (1994). Complexation of carbonate species at the goethite surface - implications for adsorption of metal-ions in natural-waters. *Geochim. Cosmochim. Acta* **58**(9): 2073.

Villalobos, M., and J. O. Leckie (2000). Carbonate adsorption on goethite under closed and open co2 conditions. *Geochim. Cosmochim. Acta* **64**(22): 3787.

Villalobos, M., and J. O. Leckie (2001). Surface complexation modeling and ftir study of carbonate adsorption to goethite. *J. Colloid Interface Sci.* **235**(1): 15.

Villalobos, M., M. A. Trotz, and J. O. Leckie (2001). Surface complexation modeling of carbonate effects on the adsorption of cr(vi), pb(ii), and u(vi) on goethite. *Environ. Sci. Technol.* **35**(19): 3849.

Wijnja, H., and C. P. Schulthess (1999). Atr-ftir and drift spectroscopy of carbonate species at the aged gamma-al2o3/water interface. *Spectroc. Acta Pt. A-Molec. Biomolec. Spectr.* **55**(4): 861.

Wijnja, H., and C. P. Schulthess (2000). Vibrational spectroscopy study of selenate and sulfate adsorption mechanisms on fe and al (hydr)oxide surfaces. *J. Colloid Interface Sci.* **229**(1): 286.

Wijnja, H., and C. P. Schulthess (2001). Carbonate adsorption mechanism on goethite studied with atr- ftir, drift, and proton coadsorption measurements. *Soil Sci. Soc. Am. J.* **65**(2): 324.

Zeltner, W. A., and M. A. Anderson (1988). Surface-charge development at the goethite aqueous-solution interface - effects of co2 adsorption. *Langmuir* **4**(2): 469.

6

Competitive Adsorption of Phosphate and Carbonate on Goethite

Abstract

Competitive adsorption of phosphate and carbonate on goethite has been quantitatively studied, since these anions are widely present in soils, sediments, and other natural systems. Metal hydroxide surfaces are positively charged at normal range of pH and are often responsible for binding of anions such as phosphate and carbonate. Adsorption edges of phosphate were performed in a binary system containing phosphate and carbonate, as a function of phosphate and carbonate loading and background salt concentration. It was compared with adsorption of carbonate in a 'single ion' system. The adsorption data were described using the CD model for inner- and outersphere surface complexation. The charge distribution of innersphere surface complexes of phosphate and carbonate was constrained using quantum chemical calculation. The constants for carbonate species were derived from modeling of carbonate-phosphate interaction data. These obtained constants were used to predict the carbonate adsorption in absence of phosphate with good results. The carbonate adsorption data were successfully described using an innersphere bidentate complex, which partly interacts with sodium, resulting in an innersphere sodium-carbonate surface complex. A monodentate outersphere sodium-bicarbonate complex may form at relatively high pH and high carbonate loading. This complex becomes non-protonated at a higher pH range. At low loading of carbonate, the bidentate complex strongly dominates the carbonate adsorption.

Keywords: phosphate; carbonate; adsorption; diffuse double layer; basic Stern; iron oxide; goethite; CD model; MUSIC model; surface speciation; IR spectroscopy;

Introduction

Anion and cation adsorption at the solid-solution interface of minerals plays an important role in processes in the natural environment. Reactive surfaces are very important in bioavailability, retention, and transport of ions. Clay minerals and organic matter provide negative charge in soils and sediments. These surfaces are important for cation binding, like binding of the macro-elements Na^{+1}, K^{+1}, Ca^{+2}, Mg^{+2} and of trace elements, in particular heavy metal cations. Al and Fe (hydr)oxides have a positive surface charge. This surface charge can be compensated by specifically bound oxyanions like SO_4^{-2}, CO_3^{-2}, and PO_4^{-3}.

The binding of cations and oxyanions on metal oxide surfaces can be described with surface complexation models. For application of surface complexation models in

natural systems, information is needed with respect to the binding of those ions that are omnipresent. Phosphate is an anion, which is present in the environment at a rather low concentration level (often 1-10 μM scale). However, phosphate ions have a very high affinity for metal oxide surfaces of Al and Fe. It implies that phosphate will be a dominant ion at the surface. This ion strongly influences the particle charge and therefore the binding of other anions and cations. A macro-element like calcium is a typical example of an ever-present cation that has a considerable interaction with phosphate. The process can be considered as cooperative binding. The variation in Ca^{2+} activities is rather high, ranging from 10^{-5} M in river waters of the Amazon to 10^{-2} M in seawater and soils. This variation influences the PO_4^{-3} adsorption in the pH range above 5 (Rietra *et al.*, 2001).

At low pH (pH<5), sulfate ions are a competitor for phosphate (Geelhoed *et al.*, 1997). Sulfate is less strongly bound to Fe oxides in comparison with phosphate. However, the lower affinity is compensated by a higher concentration (1 mM scale) in the environment, in particular in the industrial areas with air (SO_2) pollution.

In this study, we will focus on another ubiquitous present oxyanion, i.e. (bi)carbonate. The concentration of this anion is related to the local partial CO_2 pressure and the pH. In ground water, the natural concentration range is 10^{-4}-10^{-2} mM. The dissolved forms of CO_2, i.e. bicarbonate and carbonate, may adsorb onto metal oxide surfaces. This process induces competition of carbonate with phosphate. In the Olsen phosphate extraction procedure (Olsen and Dean, 1954), the competitive interaction between phosphate and bicarbonate is deliberately used to desorb PO_4^{-3} from soil.

Carbonate adsorption has been studied as a ‘single ion’ system (Vangeen *et al.*, 1994), (Villalobos and Leckie, 1999), (Villalobos and Leckie, 2000) and in interactions with other ions like arsenate (Arai *et al.*, 2004), uranyl (Wazne *et al.*, 2003), (Villalobos *et al.*, 2001), and chromate and lead (Villalobos *et al.*, 2001). With IR spectroscopy, the adsorption mechanism of carbonate has been studied (Villalobos and Leckie, 2001), (Wijnja and Schulthess, 2001). Initially, it has been concluded for goethite (FeOOH) that carbonate ions are adsorbed as a monodentate complex. Recently, Hiemstra et al. (Hiemstra *et al.*, 2004, Ch 5) have reinterpreted the spectroscopy data and argued that bidentate surface complexation is more likely.

In the present study, we will measure PO_4–CO_3 interaction. The interaction will be described with the charge distribution (CD) model for inner- and outersphere surface complexation (Rahnemaie *et al.*, Ch 2). For phosphate, we will use the parameters derived previously by Rahnemaie et al. (Rahnemaie *et al.*, Ch 4). The authors have derived the CD values of adsorbed complexes from quantum chemical optimized geometries of the various phosphate complexes and interpreted with the

Brown bond valence approach (Brown and Altermatt, 1985), (Brown, 2002). The same approach will be followed here to derive the CD values of adsorbed carbonate. For the description of the CO_3-PO_4 interaction only the affinity constant for the surface complex(es) will be used as adjustable parameters. The CD model for inner- and outersphere surface complexation will be used to describe the CO_3 adsorption in a 'single ion' system in comparison with CO_3-PO_4 competition adsorption data.

Material and methods

Preparation of reagents

Without precautions, preparation of solutions in contact with the atmosphere will lead to dissolution of CO_2. To prevent this source of contamination, all chemicals (Merck p.a.), except carbonate solutions, were made under purified N_2 atmosphere and stored for a short time in polyethylene bottles to be free of silica. The acid solutions were stored in glass bottles to avoid contamination by organic materials (Rahnemaie *et al.*, Ch 4). A stock solution of NaOH was prepared CO_2-free from a highly concentrated 1:1 NaOH/H_2O. The mixture was centrifuged to remove any solid Na_2CO_3. The sub-sample of supernatant was pipetted into ultra pure water and stored in a desiccator, equipped with a CO_2 absorbing column. The ultra pure water (≈0.018 dS/m) was used throughout the experiments. It has been pre-boiled to remove dissolved CO_2 before using it in the experiments. The experiments were done in a constant temperature room (20-22 ^oC).

Preparation and characterization of the goethite

The goethite suspension was prepared based on the method of Atkinson et al. (Atkinson *et al.*, 1967), as described in detail by Hiemstra et al. (Hiemstra *et al.*, 1989). A freshly prepared 0.5 M $Fe(NO_3)_3$ was slowly titrated with 2.5 M NaOH to pH 12. The suspension was aged for 4 days at 60°C and subsequently dialyzed in ultra pure water. Before using it in the experiments, the goethite suspension was acidified (pH≈5) to desorb and remove (bi)carbonate, by continuously purging with N_2 for at least one day. The BET(N_2) specific surface area of this goethite equals 85 $m^2\ g^{-1}$. The same batch of goethite has been previously used by Rahnemaie et al.(Rahnemaie *et al.*, Ch 4).

The surface charge of goethite was measured in $NaNO_3$ solutions. A sample of goethite was titrated forward and backward by base and acid within the pH range of

almost 4 to 10.5. The temperature was fixed at 20±0.1 °C using a thermo stated reaction cell. The details of experimental setup and data handing is given elsewhere (Rahnemaie *et al.*, Ch 2).

Carbonate-Phosphate Adsorption edges in a binary ion system

Adsorption experiments were performed in individual gas-tight 23.6 ml low-density polyethylene bottles with fixed amounts of salt, goethite, carbonate, and phosphate at different pH values.

All solutions, except (bi)carbonate, were added to the bottles under a clean N_2 atmosphere to avoid carbonate contamination. A certain amount of HNO_3 or NaOH was added to the vessels, in order to obtain final pH values within the relevant pH range. The carbonate solution was added at the end after the N_2 flushing was stopped. The pH range in the experiments was limited to values higher than 6.5 to minimize the amount of carbonate in the gas phase of the bottle (0.18 $l_{gas}/l_{solution}$). In the modeling, we corrected for the amount of carbonate as CO_2 in the gas phase of the bottles by calculation. $NaNO_3$ was used to obtain the intended concentration of the suspensions. The final volume of the suspensions was 20 ml. The bottles were equilibrated for 24 hours in an end-over-end shaker at 20-22 ^{o}C. After centrifugation, a sample of the supernatant was taken for phosphate analysis. Phosphate concentration was determined using an adapted molybdate blue method. The pH of the suspensions was measured in the re-mixed suspensions. For each data point, the total concentration of components of the system was calculated based on a book keeping of the concentrations of the added solutions.

The adsorption experiments were performed at the same total amount of phosphate and various levels of (bi)carbonate. The total initial phosphate concentration was 0.4 mmol l^{-1}. The added initial carbonate concentration was 0, 0.03, 0.1, 0.2, or 0.5 mol l^{-1}. The total background electrolyte concentration was 0.5 mol l^{-1} Na^{+}, which was achieved by adding the appropriate amount of $NaNO_3$. The experiments were done at two different levels of goethite, i.e. 3 and 9 g l^{-1}, resulting in two levels of loading of phosphate and a wide range of carbonate concentration.

An additional system was prepared at lower salt concentration. In these experiments, four levels of carbonate were used, including 0, 0.05, 0.1 and 0.2 mol l^{-1}. The total amount of sodium was adjusted to 0.2 mol l^{-1}, The systems contained 0.4 mmol l^{-1} phosphate and 6 g l^{-1} goethite. The goethite used in this set of experiments was from a different batch. It was also prepared using the above mentioned method. However, it has a slightly higher surface area (98.6 m^2 g^{-1}).

The amount of adsorbed phosphate was calculated from the difference between the total initial phosphate concentration and the final equilibrium concentration.

Carbonate Adsorption edges in a 'single ion' system

In order to study the carbonate adsorption in the absence of any specific competitor, adsorption edges of carbonate were measured in a system without phosphate. Three levels of carbonate (1.2, 2.2, and 3.2 mmol l^{-1}) were used. The systems contained 10 g l^{-1} goethite and 0.1 mol l^{-1} $NaNO_3$, in the pH range of 6.5 to 10.5. The used goethite was from the second batch with the surface area equals 98.6 m^2 g^{-1}. After equilibration and centrifugation, a sample of supernatant was taken for analysis. The carbonate concentration in the solution phase was measured with a TOC analyzer. The TOC analyzer was adapted to measure the carbonate concentration by excluding the acidification sequence and the procedure was carefully checked by measuring a series of organic and inorganic standard solutions.

Results and discussion

Quantum chemical derived CD values

The surface structure of adsorbed carbonate on goethite has been studied by in situ FTIR spectroscopy (Wijnja and Schulthess, 2001), (Villalobos and Leckie, 2001). The data have been reinterpreted by Hiemstra at al. (Hiemstra *et al.*, 2004, Ch 5). They have concluded that carbonate is adsorbed as a bidentate innersphere surface complex.

Rahnemaie et al. (Rahnemaie *et al.*, Ch 4) have used a method to derive the charge distribution of adsorbed phosphate complexes using quantum chemical calculation. Based on this method, the geometry of the bidentate surface complex of carbonate was derived using the software of Wavefunction (Spartan'04). The starting point in the calculation is a cluster with two Fe oxide octahedra serving as a template to mimic the goethite mineral (Rahnemaie *et al.*, Ch 4). The Fe-O distances (d=196 and 210 pm) and angles of the two octahedra represent the values found for goethite (Hazemann *et al.*, 1991). Additional protons are added resulting in the zero-charged cluster $Fe_2(OH)_6(OH_2)_4$ (z=0), which is given in Figure 1.

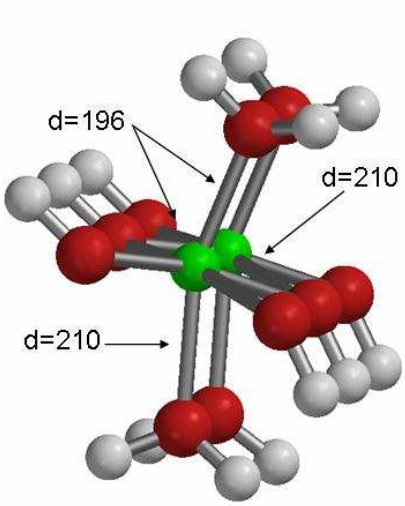

Figure 1. Two Fe(III)-O octahedra with Fe-O distances and angles as found in goethite (α-FeOOH). Big black spheres are oxygen, small white spheres are proton, and central gray spheres are iron.

The bidentate CO_3 complex was defined by exchanging both H_2O molecules on the top of the cluster against CO_3. These two exchanged ligands (Figure 1) are equivalent with the singly coordinated surface groups at the 110 face of goethite. The geometry optimizations were done using density functional theory (DFT). Pseudo potentials, defined in Spartan‘04 as LACVP+** (Los Alamos Core Valence Potentials) were used. This set comprises the 6-31+G** basis set for main group elements H-Ar. The final geometry was calculated with the Becket Perdue (BP86) model (Kong *et al.*, 2000) as presented in Figure 2.

In order to explore the effect of hydration, additional calculations were done by defining extra water molecules that interact via H bridges (O-H**…**O) with the bound CO_3^{-2} ion. We defined one H_2O per common O ligand in both Fe-O-C bonds. The non-coordinated oxygen of CO_3^{-2} was allowed to interact with three water molecules via O-H**…**H bridges. The results of the calculations are given in Table 1.

In Table 1, the O-C distance refers to the distance between the common O ligand and the C ion. The variation in both distances is indicated with a ± symbol. The C-O distance in Table 1 refers to the bond between the C ion and the outer O ligand. In addition, the Fe-O distance between the Fe ion and the common oxygen and the Fe-C distance are given. As shown in Table 1, hydration leads to rearrangements in the surface complex, as previously also observed for phosphate (Rahnemaie *et al.*, Ch 4).

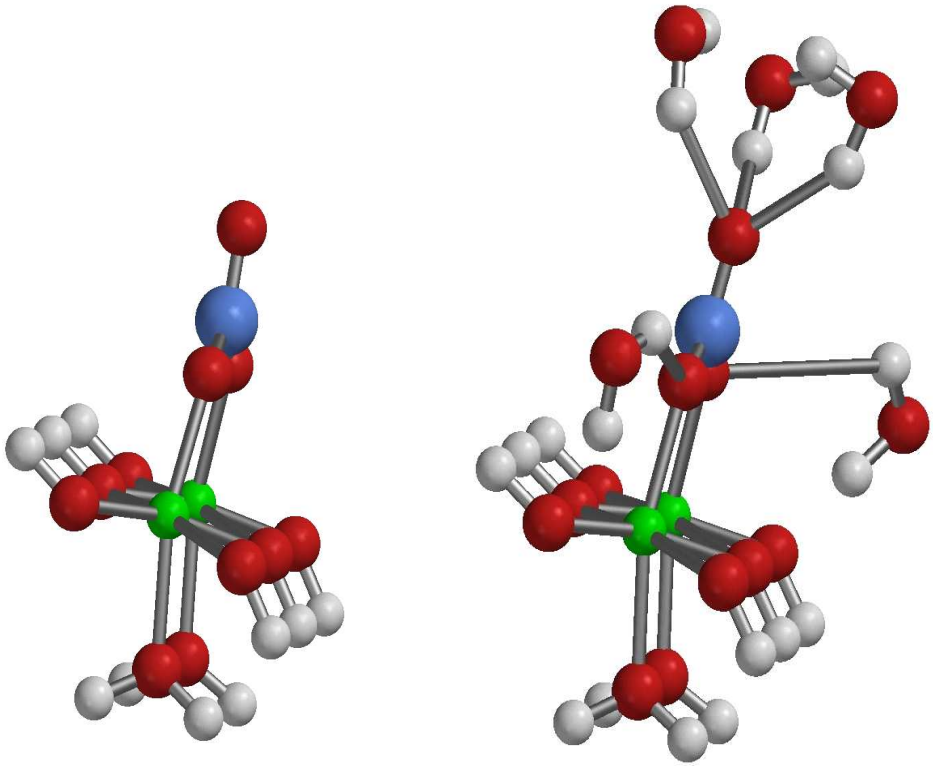

Figure 2. Two Fe(III)-O octahedra with a bidentate carbonate surface complex. Left hand side, the complex is formed by exchanging the CO_3^{-2} species with two-coordinated H_2O molecules that are equivalent with singly coordinated groups at the goethite interface. Right hand side, the hydrated bidentate CO_3 complex with one water molecule coordinating to each common oxygen of the carbonate complex and three water molecules are coordinating via H bonds with the outer oxygen ligand.

Table 1. The calculated average and variation (±) in distances (pm) in the geometry of non-hydrated and hydrated carbonate complexes optimized with the DFT-B86 model.

Species	O-C	C-O	Fe-O	Fe-C
≡Fe_2O_2CO non-hydrated	133.1±0.0	126.7	200.4±0.0	304.3±0.0
≡Fe_2O_2CO hydrated	131.3±0.1	129.3	203.1±0.4	303.6±0.8

The optimized C-O bonds were interpreted with the Brown bond valence approach (Brown and Altermatt, 1985), relating the bond valence **S** to the distance R as:

$$s = e^{-(R-R_0)/B} \quad [1]$$

in which B is a constant and R_0 is the element specific parameter. The value of R_0 is chosen such that the sum of the bond valences around the C ion corresponds to the formal C valence (z=+4). Using the B value equal to 42.1 pm leads to soft bond valences. The CD values are given in Table 2 for the non-hydrated as well as hydrated options. The results illustrate that the presence of hydration water leads to a more equal distribution of carbon charge over the three ligands. In case of an equal charge distribution (Pauling bond valence of 0.67 v.u.), the interfacial CD value would have been n_o=-1.33 v.u. and n_1=-0.67 v.u. The values for the hydrated surface species were assumed to be representative for the carbonate surface complex at the goethite water interface.

Table 2. CD values (n_0 and n_1 with $n_0 + n_1 = -2$ v.u.) based on the optimized geometries as given in Table 1 using soft bond valences (B=42.1).

Species	Non-hydrated		Hydrated	
	n_0	n_1	n_0	n_1
$\equiv Fe_2O_2CO$	-1.49	-0.51	-1.39	-0.61

Modeling primary charging

Rahnemaie et al. (Rahnemaie *et al.*, Ch 2) have modeled the primary charge of goethite using a charge distribution approach for electrolyte ions. The charge of the electrolyte ions is distributed over the two outer electrostatic planes of a Three Plane (TP) model. The relevant parameters are given in Table 3 and have been applied in the modeling of our experiments.

Table 3. Goethite interface parameters of Rahnemaie et al. (Rahnemaie *et al.*, Ch 2). The ion pair formation constants are based on the charge distribution of electrolyte ions in the outer part of the compact part of the double layer. The proton affinity constant for singly and triply coordinated surface groups was set to log K_H=9.0.

Ions	n_0	n_1	n_2	log K
Na^{+1}	0	0.50	0.50	-0.27
NO_3^{-1}	0	-0.67	-0.33	-0.53
C_1 F m^{-2}	1.00			
C_2 F m^{-2}	0.89			

Surface chemistry of phosphate

The phosphate surface complexation on goethite has been studied by Tejedor-Tejedor et al. (Tejedor-Tejedor and Anderson, 1990), using in situ CIR-FTIR. The main surface phosphate species identified is a bidentate surface complex. This complex is protonated at low pH. The fraction of protonated bidentate complexes increases with increasing surface coverage, which is due to the change of the particle charge induced by the binding of negatively charged phosphate. At high pH levels, some monodentate complexation may take place.

Recently, Rahnemaie et al. (Rahnemaie *et al.*, Ch 4) have interpreted the adsorption of PO_4 with the Charge Distribution (CD) model for inner- and outersphere surface complexation. They have used quantum chemical calculation to derive the geometry of the various surface complexes and derived the corresponding charge distribution. They have shown that phosphate is mainly adsorbed as a bidentate complex at low and intermediate PO_4 loading. At low pH and a relatively high PO_4 loading, phosphate is also adsorbed as a protonated monodentate complex. In the modeling, we used the phosphate adsorption parameters derived by Rahnemaie *et al.* (Rahnemaie *et al.*, Ch 4) as represented in Table 4.

Table 4. Surface speciation of phosphate as derived from modeling of phosphate adsorption edges using the CD model for inner- and outersphere surface complexation (Rahnemaie *et al.*, Ch 4).

Species	n_0	n_1	n_2	Log K
$FeOPO_3$	-0.83	-2.17	0	20.14 ± 0.07
$FeOPO(OH)_2$	-0.62	-0.38	0	29.90 ± 0.19
$Fe_2O_2PO_2$	-1.63	-1.37	0	29.54 ± 0.03
Fe_2O_2POOH	-1.42	-0.58	0	34.02 ± 0.05
$Fe_2O_2PO_2Na$	-1.42	-0.58	0	28.95 ± 0.02
$FeOPO_2OHNa$	-0.68	-1.32	1	27.89 ± 0.04

Phosphate-carbonate interaction

In Figure 3, the experimental phosphate adsorption is given as a function of pH, carbonate and phosphate loading, and electrolyte concentration. The data of Figure 3a, 3b, and 3c respectively refer to three levels of goethite concentration, i.e. 3, 9, and 6 g l^{-1}, which leads to 3 levels of phosphate loading. The salt concentration is 0.5 molar in Figure 3a and 3b, and 0.2 molar in Figure 3c.

The adsorption data show that carbonate ions compete with phosphate species for the surface sites. With increasing CO_3, the phosphate concentration in solution

increases due to decreasing adsorption of PO_4. The competitive effect of a certain CO_3 concentration is larger at a lower PO_4 level (compare Figure 3a and 3b).

The experimental data show that the maximum interaction between carbonate and phosphate ions takes places at the lower part of the pH range of our study. The competitive interaction of CO_3 decreases as the pH increases. It is very weak at pH above 10.5. These observed effects are partly due to the adsorption behavior of CO_3. As shown by Villalobos and Leckie ((Villalobos and Leckie, 2000), the binding of CO_3 in a closed system has a maximum value at a pH of about 6-7. It decreases at higher pH values.

CD-Modeling

Figure 3 presents the model description of all phosphate adsorption data, using the PO_4 parameters of Rahnemaie et al. (Rahnemaie *et al.*, Ch 4) given in Table 4. The affinity constants for the carbonate species were optimized by a simultaneous fit to all data of Figure 3. The CD modeling revealed that only using the bidentate carbonate surface complex, $\equiv Fe_2O_2CO$, does not lead to a satisfactory description of the interaction. The data were described well when formation of a sodium-bicarbonate surface complex, i.e. $\equiv Fe_2O_2CONa$, was included. It indicates that the bidentate carbonate surface species may interact with a sodium ion. Such an interaction is also found for CO_3^{-2} in solution with the formation of $NaCO_3^{-1}(aq)$ and $Na_2CO_3^{0}(aq)$. We note that a similar complex has been suggested by Villalobos and Leckie (Villalobos and Leckie, 2000) and Hiemstra et al. (Hiemstra *et al.*, 2004, Ch 5).

One may also expect the formation of outersphere surface complexes for carbonate at high pH, since it has been found for similar anions (in terms of charge) such as selenate and sulfate, by in situ FTIR spectroscopy (Peak *et al.*, 1999), (Wijnja and Schulthess, 2000). Formation of an outersphere surface complex has not been detected for carbonate by spectroscopy, which might be related to the studied pH range. However, in our experiment, including a monodentate outersphere $NaHCO_3$ complex, i.e. $FeOH\mathbf{\ldots}NaHCO_3$, which becomes non-protonated at higher pH range, i.e. $FeOH\mathbf{\ldots}NaCO_3$, leads to a better description of the adsorption data at the mid (≈ 8-10) and high pH range (>10). The charge distribution value of these complexes was derived from modeling of the adsorption data.

The reaction of innersphere and outersphere surface complexes of carbonate were formulated in the CD model based on the equations given in Table 5. The optimized affinity constants of the adsorbed carbonate complexes and their charge distribution based on the quantum chemical calculation for innersphere complexes or based on the optimization for outersphere complexes are represented in Table 6.

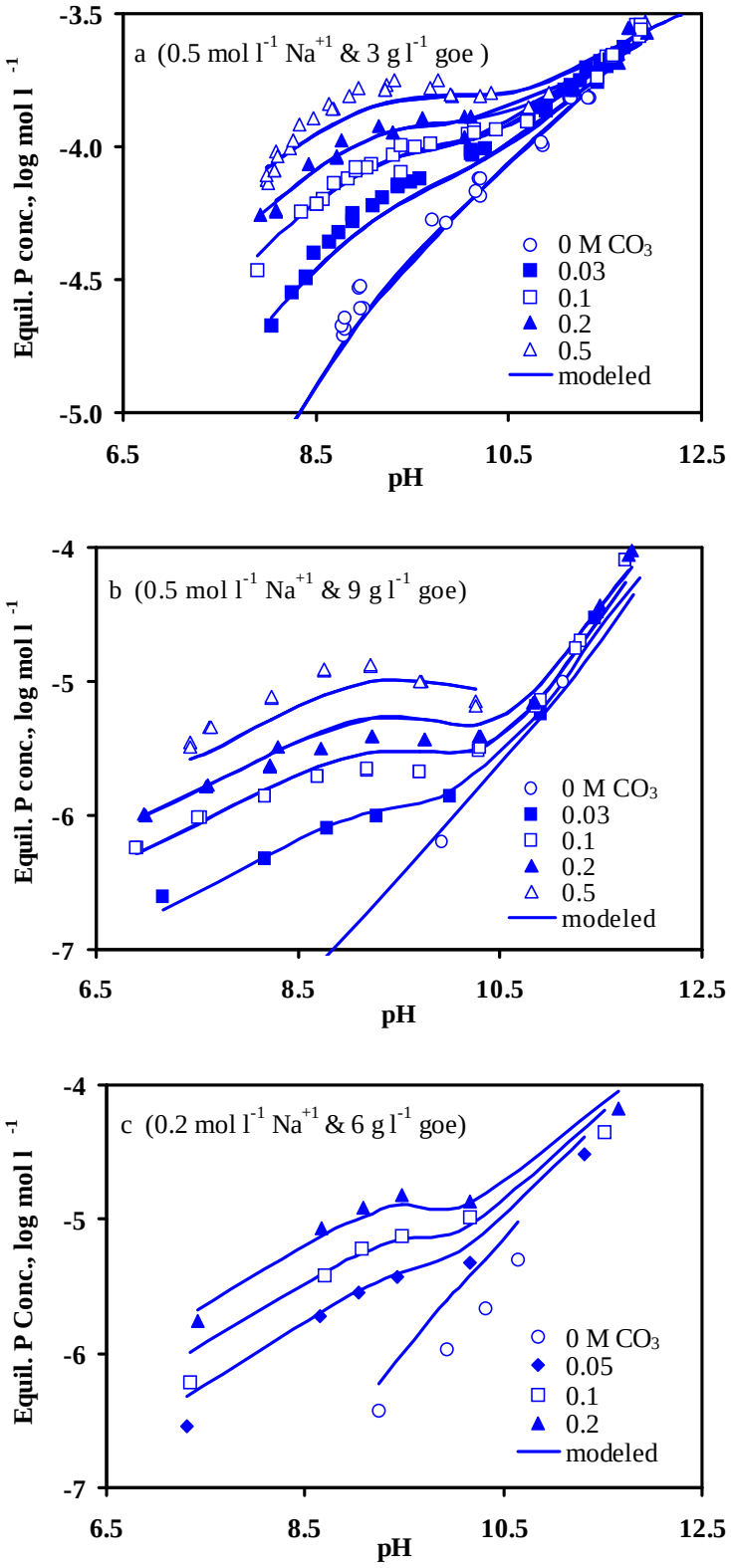

Figure 3. Experimental data and model description of phosphate adsorption edges as a function of different levels of carbonate, pH, and salt concentration. The total amount of phosphate is 0.4 mmol l^{-1}. The goethite concentration is 3, 9, and 6 g l^{-1} in Figure 3a, 3b and 3c respectively, which leads to three levels of phosphate loading. The lines are the simultaneous model description of the

equilibrium phosphate concentration. The modeling was done with the CD model for inner- and outersphere surface complexation using the phosphate surface speciation given by Rahnemaie et al. (Rahnemaie *et al.*, Ch 4), and the electrolyte parameters of Rahnemaie et al. (Rahnemaie *et al.*, Ch 2). The affinity constants of adsorbed carbonate complexes were optimized on the data as well as the CD values for the outersphere complexes.

Table 5. Carbonate reactions with the singly coordinated groups at goethite surface. The n_0 and n_1 values define the charge distribution of a surface complex.

Reaction	$\log K$
$\equiv 2FeOH^{-1/2} + 2H^{+1}(aq) + CO_3^{-2}(aq) \Leftrightarrow \equiv Fe_2O_2^{n_0+1}CO^{n_1} + 2H_2O$	$\log K_{Fe_2O_2CO}$
$\equiv 2FeOH^{-1/2} + 2H^{+1}(aq) + Na^{+1}(aq) + CO_3^{-2}(aq) \Leftrightarrow \equiv Fe_2O_2^{n_0+1}CO^{n_1}Na^{+1} + 2H_2O$	$\log K_{Fe_2O_2CONa}$
$\equiv FeOH^{-1/2} + H^{+1}(aq) + Na^{+1}(aq) + CO_3^{-2}(aq) \Leftrightarrow \equiv FeOH^{-1/2}\cdots^{n_1} NaHCO_3^{n_2}$	$\log K_{FeOH^{-1/2}\cdots NaHCO_3}$
$\equiv FeOH^{-1/2} + Na^{+1}(aq) + CO_3^{-2}(aq) \Leftrightarrow \equiv FeOH^{-1/2}\cdots^{n_1} NaCO_3^{n_2}$	$\log K_{FeOH^{-1/2}\cdots NaCO_3^{-1}}$

Table 6. Surface speciation of carbonate as derived from modeling of the carbonate-phosphate adsorption edges. The modeling was done using the CD approach for the inner- and outersphere surface complexes.

Species	n_0	n_1	n_2	log K
Fe_2O_2CO	-1.39	-0.61	0	21.70 ± 0.07
Fe_2O_2CONa	-1.39	-0.61	1[a]	22.38 ± 0.15
$FeOH\ldots NaHCO_3$	0	0.46 ± 0.06	-0.46 ± 0.06	12.72 ± 0.07
$FeOH\ldots NaCO_3$	0	-0.12 ± 0.30	-0.88 ± 0.30	2.13 ± 0.10

[a] The charge was placed here by definition since the model showed that almost the total charge remains at this plane

With reference to Figure 3, the model description is slightly different for different loading. It may relate to the relatively different adsorption of carbonate surface complexes at different loading. Individual modeling of these three data sets revealed that at higher loading of carbonate and phosphate species, the Fe_2O_2CONa species is of more importance than at low loading.

Figure 4 illustrates the calculated phosphate and carbonate adsorption edges based on the total adsorbed phosphate and carbonate at the surface, using the parameters derived from the data in Figure 3.

Figure 4a, 4b, and 4c demonstrate the effect of different levels of carbonate on phosphate adsorption. Figure 4a shows that the addition of carbonate ions decreases the phosphate adsorption. This effect becomes stronger with increasing the carbonate concentration. However, in relative terms the effect decreases. Figure 4b and 4c show the situation at a lower loading of goethite with phosphate and carbonate ions. Note that the amount adsorbed in Figure 4b is roughly one third of the amount adsorbed in Figure 4a due to the lower loading.

Figure 4c has an intermediate loading, between 4a and 4b, and a lower salt level. The decrease in salt level will lead to a lowering of the electrostatic interactions. The net electrostatic effect on the phosphate binding is for these data always repulsive, meaning that the lowering in salt will lead to a lower amount adsorbed. It is clear from the results that loading is the dominant factor.

Figure 4d, 4e, and 4f demonstrate the carbonate adsorption edges based on the total adsorbed carbonate at the surface, which were derived from the phosphate-carbonate adsorption edges (Figure 3). The figures show that carbonate adsorption is increased with increasing the carbonate loading. The surface coverage with carbonate is for these conditions very high and is higher than the amount of phosphate adsorbed. The value of 3 $\mu mol\ m^{-2}$ is close to the theoretical adsorption maximum assuming bidentate adsorption. The relative adsorption of carbonate is increased when the total number of surface sites per liter solution is increased (For instance, Figure 4e vs. 4d).

The adsorption of carbonate in different carbonate loading is relatively less dependent on pH than phosphate, since the availability of surface sites is strongly regulated by phosphate adsorption. The figures show that the maximum adsorption of carbonate is at about pH 7-9, which depends on the loading and salt concentration.

Adsorption of carbonate in a 'single ion' system

The binding properties of CO_3 were derived from a binary system, containing carbonate and phosphate. Only the affinities of adsorbed carbonate species and the CD values of outersphere surface complexes of carbonate were optimized. The adsorption of carbonate in a 'single ion' system was measured to examine whether the CD model with derived affinities is capable to predict carbonate adsorption in a 'single ion' system, at a much lower carbonate loading and background salt concentration. In fact, this system is much closer to situations that normally occur in natural systems.

In Figure 5a the experimental data of the carbonate adsorption edges are given as a function of pH and carbonate concentration. The calculated lines are pure model prediction using the values of Table 6. It shows that within the uncertainty and taking

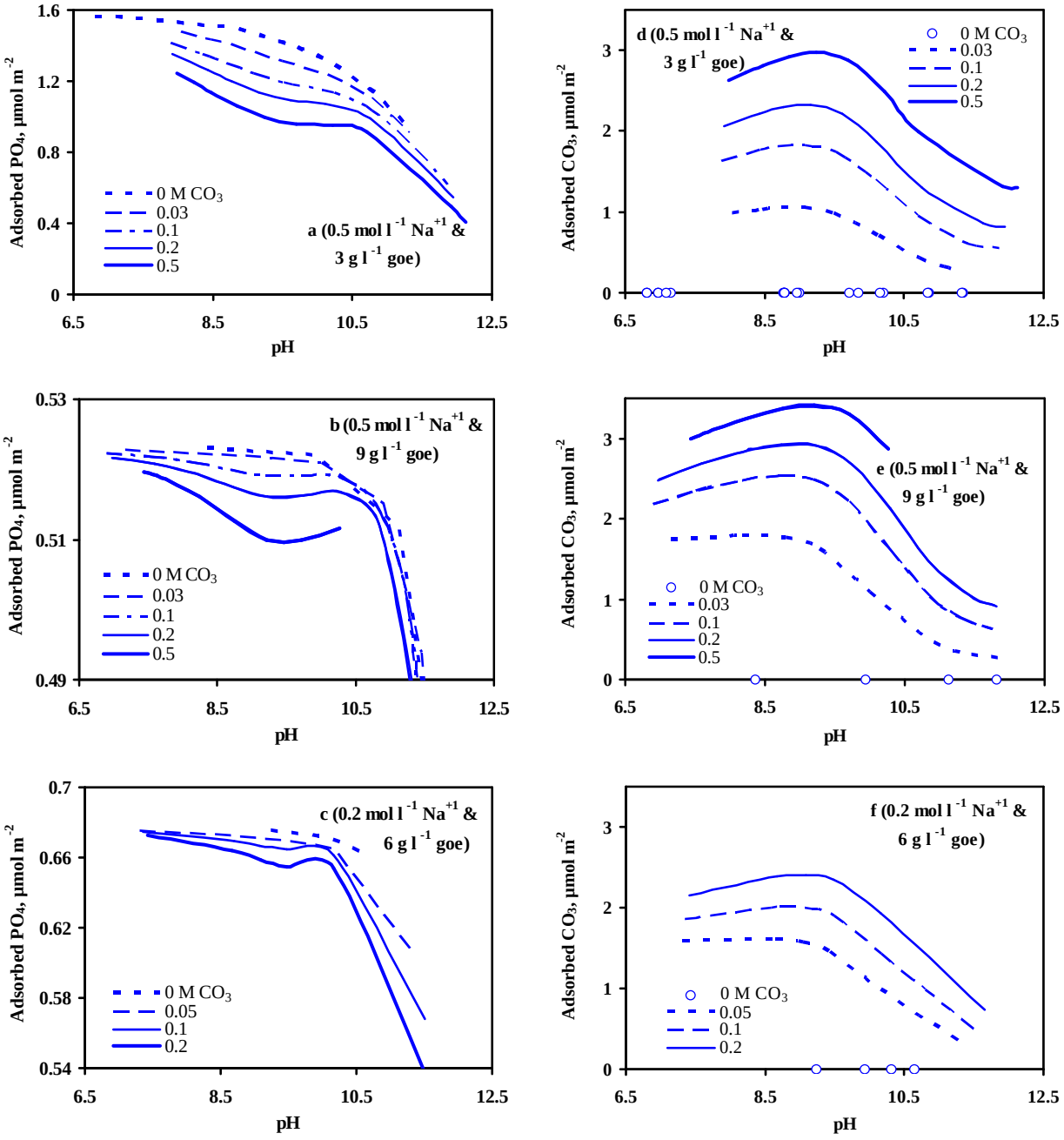

Figure 4. Phosphate and carbonate adsorption edges as a function of pH, phosphate and carbonate loading, and salt concentration based on the amount of adsorbed ion at the surface. The data were derived from phosphate-carbonate adsorption edges (Figure 3).

into account the large differences between the experimental conditions, the model can successfully predict the carbonate adsorption edges.

To illustrate the relative importance of carbonate surface complexes, the surface speciation of carbonate for these conditions is given in Figure 5b for a level of carbonate loading. It shows that in relatively low ionic strength (0.1 M), which is

closer to the natural media, the bidentate complex dominates the carbonate adsorption. The sodium-carbonate surface complex contributes weakly in carbonate adsorption below pH 9. The monodentate outersphere $NaHCO_3$ complex becomes important above pH 8, while the monodentate outersphere $NaCO_3$ complex almost has no effect in studied pH range.

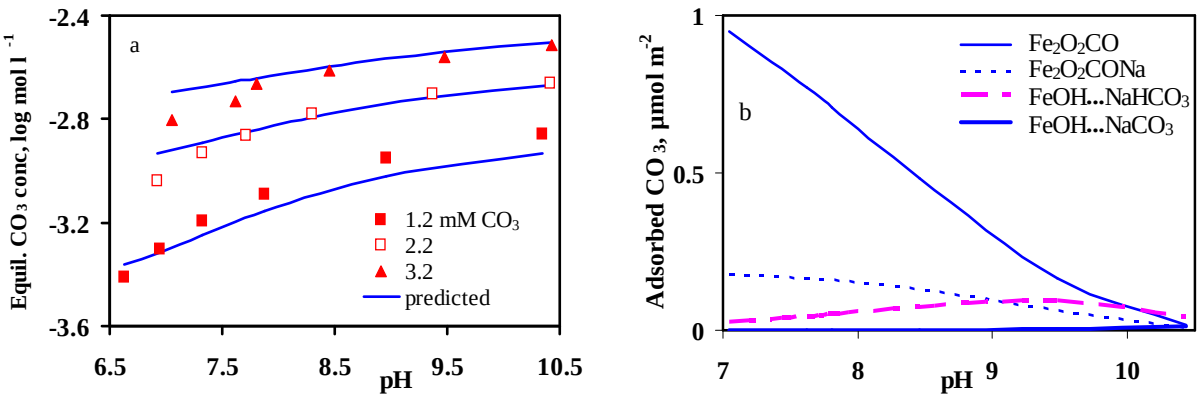

Figure 5. (a) experimental data of carbonate adsorption edges in a single ion system as a function of pH and carbonate concentration in 0.1 M $NaNO_3$. The lines show pure predicted equilibrium carbonate concentration taking into account the carbonate surface speciation as given in Table 6. Figure b shows the corresponding surface speciation of adsorbed carbonate complexes for 3.2 mM total carbonate at 10 g l^{-1} goethite.

Modeling of the adsorption data using fitted CD value

The charge distribution of adsorbed ions has often been used as a fitting parameter (Hiemstra and VanRiemsdijk, 1996), (Rietra *et al.*, 2001), (Hiemstra *et al.*, 2004, Ch 5), (Tadanier and Eick, 2002). To compare the quality of the fitting and the calculated CD values with the above given approach, the adsorption data of phosphate and carbonate were modeled in such a way that the CD value of phosphate and carbonate adsorbed complexes were treated as fitting parameters. The CD value and affinity of adsorbed phosphate complexes were taken from Rahnemaie et al. (Rahnemaie *et al.*, Ch 4), while the CD and affinity of adsorbed carbonate complexes were optimized on the data. The result is given in Table 7.

Results show that the fitted CD of carbonate complex is relatively close to the one derived from quantum chemical calculation. The model description is almost the same as in the previous option.

Table 7. The surface speciation of carbonate at goethite surface as derived from modeling of the carbonate-phosphate adsorption edges. The modeling was done using the CD model for inner- and outersphere surface complexes. The surface speciation of phosphate was used according to Rahnemaie et al. (Rahnemaie *et al.*, Ch 4).

Species	n_0	n_1	n_2	log K
$Fe_2O_2PO_2$	-1.26	-1.74	0	29.92
Fe_2O_2POOH	-0.85	-1.15	0	36.37
$Fe_2O_2PO_2Na$	-1.44	-0.88	0.32	29.56
Fe_2O_2CO	-1.09 ± 0.03	-0.91 ± 0.03	0	22.31 ± 0.06
Fe_2O_2CONa	-	-	-	-
FeOH**…**$NaHCO_3$	0	0.55 ± 0.05	-0.55 ± 0.05	13.20 ± 0.13
FeOH**…**$NaCO_3$	0	0	-1[a]	2.34 ± 0.17

[a] The charge was placed by definition since the model showed that almost the total charge remains at this plane

Conclusions

- The CD model for inner- and outersphere surface complexation can successfully describe carbonate adsorption data using the derived charge distribution from quantum chemical calculation. In the CD model, the charge distribution was used for adsorbed ions of phosphate, carbonate, and salt ions, which were adsorbed either as inner- or as outersphere surface complexes.
- Carbonate ions bind mainly as an innersphere bidentate surface complex. At high salt concentration, a sodium-carbonate complex contributes to the carbonate adsorption. At high carbonate loading and relatively high pH, an outersphere monodentate sodium-bicarbonate complex, i.e. FeOH**…**$NaHCO_3$, may form. This complex becomes non-protonated at higher pH range.
- Carbonate binds much weaker than phosphate at the goethite surface.
- Maximum adsorption of carbonate take places at pH 7-9, which depends on the carbonate loading and the ionic strength.

Acknowledgments

The authors thank the Ministry of Science, Research, and Technology of Iran (MSRT) for financial support and Mr. A Korteweg (Laboratory of Physical and Colloid Chemistry) for the BET analysis.

References

Arai, Y., D. L. Sparks, and J. A. Davis (2004). Effects of dissolved carbonate on arsenate adsorption and surface speciation at the hematite-water interface. *Environ. Sci. Technol.* **38**(3): 817.

Atkinson, R. J., P. A.M., and J. P. Quirk (1967). Adsorption of potential-determining ions at the ferric oxide-aqeous electrolyte interface. *J. Physic. Chem.* **71**: 550.

Brown, I. D. (2002). The chemical bond in inorganic chemistry: The bond valence model. Oxford, Oxford University Press.

Brown, I. D., and D. Altermatt (1985). Bond-valence parameters obtained from a systematic analysis of the inorganic crystal-structure database. *Acta Crystallographica Section B-Structural Science* **41**(AUG): 244.

Geelhoed, J. S., T. Hiemstra, and W. H. Vanriemsdijk (1997). Phosphate and sulfate adsorption on goethite: Single anion and competitive adsorption. *Geochim. Cosmochim. Acta* **61**(12): 2389.

Hazemann, J. L., J. F. Berar, and A. Manceau (1991). Rietveld studies of the aluminium-iron substituation in synthetic goethite. *Material Science Forum* **79**: 821.

Hiemstra, T., J. C. M. Dewit, and W. H. Vanriemsdijk (1989). Multisite proton adsorption modeling at the solid-solution interface of (hydr)oxides - a new approach .2. Application to various important (hydr)oxides. *J. Colloid Interface Sci.* **133**(1): 105.

Hiemstra, T., R. Rahnemaie, and W. H. Van Riemsdijk (2004, Ch 5). Surface complexation of carbonate on goethite: Ir spectroscopy, structure and charge distribution. *J. Colloid Interface Sci.* **278**(2): 282.

Hiemstra, T., and W. H. Vanriemsdijk (1996). A surface structural approach to ion adsorption: The charge distribution (cd) model. *J. Colloid Interface Sci.* **179**(2): 488.

Kong, J., C. A. White, A. I. Krylov, D. Sherrill, R. D. Adamson, T. R. Furlani, M. S. Lee, A. M. Lee, S. R. Gwaltney, T. R. Adams, et al. (2000). Q-chem 2.0: A high-performance ab initio electronic structure program package. *Journal of Computational Chemistry* **21**(16): 1532.

Olsen, S. R., and L. A. Dean (1954). Estimation of available phosphorus in soils by extraction with sodium bicarbonate. *Washington, D.C. : U.S. Dept. of Agriculture* **19**.

Peak, D., R. G. Ford, and D. L. Sparks (1999). An in situ atr-ftir investigation of sulfate bonding mechanisms on goethite. *J. Colloid Interface Sci.* **218**(1): 289.

Rahnemaie, R., T. Hiemstra, and W. H. Van Riemsdijk (Ch 2). A new surface structural approach to ion adsorption: Tracing the location of electrolyte ions.

Rahnemaie, R., T. Hiemstra, and W. H. Van Riemsdijk (Ch 4). Phosphate adsorption on the goethite: Surface speciation in relation to charge distribution.

Rietra, R., T. Hiemstra, and W. H. Van Riemsdijk (2001). Interaction between calcium and phosphate adsorption on goethite. *Environ. Sci. Technol.* **35**(16): 3369.

Tadanier, C. J., and M. J. Eick (2002). Formulating the charge-distribution multisite surface complexation model using fiteql. *Soil Sci. Soc. Am. J.* **66**(5): 1505.

Tejedor-Tejedor, M. I., and M. A. Anderson (1990). Protonation of phosphate on the surface of goethite as studied by cir-ftir and electrophoretic mobility. *Langmuir* **6**(3): 602.

Vangeen, A., A. P. Robertson, and J. O. Leckie (1994). Complexation of carbonate species at the goethite surface - implications for adsorption of metal-ions in natural-waters. *Geochim. Cosmochim. Acta* **58**(9): 2073.

Villalobos, M., and J. O. Leckie (1999). Carbonate adsorption onto goethite. A chemical, modeling and spectroscopic study. *Abstr. Pap. Am. Chem. Soc.* **217**: 023.

Villalobos, M., and J. O. Leckie (2000). Carbonate adsorption on goethite under closed and open co2 conditions. *Geochim. Cosmochim. Acta* **64**(22): 3787.

Villalobos, M., and J. O. Leckie (2001). Surface complexation modeling and ftir study of carbonate adsorption to goethite. *J. Colloid Interface Sci.* **235**(1): 15.

Villalobos, M., M. A. Trotz, and J. O. Leckie (2001). Surface complexation modeling of carbonate effects on the adsorption of cr(vi), pb(ii), and u(vi) on goethite. *Environ. Sci. Technol.* **35**(19): 3849.

Wazne, M., G. P. Korfiatis, and X. G. Meng (2003). Carbonate effects on hexavalent uranium adsorption by iron oxyhydroxide. *Environ. Sci. Technol.* **37**(16): 3619.

Wijnja, H., and C. P. Schulthess (2000). Vibrational spectroscopy study of selenate and sulfate adsorption mechanisms on fe and al (hydr)oxide surfaces. *J. Colloid Interface Sci.* **229**(1): 286.

Wijnja, H., and C. P. Schulthess (2001). Carbonate adsorption mechanism on goethite studied with atr- ftir, drift, and proton coadsorption measurements. *Soil Sci. Soc. Am. J.* **65**(2): 324.

7

Determination of the Effective Reactive Surface Area of Metal (Hydr)oxides in Soils

Abstract

Any application of surface complexation modeling in multicomponent systems like soils and sediments requires information on the reactive surface area (RSA) of the various reactive phases. Gas adsorption, which is used to measure the RSA in model systems like a pure mineral, is problematic for soils since they are heterogeneous. An approach has been developed to estimate the effective RSA of metal oxides in soils by means of surface complexation modeling. This approach uses the CD model for inner- and outersphere surface complexation with defined binding parameters to link the effective reactive surface area to the total amount of a reversibly bound ion. For this purpose, phosphate was chosen, since it does not bind to the organic phase and since it is present in all biogeochemical environments. The adsorption parameters of phosphate, carbonate, calcium, and relevant ion pairs were implemented in the model. The model was successfully applied to a series of phosphate extraction data, using the sodium-bicarbonate extraction. The effective RSA and the amount of reversibly bound phosphate in the soil were fitted. The calculated effective reactive surface area strongly correlates with the oxalate extraction method. The model shows that there is a considerable amount of reversibly bound phosphate at oxidic mineral surfaces. At 0.5 M sodium bicarbonate concentration (adjusted to pH 8.5) and about 1/20 soil-solution ratio only about 25% of the total adsorbed phosphate is extracted from soils. These conditions are in accordance with the widely used Olsen phosphate extraction method that is used in soil science to estimate phosphate availability.

Keywords: Surface complexation; Surface area; Phosphate; Sodium bicarbonate; Extraction; Olsen extraction method; CD model; MUSIC model;

Introduction

The surface composition of natural particles and the solution composition in natural systems are continuously changing, since these systems are thermodynamically open and multicomponent. Any change in the system composition may lead to a change in the competitive and cooperative adsorption of ions. Surface complexation models (SCM) have been developed to account for the complex interaction between ions and mineral surfaces. Ideally, surface complexation models may predict changes in the situation where the experimental data are not available or difficult to achieve.

Mineral surfaces are usually charged, radiating an electric field, which interacts with adsorbing ions. Surface complexation models account for the electrostatic interaction. Electrostatic models require an expression per unit of reactive surface area (RSA). Any application of electrostatic surface complexation models to natural systems like soils, sediments, and aquatic media requires information on the reactive surface area.

In model systems with a single metal oxide, the surface area is usually determined by gas adsorption (BET method). This method cannot be used in natural soils since soils are heterogeneous in the sense that part of the surface will be non-reactive. Several approaches have been used to estimate the reactive surface area of soil materials, in particular focusing on Fe and Al (hydr)oxides.

Most frequently, soils are extracted to determine the amount of Fe and/or Al (hydr)oxides. Extraction with Dithionite-Citrate-Bicarbonate (DCB) (Mehra and Jackson, 1960), or NH_4-oxalate (Schwertm, 1973), (Kinniburgh and Smedley, 2001), (Weng *et al.*, 2001), or ascorbate (Kostka and Luther, 1994), (Meima and Comans, 1998) are interpreted as yielding respectively the total and the reactive fraction of iron (hydr)oxides. The next step is the transformation of the extracted amount to a corresponding surface area. The specific surface area of reactive iron oxides is usually assumed to be equal to the surface area of Hydrous Ferric Oxide, HFO (Davis *et al.*, 1978), (Dzombak and Morel, 1990). The DCB extraction may represent the sum of the reactive and the more crystalline Fe fraction of soils. Goethite is the dominant Fe-oxide mineral in most soils. The surface area of goethite may be in the order of 20-100 $m^2\ g^{-1}$, based on the measured values for synthetic goethites.

Another approach is to apply SCM with known binding parameters to soil adsorption data and fit the effective reactive surface area of metal oxides, needed to explain the experimental adsorption (Lofts and Tipping, 1998). If adsorption data of heavy metals are used, the major disadvantage is that the metal binding in soils is often dominated by the organic fraction of the soil (Weng *et al.*, 2001). To assess a realistic apparent effective reactive surface area for metal soil oxides the use of a dominant binding anion is more appropriate. Phosphate can be considered as a good candidate.

Phosphorus is an essential nutrient for organisms and therefore present in most biogeochemical environments. If expressed per unit surface area, it is available in large quantities in soils and sediments, even at very low solution concentrations. This is due to the very high affinity character of this anion for Al and Fe (hydr)oxides. Moreover, the ubiquitous presence of phosphate in soils and sediments implies that the charge properties of metal oxides are strongly influenced by the presence of adsorbed phosphate. It puts forward that any successful application of SCM in natural systems will benefit from the incorporation of this ion in the description of the adsorption of

other ions under study. In addition, one should account for Ca^{+2} as an omnipresent ion, since it may strongly interact with phosphate (Rietra *et al.*, 2001b).

The accommodation of PO_4 in surface complexation modeling requires information on the initial reversible adsorbed phosphate fraction. There are several methods to estimate the available P fraction in soils. These methods use salt, acidic, or basic solutions to desorb readily extractable P from soil. Olsen and Dean (Olsen and Dean, 1954) proposed a method to estimate plant available phosphorus in the soils. The Olsen method uses 0.5 M $NaHCO_3$ adjusted to pH 8.5 to extract P from soils. In this method, increase of soil pH leads to a decrease of the cooperative adsorption of Ca, which may stimulate desorption of P from soil. Carbonate ions at a high concentration will be able to compete with the phosphate ions for the same sites on the mineral surfaces. The competition will release a part of the adsorbed phosphate ions (Rahnemaie *et al.*, Ch 6). A second function of bicarbonate ions is the simultaneous decrease of the Ca^{+2} activity by producing less soluble calcium carbonate. A lower Ca^{+2} activity will decrease the calcium binding at the metal oxide surface and decrease the cooperative interaction with adsorbed phosphate ions (Rietra *et al.*, 2001b). As a result, more phosphate will desorb. A lower Ca^{+2} activity also contributes to the elimination of the precipitation of secondary Ca-phosphates. A third effect of a high HCO_3^{-1} concentration is the buffering of the pH at a high value, where the phosphate binding is less significant. This triple action makes 0.5 M $NaHCO_3$ a relevant P extractant for both acid and calcareous soils.

The aim of this study is to use the $NaHCO_3$ extraction method to determine the effective reactive surface area of the metal oxides in soils. Simultaneously, the reversible phosphate fraction can be determined. The extraction will be interpreted with surface complexation modeling. In this system, the interactions are strongly dominated by PO_4^{-3} and CO_3^{-2}, while the ionic strength and the ions in double layer are fully dominated by the Na^+ and HCO_3^{-1} ions. Moreover, binding of sulfate at the high pH (8.5) is not relevant (Rietra *et al.*, 2001a) and any influence of Ca^{+2} will be limited (low Ca^{+2} activity). The created system contains most ingredients to treat it as a semi-binary system.

To test the method for the determination of the surface area, we will use an excellent and extensive data set published by Barrow and Shaw (Barrow and Shaw, 1976b), (Barrow and Shaw, 1976c), (Barrow and Shaw, 1976a) comprising a series of experiments done on two Australian soils. We will evaluate the main characteristics of these data sets, i.e. the effect of variation in the bicarbonate concentration and soil-solution ratio on the amount of soil extractable phosphorus. These data will be analyzed with the Charge Distribution (CD) model for inner- and outersphere surface complexation (Rahnemaie *et al.*, Ch 2). The model parameters are taken from

Rahnemaie et al. (Rahnemaie *et al.*, Ch 2), (Rahnemaie *et al.*, Ch 3), (Rahnemaie *et al.*, Ch 4), (Rahnemaie *et al.*, Ch 6). Authors have studied the effect of the electrolyte ions on the surface charge and the effects of carbonate and phosphate loading, pH, and ionic strength on the adsorption of phosphate by goethite in single ion and PO_4-CO_3 competition systems.

Theory and concept

In metal oxide systems, phosphate ions can be adsorbed on the surface or be present in solution. The total amount in the system is represented by the sum of the ions in both compartments of the system:

$$T_P = A_r \Gamma_P + \rho^{-1} C_P \quad [1]$$

in which T_P is total reversibly bound fraction of adsorbed phosphate in mol kg^{-1}, A_r is specific effective reactive surface area in m^2 kg^{-1}, Γ_P is the amount of adsorbed phosphate in mol m^{-2}, ρ is solid-solution ratio in kg l^{-1} and C_P is the solution concentration of phosphate in mol l^{-1}. In soil, the total amount of phosphate is usually different from the reversibly bound fraction T_P, since part of the phosphate may be present in Ca, Al, and Fe phosphate minerals, or occluded in metal hydroxide precipitates. Via an extraction of the soil, the ortho-phosphate concentration C_P in solution is experimentally determined.

The phosphate adsorption isotherm is the actual link between the solution concentration, C_P, and its concentration on the surface, Γ_P. Surface complexation models are the typical tool to derive the adsorption Γ_P on the basis of the measured concentration C_P in solution. The total amount of reversibly bound phosphate T_P can be found for a given solid solution ratio ρ, once the effective reactive surface area A_r is known. Both parameters (T_P and A_r) are unknown, but can be derived in principle by analyzing the solution concentration C_P in extracts with two (or more) different solid-solution ratios ρ, and corresponding calculation of Γ_P for these systems with the CD model.

Soil characteristics and method of experiments

Barrow and Shaw (Barrow and Shaw, 1976c) studied the effect of the period of desorption, the effect of soil-solution ratio, the bicarbonate concentration, and the pH

on the amount of extractable phosphorous from the soil. They used sodium bicarbonate as an extraction solution. The main difference with the Olsen extraction is the much longer extraction time (16 hours vs. 30 minutes).

Barrow and Shaw used in their experiments mainly a native yellowish-brown loamy sandy soil (Bakers Hill), which had never been fertilized with phosphate (Barrow and Shaw, 1976b). The pH of the soil in 0.01 M calcium chloride is 5.5. The soil has a CEC of 103 meq kg^{-1}, which binds exchangeable sodium 1.3, potassium 3.8, magnesium 9.6, and calcium 34 meq kg^{-1}. The extractable amount of iron and aluminum was determined with NH_4 oxalate extraction (Coffin method) resulting in 0.24% Fe and 0.17% Al (Barrow and Shaw, 1976b), which are equivalent with 0.46% $Fe(OH)_3$ and 0.49% $Al(OH)_3$.

Since the native soil had never been fertilized by phosphorus, the amount of P in the soil is expected to be low. The effect of the bicarbonate concentration on the desorption of the phosphate has been studied by adding a certain amount of P (400 mg P kg^{-1} soil equal to 12.9 mmol P kg^{-1} soil) to the soil sample that has been incubated at 70 ^{o}C for 3.75 days. It has been shown that this treatment is equivalent with an equilibration time at 25 ^{o}C of about 320 days (Barrow and Shaw, 1976c). The sub samples were extracted (16 hours) with sodium bicarbonate solution, ranging from 0 to 1 molar. NaCl was added to these extraction solutions to reach a Na^+ concentration of 1 M. A range of soil-solution ratios was used in the extraction, i.e. 1/6, 1/12, 1/24, 1/60, 1/120, 1/300. The phosphate and carbonate concentration has been measured from samples of the supernatant after centrifuging and filtering.

In a second experiment, Barrow and Shaw (Barrow and Shaw, 1976b) have used a different soil, i.e. a loamy soil from Wungong, Western Australia. The pH of this soil was measured in 0.01 M $CaCl_2$ as 5.4. The CEC of the soil was 131 meq kg^{-1}. It has exchangeable sodium 3.1, potassium 2.4, magnesium 2.1, and calcium 30 meq kg^{-1}. The extractable amount of iron and aluminum was determined with a NH_4 oxalate extraction (Coffin method) resulting in 5.4% Fe and 1.0% Al (Barrow and Shaw, 1976b), which are equivalent with 10.32% $Fe(OH)_3$ and 2.89% $Al(OH)_3$. In this experiment, four levels of phosphate (600, 900, 1200, and 1500 mg P kg^{-1} soil) have been added to the soil samples and then incubated for 21 days at 25 ^{o}C. After that, samples were shaken for 16 hours with 0.5 M sodium bicarbonate.

Surface complexation modeling

In this study, the adsorption behavior, i.e. the link between Γ_P and C_P, was calculated with the CD model for inner- and outersphere surface complexation

(Rahnemaie *et al.*, Ch 2) for the variable conditions used in the experiments of Barrow and Shaw. The model parameters (Table 1) have been determined studying electrolyte ion binding and the carbonate-phosphate interaction on goethite (Rahnemaie *et al.*, Ch 2), (Rahnemaie *et al.*, Ch 3), (Rahnemaie *et al.*, Ch 4), (Rahnemaie *et al.*, Ch 6). In this approach, we will implicitly assume that all oxidic surfaces present behave similar to goethite. The surface area that is determined in this way is thus not equal to the area of goethite in the soil but should be seen as an effective RSA for the mixture of metal (hydr)oxides.

Table 1. The affinity of ion pairs, phosphate, and carbonate and the charge distribution of adsorbed complexes at the solid-solution interface of goethite (Rahnemaie *et al.*, Ch 2), (Rahnemaie *et al.*, Ch 3), (Rahnemaie *et al.*, Ch 4), (Rahnemaie *et al.*, Ch 6). The capacitances of inner and outer Stern layers were respectively set equal to 1.0 and 0.89 F m^{-2}.

Species	$\mathbf{n_0}$	$\mathbf{n_1}$	$\mathbf{n_2}$	**log K**
$FeOH_2$	1	0	0	9.0
Fe_3OH	1	0	0	9.0
FeOH-Na	0	0.5	0.5	-0.27
Fe_3O-Na	0	0.5	0.5	-0.27
$FeOH_2$-Cl	1	-1	0	8.34
Fe_3OH-Cl	1	-1	0	8.34
FeOHCa	0.22	1.78	0	3.21
Fe_3OCa	0.22	1.78	0	3.21
FeOHCaOH	0.22	0.78	0	5.48
Fe_3OCaOH	0.22	0.78	0	5.48
FeOH-Ca	0	2	0	3.15
Fe_3O-Ca	0	2	0	3.15
$Fe_2(OH)_2Mg$	0.60	1.40	0	4.39
Fe_6O_2Mg	0.60	1.40	0	4.39
$Fe_2(OH)_2MgOH$	0.60	0.40	0	7.63
Fe_6O_2MgOH	0.60	0.40	0	7.63
$FeOPO_3$	-0.83	-2.17	0	20.14
$FeOPO(OH)_2$	-0.62	-0.38	0	29.90
$Fe_2O_2PO_2$	-1.63	-1.37	0	29.54
Fe_2O_2POOH	-1.42	-0.58	0	34.02
$FeOPO_2(OH)Na$	-0.68	-1.32	1	27.89
$Fe_2O_2PO_2Na$	-1.42	-0.58	0	28.95
Fe_2O_2CO	-1.39	-0.61	0	21.70
Fe_2O_2CONa	-1.39	-0.61	1	22.38
$FeOH\text{-}NaHCO_3$	0	0.46	-0.46	12.72
$FeOH\text{-}NaCO_3$	0	-0.12	-0.88	2.13

Results and discussion

Bakers Hill soil

Figure 1 illustrates, for the Bakers Hill soil, the effect of bicarbonate concentration on the phosphate concentration C_P in the extraction solution for various soil-solution ratios ρ. The data show that the total amount of the extracted phosphate increases with the bicarbonate concentration. The equilibrium phosphate concentration C_P decreases with decreasing soil-solution ratio.

The experimental data were modeled using the CD model for inner- and outersphere surface complexation, taking into account the phosphate and carbonate surface speciation as described in Table 1. The total effective reactive surface area A_r of metal hydroxides and the total amount of phosphate are the parameters, which were adjusted on the experimental data. The lines in Figure 1 show that the model can successfully describe the experimental data. The deviation of the model description is higher for small solid-solution ratios. This might be due to disequilibrium at low solid-solution ratios because of short extraction time. This may in particular be true for solid-solution ratios above about 1:50 as shown by Barrow and Shaw (Barrow and Shaw, 1975).

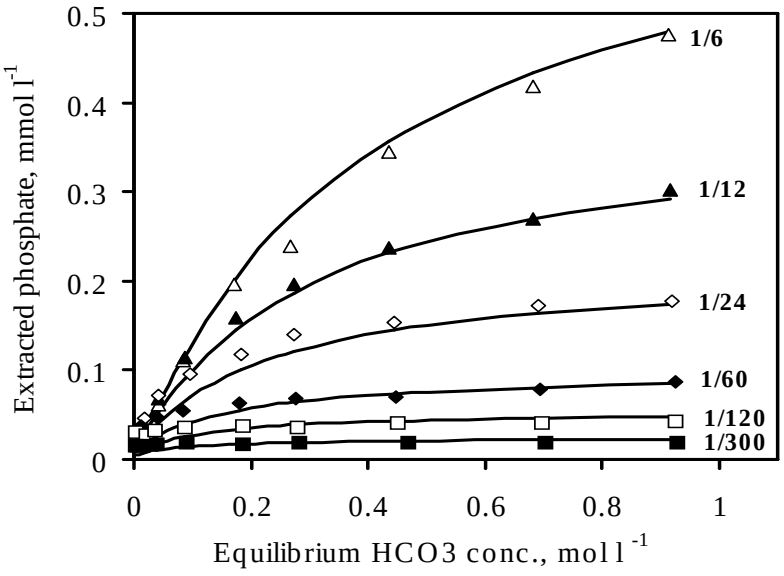

Figure 1. Effect of bicarbonate concentration and soil-solution ratio on the extracted phosphate from the Bakers Hill soil that was incubated with 400 mg P kg^{-1} soil at 70 ^{o}C for 3.75 days. The experimental data were taken from Barrow and Shaw (Barrow and Shaw, 1976c). The lines show the description of the phosphate concentration in the extraction solution using the CD model for inner- and outersphere surface complexation.

The fitted effective reactive surface area, A_r, was found to be 4.7±0.2 m^2 g^{-1}. The reversible phosphate fraction was found to be 308±10 mg P kg^{-1} or 9.94 mmol kg^{-1}, which is equivalent with about 3/4 of the added phosphate. The corresponding loading is 2.17 μmol m^{-2}. This indicates that the total amount of reactive P that was found in the calculation is smaller than the amount of P that has been added to the soil, which may denote the effect of long-term reactions on lowering the total extractable P.

It is interesting to notice that only a small fraction (about 2-50 %) of the added phosphate is really extracted. The major part remains adsorbed, illustrating the high affinity character of the phosphate binding and the relatively low competition power of carbonate. The amount of extracted phosphate depends on the bicarbonate concentration and soil-solution ratio. The bicarbonate concentration has a positive effect on the amount of extractable phosphate. For a specific soil-solution ratio, the extractable phosphate is increased with increasing the bicarbonate concentration. The total amount of extracted phosphate has an inverse relationship with the soil-solution ratio, which is due to the lower P concentration at low solid-solution ratio. The phosphate concentration in solution decreases with decreasing soil-solution ratio. The effects of bicarbonate concentration and soil-solution ratio on the total extracted phosphate and total adsorbed phosphate are illustrated in Figure 2.

There is no independent information available on the initial P level in the Bakers Hill soil. Barrow and Shaw has reported 200 mg P kg^{-1} soil as a total acid soluble P in a comparable soil near Bakers Hill (Barrow, 1974). Summation of this value with the added phosphate leads to a value of about 600 mg P kg^{-1} soil, meaning that only about 50% of total phosphate is reactive and of maximum about 30% of the total phosphate has been extracted by the sodium-bicarbonate solution.

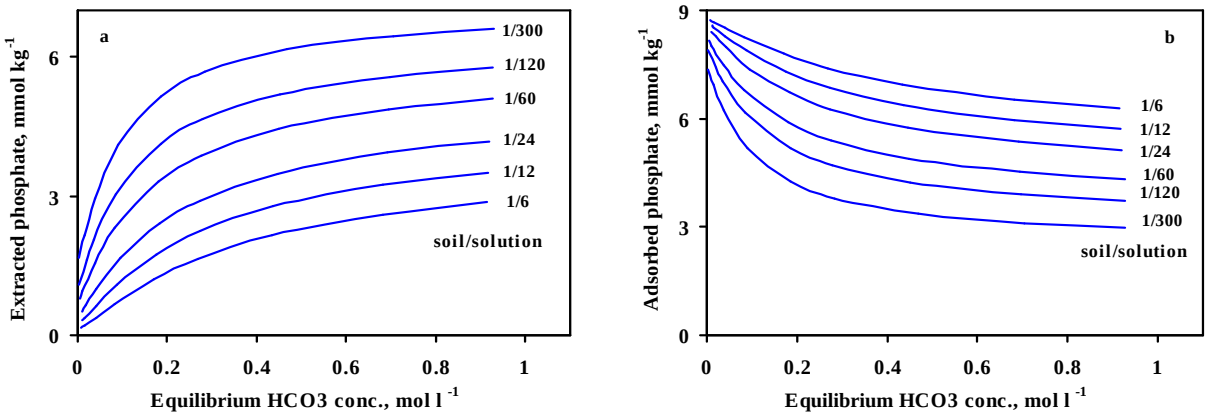

Figure 2. The model calculation of (a) total extracted and (b) adsorbed phosphate as a function of bicarbonate concentration and soil-solution ratio. The calculation was done using the CD model for inner- and outersphere surface complexation with respect to the data of Figure 1.

Wungong soil

Barrow and Shaw (Barrow and Shaw, 1976b) have also studied the extraction of phosphate for a very different type of soil, i.e. the Wungong soil. This soil is characterized by a much higher amount of extractable Fe and Al. The soil is rich in metal oxides.

The effect of phosphate loading on the amount of extracted phosphate was measured at different soil-solution ratios on samples of Wungong soil by adding four levels of phosphate. The added amounts of P are much larger than for Bakers Hill soil, since this soil has a much higher P buffer capacitance, due to the high content of metal oxides. The Wungong soil was incubated during only 21 days at 25 ^{o}C. This reaction time is rather small compared to the previously discussed Bakers Hill soil.

Figure 3 illustrates the experimental data and the model description. It shows that the amount of extracted phosphate is increased with increasing the added phosphate at all different soil-solution ratios.

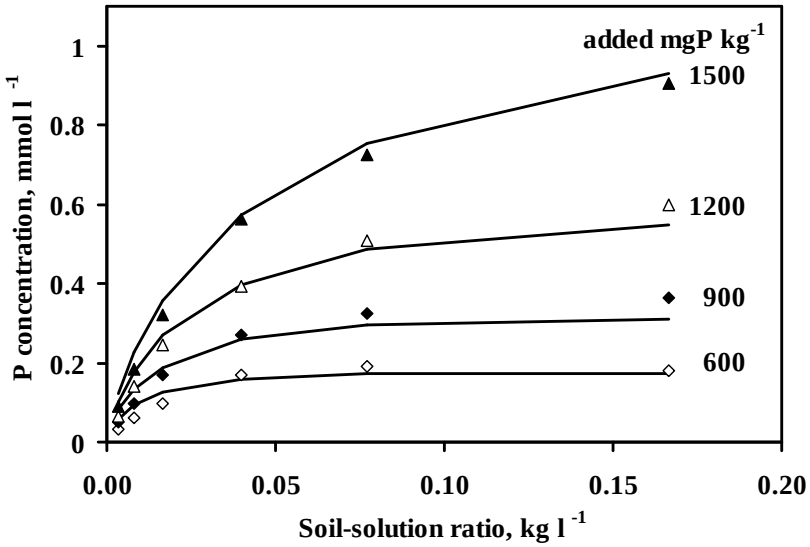

Figure 3. The effect of phosphate loading on the extracted phosphate from Wungong soil as a function of soil-solution ratio

The P concentration in the $NaHCO_3$ extract was described very well using only one effective reactive surface area A_r (46±1 m^2 g^{-1} soil) and a linear relation between the amount of phosphate added and total amount of adsorbed P in the soil (T_P). The initial amount of P in this soil was found to be 1550±40 mg P kg^{-1}. This value is much larger than the initial amount for the Bakers Hill soil. This is not surprising since this soil has much higher metal oxide content (15 times) than the Bakers Hill soil.

A linear relationship may be expected as a first order approximation between the effective reactive surface area and the amount of metal hydroxides in soil. In Figure 4, the relation is given for the two soils studied. It shows that the amount of metal hydroxides in these soils is linearly related to the effective reactive surface area. This relation between the surface area and the Fe+Al content can be used to calculate the apparent specific surface area of the reactive metal (hydr)oxides in the soil. It yields a specific surface area of about 360±50 m^2 g^{-1}. This agrees with the idea that an oxalate extraction removes especially the finest particles in an extraction. It is also possible to explain the data points based on two Fe and Al oxide fractions; a fraction of amorphous Fe and Al (hydr)oxides with approximately 800 m^2 g^{-1} and a fraction of crystalline Fe and Al (hydr)oxides with approximately 100 m^2 g^{-1}. The fraction of each type (smaller and bigger particles) of (hydr)oxide can thus be derived from the calculated specific surface area. For this example roughly 50% of the total metal (hydr)oxide fraction is amorphous.

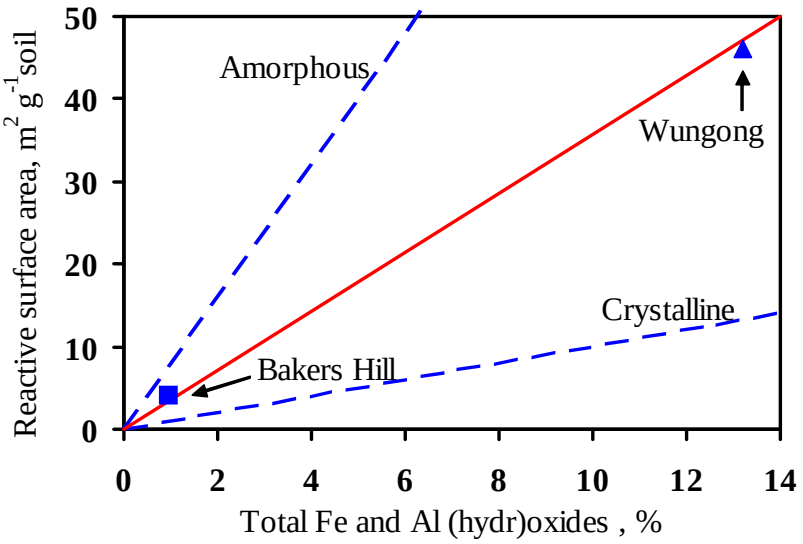

Figure 4. Relation between calculated effective reactive surface area per gram of soil and the total amount of metal hydroxides in the Bakers Hill soil and Wungong soil. The dotted lines indicate a hypothetical presence of amorphous and crystalline iron oxides in soil, with a high (800 m^2 g^{-1}) and low (100 m^2 g^{-1}) specific surface area. A combination of these two kinds of oxides leads to the calculated value for the effective reactive surface area.

Effect of Ca^{+2} and Mg^{+2}

It has been shown that calcium can have a considerable influence on the adsorption of phosphate in soils (Rietra *et al.*, 2001b). In the calculation, the binding of calcium was taken into account, using as a restriction that the Ca^{+2} activity is

determined in the extract solution via the solubility of calcite. The calculation shows that calcium adsorption is important at low carbonate concentration. This denotes the presence of calcium adsorption interaction with phosphate. However, this effect becomes less important with increasing the carbonate concentration. At 0.5 M carbonate concentration, which is corresponding with the recommended value in the Olsen method, calcium almost has no adsorption interaction with phosphate.

In addition to calcium, magnesium may also interact with phosphate in soils. Magnesium shows higher affinity for surface sites than calcium does (Rahnemaie *et al.*, Ch 3) and it stimulates the binding of phosphate by goethite (Geelhoed, 1998). Therefore, in the calculation, the binding of Mg was taken into account, using as a restriction that the Mg^{+2} activity is determined via the solubility of $MgCO_3$. The calculation shows that Mg adsorption is important at low carbonate concentration. This effect decreases dramatically with increasing the carbonate concentration.

These calculations imply that the calcium and magnesium adsorption cannot be ignored in the calculations, when the carbonate concentration is low. The effect of the carbonate concentration and the soil-solution ratio on the calcium and magnesium adsorption is respectively given in Figure 5a and 5b, which have been calculated based on the data of Bakers Hill soil.

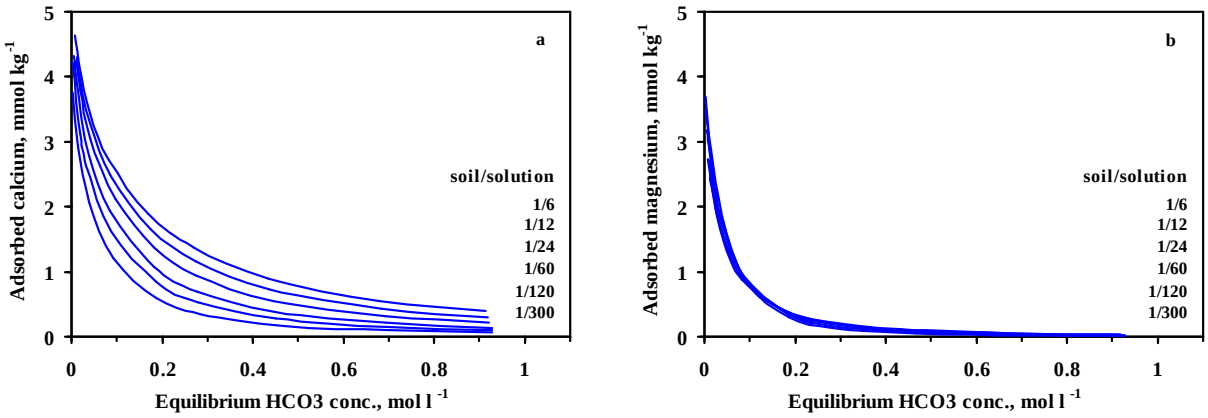

Figure 5. Effect of carbonate and soil-solution ratio on the calcium and magnesium adsorption on the metal (hydr)oxide fraction of the soil. The calculation was done using the CD model for inner- and outersphere surface complexation based on the data of Bakers Hill soil.

Conclusions

- The parameterized CD model is able to describe the effect of variation in $NaHCO_3$ concentration and solid-solution ratio on the P concentration in the extraction solution.

- There is a considerable amount of adsorbed phosphate at the mineral surfaces even in pristine soils with respect to phosphate. This amount of adsorbed phosphates correlates with the amount of Fe and Al (hydr)oxides.
- Sodium bicarbonate extraction, based on the Olsen's method (0.5 M $NaHCO_3$ at pH 8.5), desorb about 25% of the total adsorbed phosphate from soils.
- The calculated effective reactive surface area of soils strongly correlates with the oxalate extractable fraction. The apparent specific surface area of this fraction is about 360 $m^2\ g^{-1}$.
- Calcium and magnesium affect on the phosphate adsorption at low carbonate concentration

Acknowledgments

The authors thank the Ministry of Science, Research, and Technology of Iran (MSRT) for financial support and Mr. M. Keizer for making various adjustments in the ECOSAT software allowing new fitting options.

References

Barrow, N. J. (1974). Effect of previous additions of phosphate on phosphate adsorption by soils. *Soil Sci.* **118**(2): 82.

Barrow, N. J., and T. C. Shaw (1975). The slow reactions between soil and anions. 2. Effect of time and temperature on the decrease in phosphate concentration in the soil solution. *Soil Sci, Feb* **119**(2): 167.

Barrow, N. J., and T. C. Shaw (1976a). Sodium bicarbonate as an extractant for soil phosphate .3. Effects of buffering capacity of a soil for phosphate. *Geoderma* **16**(4): 273.

Barrow, N. J., and T. C. Shaw (1976b). Sodium bicarbonate as an extractant for soil phosphate. 1. Separation of the factors affecting the amount of phosphate displaced from soil from those affecting secondary adsorption. *Geoderma, Sept* **16**(2): 91.

Barrow, N. J., and T. C. Shaw (1976c). Sodium bicarbonate as an extractant for soil phosphate. 2. Effect of varying the conditions of extraction on the amount of phosphate initially displaced and on the secondary adsorption. *Geoderma, Sept* **16**(2): 109.

Davis, J. A., R. O. James, and J. O. Leckie (1978). Surface ionization and complexation at the oxide/water interface. 1. Computation of electrical double layer properties in simple electrolytes. *J. Colloid Interface Sci.* **63**: 480.

Dzombak, D. A., and F. M. M. Morel (1990). Surface complexation modelling: Hydrous ferric oxide. New York, John Wiely & Sons.

Geelhoed, J. S. (1998). Phosphate availability in the soil-root system: Integration of oxide surface chemsitry, transport and uptake. PhD thesis, Department of Soil Quality. Wageningen, Wageningen UR.

Kinniburgh, D. G., and P. L. Smedley (2001). Arsenic contamination of ground water in bangladesh, British Geological Survey Report**:** Chapter 11.

Kostka, J. E., and G. W. Luther (1994). Partitioning and speciation of solid-phase iron in salt-marsh sediments. *Geochim. Cosmochim. Acta* **58**(7): 1701.

Lofts, S., and E. Tipping (1998). An assemblage model for cation binding by natural particulate matter. *Geochim. Cosmochim. Acta* **62**(15): 2609.

Mehra, O. P., and M. L. Jackson (1960). Iron oxide removal from the soils and clays by a dithionite-citrate system buffered with sodium bicarbonate. *Clays and Clay Minerals* **7**: 317.

Meima, J. A., and R. N. J. Comans (1998). Application of surface complexation precipitation modeling to contaminant leaching from weathered municipal solid waste incinerator bottom ash. *Environ. Sci. Technol.* **32**(5): 688.

Olsen, S. R., and L. A. Dean (1954). Estimation of available phosphorus in soils by extraction with sodium bicarbonate. *Washington, D.C. : U.S. Dept. of Agriculture* **19**.

Rahnemaie, R., T. Hiemstra, and W. H. Van Riemsdijk (Ch 2). A new surface structural approach to ion adsorption: Tracing the location of electrolyte ions.

Rahnemaie, R., T. Hiemstra, and W. H. Van Riemsdijk (Ch 3). Inner- and outersphere complexation of ions at the goethite-solution interface.

Rahnemaie, R., T. Hiemstra, and W. H. Van Riemsdijk (Ch 4). Phosphate adsorption on the goethite: Surface speciation in relation to charge distribution.

Rahnemaie, R., T. Hiemstra, and W. H. Van Riemsdijk (Ch 6). Competitive adsorption of phosphate and carbonate on the goethite.

Rietra, R., T. Hiemstra, and W. H. Van Riemsdijk (2001a). Comparison of selenate and sulfate adsorption on goethite. *J. Colloid Interface Sci.* **240**(2): 384.

Rietra, R., T. Hiemstra, and W. H. Van Riemsdijk (2001b). Interaction between calcium and phosphate adsorption on goethite. *Environ. Sci. Technol.* **35**(16): 3369.

Schwertm, U. (1973). Use of oxalate for fe extraction from soils. *Canadian Journal of Soil Science* **53**(2): 244.

Weng, L. P., E. J. M. Temminghoff, and W. H. Van Riemsdijk (2001). Contribution of individual sorhents to the control of heavy metal activity in sandy soil. *Environ. Sci. Technol.* **35**(22): 4436.

Summary

In English

Mobility and bioavailability of ions in natural systems, such as soils and sediments, is strongly influenced by the physical and chemical properties of the porous media. The composition of the porous media can vary widely, which complicated the development of prediction models for mobility and bioavailability. Adsorption and desorption of ions in the environment is always a multicomponent process. Metal (hydr)oxides dominate the adsorption of anions in soils, since these mineral are positively charged at the normal pH range in soils. Goethite is perhaps one of the most important crystalline metal (hydr)oxides in environmental systems.

Among anions, phosphate and carbonate are omnipresent in natural systems. These ions interact with adsorption of other ions and with themselves. Phosphate is a nutrient for organisms and an important element in studying the interactions of the solid-solution interface of minerals. Carbonate is also very important. It has been shown that carbonate competes with anions for the surface sites while it sometimes encourages the adsorption of other ions.

Moreover, electrolyte ions, such as Li^{+1}, Na^{+1}, K^{+1}, Cs^{+1}, Ca^{+2}, Mg^{+2}, Cl^{-1}, and NO_3^{-1} are present in natural systems. These ions play an important role in the development of the surface charge at the solid-solution interface of minerals. It has been shown that some of these ions like Li^{+1}, Na^{+1}, K^{+1}, Cs^{+1}, Cl^{-1}, and NO_3^{-1} are mainly adsorbed as outersphere surface complexes. Calcium and magnesium may adsorb partly as an innersphere and party as an outersphere surface complex, depending on the solution concentration and the pH of the medium.

Adsorption models should at least obey the macroscopic laws of thermodynamics. These macroscopic laws are valid irrespective the molecular level detail of the adsorption process. This may seem as an advantage and one may be tempted to ignore the molecular level detail. However, due to its nature the thermodynamic concept does theoretically not necessarily predict the behavior of a multicomponent system, if the model has been calibrated only in simple systems. The closer the model is to physical reality the more likely it is that the predictive capabilities are good.

The challenge is thus to take into account the structural information of adsorbed ions and of surface sites as much as possible in the adsorption modeling. The CD model may be considered the most physically realistic model among the various surface complexation models. This model uses the coordination and structure for the adsorbed ions on the basis of available spectroscopic information. In the CD model, a spatial charge distribution is assumed for the innersphere surface complexes. The outersphere surface complexes have been treated as point charges so far.

Improvement of the surface complexation model in order to account for the surface structure and the structure of outersphere and innersphere surface complexes is an interesting and an important goal in ion adsorption modeling. In *Chapter 2 and 3* of this thesis, a new surface structural approach is introduced, which accounts for the variable position of outersphere surface complexes. This approach is based on the CD model, meaning that the position of the outersphere surface complexes is traced by calculation of the charge distribution in the interface. Based on this approach, the outersphere complexes at the solid-solution interface of minerals are not treated as point charges anymore. The model uses a Three Plane model in which the innersphere surface complexes are located between the surface (0-plane) and 1-plane and the outersphere surface complexes are located between the 1-plane and the head end of the DDL (2-plane). The model calculation shows that the minimum distance of approach of adsorbed ions depends on the finite size of ions and their degree of hydration, which determine their relative distances to the surface of minerals.

It has been shown in *Chapter 4* that the new approach can successfully describe the adsorption of phosphate in a ‘single ion’ system as a function of pH, phosphate loading, and salt concentration. The new approach revealed that phosphate may also adsorb as a sodium-phosphate complex. Using previous approaches, it could not be detected since the counter electrolyte ions were located closer to the surface. This leads to a much higher interaction with the surface groups and therefore no need for a sodium-phosphate complex. The charge distribution of adsorbed complexes like phosphate species has been often derived by fitting the adsorption data with the model. A new approach was used in *Chapter 4* in order to calculate the charge distribution value using quantum chemical calculation. The derived values using this technique were used in the modeling of phosphate adsorption data. It has been also shown in *Chapter 4* that the new approach gives a reasonable good prediction of the zeta potential, considering it is identical with the potential at the head end of DDL (2-plane), and a perfect prediction of the shift in the isoelectric point.

The spectroscopic studies have initially been interpreted in the literature for carbonate ions as being the result of a monodentate surface complex. However, modeling of adsorption data leads to a charge distribution value, which is realistic for a

bidentate rather than a monodentate complex. The proton co-adsorption stoichiometry also agrees with using a bidentate species for carbonate. Reinterpretation of the available spectroscopic information for carbonate in *Chapter 5* showed that in fact bidentate is a more likely interpretation than a monodentate surface complex. The new surface structure was successfully used to describe a series of carbonate adsorption data in a 'single ion' system.

In chapter 6, the competitive adsorption of carbonate and phosphate was measured as a function of pH, phosphate and carbonate loading, and salt concentration. It is considered to be a high relevant system, because of the simultaneous presence of phosphate and carbonate in most natural systems. Modeling of the data in this system also showed that carbonate ions bind mainly as an innersphere bidentate surface complex. At high salt concentration, a sodium-carbonate complex contributes to the carbonate adsorption. At high carbonate loading and relatively high pH, an outersphere monodentate sodium-bicarbonate complex may form. Maximum adsorption of carbonate take places at pH 7-9, which depends on the carbonate loading and the ionic strength.

The derived model parameters in chapters 2 to 6 cover a part of the major adsorption interaction in a complicated multicomponent system like soils. In chapter 7, this concept has been used to model the total extractable phosphate from a soil by sodium-bicarbonate solution adjusted at pH 8.5. It has been shown that the parameterized CD model for inner- and outersphere surface complexation is able to describe the effect of variation in $NaHCO_3$ concentration and solid-solution ratio on the P concentration in the extraction solution. The approach leads to an estimation of the total effective reactive surface area of metal (hydr)oxides in soils and also to a estimation of the amount of reversible bond phosphate in the soil.

Summary

In Dutch

Mobiliteit en biobeschikbaarheid van ionen in natuurlijke systemen, zoals bodem en sediment, worden sterk beïnvloed door fysische en chemische eigenschappen van de poreuze media. De samenstelling van het poreuze medium kan sterk variëren, hetgeen de ontwikkeling van modellen voor de voorspelling van mobiliteit en biobeschikbaarheid bemoeilijkt. Adsorptie en desorptie van ionen in het natuurlijke milieu is altijd een multicomponent proces. Metaal(hydr)oxides domineren de adsorptie van anionen in de bodem, omdat deze mineralen positief geladen zijn in de gebruikelijke pH traject van gronden. Goethiet is misschien één van de belangrijkste kristallijne metaal(hydr)oxides in natuurlijke systemen.

Binnen de groep van oxyanionen, zijn fosfaat en carbonaat alom vertegenwoordigd in natuurlijke systemen. Daarom gaan deze ionen een interactie aan met andere ionen die kunnen adsorberen. Fosfaat is een nutriënt voor organismen en een belangrijk element in het onderzoek naar de ioninteracties aan het mineraal/water grensvlak. Carbonaat is ook erg belangrijk. Men kan laten zien dat carbonaat in competitie is met andere anionen voor binding aan oppervlaktegroepen terwijl soms carbonaat de adsorptie van andere ionen bevordert.

In natuurlijke systemen zijn er bovendien elektrolyt ionen, zoals Li^{+1}, Na^{+1}, K^{+1}, Cs^{+1}, Ca^{+2}, Mg^{+2}, Cl^{-1}, en NO_3^{-1}, aanwezig. Deze ionen spelen een belangrijke rol in de ontwikkeling van oppervlaktelading in het grensvlak van mineralen. Men kan laten zien dat enkele van deze ionen zoals Li^{+1}, Na^{+1}, K^{+1}, Cs^{+1}, Cl^{-1}, en NO_3^{-1} voornamelijk adsorberen als zogenaamde outersphere oppervlaktecomplexen. Calcium en magnesium kunnen deels adsorberen als een zogenaamd innersphere oppervlaktecomplex en deels als outersphere oppervlaktecomplex, afhankelijk van de ionconcentratie en pH in oplossing.

Adsorptiemodellen moeten op zijn minst de macroscopische wetten van de thermodynamica respecteren. Deze macroscopische wetten gelden onafhankelijk van het moleculaire detailniveau van het adsorptieproces. Dit kan een voordeel lijken en men kan proberen het moleculaire detailniveau te ontwijken. Echter, als gevolg van de aard van het thermodynamische concept wordt het gedrag van een multi-component systeem niet noodzakelijkerwijs juist voorspeld, indien het model slechts gekalibreerd

is op enkelvoudige systemen. Hoe dichter het model de fysische werkelijkheid benadert, des te aannemelijker wordt het vermogen van een model om goed te voorspellen.

De uitdaging is dus om in de adsorptiemodellering zoveel mogelijk rekening te houden met informatie over de structuur van geadsorbeerde ionen en oppervlaktegroepen. Het CD model kan worden beschouwd als het meest fysisch-realistische model uit een reeks van oppervlaktecomplexeringsmodellen. Dit model gebruikt de coördinatie en structuur van de geadsorbeerde ionen op basis van beschikbare spectroscopische informatie. In het CD model wordt een ruimtelijke ladingsdistributie verondersteld voor innersphere oppervlaktecomplexen. De outersphere oppervlaktecomplexen zijn tot dus ver behandeld als puntladingen.

Verbetering van het oppervlaktecomplexeringsmodel waarbij rekening wordt gehouden met de oppervlaktestructuur van outersphere- en innersphere-complexen is een interessant en belangrijke doel in de modellering van ionadsorptie. In *Hoofdstuk 2 en 3* van dit proefschrift wordt een nieuwe structurele benadering geïntroduceerd die rekening houdt met de variabele positie van outersphere oppervlaktecomplexen. Deze benadering is gebaseerd op het CD model, hetgeen inhoudt dat de positie van de outersphere-oppervlaktecomplexen wordt bepaald door het berekenen van de ladingsverdeling in het grensvlak. Hiermee worden de outersphere complexen in het mineraal/water grensvlak niet langer behandeld als puntladingen. Het CD model maakt gebruik van een elektrostatisch drievlak-model waarin de lading van de innersphere-oppervlaktecomplexen geplaatst wordt tussen het oppervlak (0-vlak) en het 1-vlak en waarin de lading van de outersphere-oppervlaktecomplexen geplaatst wordt tussen het 1-vlak en het hoofdeinde van de DDL (2-vlak). De modelberekeningen laten zien dat de minimale afstand van nadering van geadsorbeerde ionen afhangt van de grootte van de ionen en hydratatie, die hun relatieve afstand tot het mineraaloppervlak bepalen.

Er wordt in *Hoofdstuk 4* aangetoond dat de nieuwe benadering de adsorptie van fosfaten succesvol kan beschrijven in een "enkelvoudig" ionsysteem als een functie van pH, fosfaatbezetting, en zoutconcentratie. De nieuwe benadering brengt naar voren dat fosfaat ook zou kunnen adsorberen als een natrium-fosfaatcomplex. Bij eerdere benaderingen kon dit niet worden waargenomen omdat de electroliet-ionen dichter bij het oppervlak waren geplaatst. Dit leidt tot een veel grotere interactie met de oppervlakgroepen waardoor de aanname van een natrium-fosfaatcomplex niet noodzakelijk was. De ladingsverdeling van geadsorbeerde complexen wordt gewoonlijk bepaald door optimalisatie van de modelparameters met behulp van de adsorptiegegevens. In *Hoofdstuk 4* wordt een nieuwe benadering gebruikt door de ladingsdistributie te berekenen met een kwantumchemisch model. De met deze techniek verkregen waarden zijn gebruikt in de modellering van de fosfaat-

adsorptiegegevens. In *Hoofdstuk 4* wordt tevens aangetoond dat de nieuwe benadering een redelijk goede voorspelling van de zeta-potentiaal geeft, wanneer de potentiaal wordt beschouwd als identiek met de potentiaal aan het hoofdeinde van de DDL (2-vlak). Daarnaast geeft het een goede voorspelling van de verschuiving van het zogenaamde iso-electrische punt.

De spectroscopische studies van carbonaationen zijn aanvankelijk in de literatuur geïnterpreteerd als het resultaat van de vorming van een zogenaamd monodentaat oppervlaktecomplex. Modellering van adsorptiegegevens leidt echter tot een ladingsverdeling, die realistischer is voor een bidentaat complex dan voor een monodentaat complex. De proton co-adsorptie stoïchiometrie is ook in overeenstemming met het gebruik van een bidentate species voor carbonaat. Herinterpretatie in *Hoofdstuk 5* van de beschikbare spectroscopische informatie voor carbonaat laat zien dat in feite een bidentaat complex een waarschijnlijker interpretatie is dan een monodentaat oppervlaktecomplex. De nieuwe oppervlaktestructuur is succesvol gebruikt om carbonaat adsorptiegegevens voor enkelvoudige ionsystemen te beschrijven.

In *Hoofdstuk 6* is de experimentele competitieve adsorptie van carbonaat en fosfaat beschreven als functie van pH, fosfaat- en carbonaatbelading, en zoutconcentratie. Het wordt beschouwd als een zeer relevant systeem, vanwege de simultane aanwezigheid van zowel fosfaat als carbonaat in veel natuurlijke systemen. Modellering van dit systeem laat ook zien dat carbonaationen hoofdzakelijk binden als een innersphere bidentaat oppervlaktecomplex. Bij een hoge zoutconcentratie, draagt ook een natrium-carbonaat complex bij aan de carbonaatadsorptie. Bij hoge carbonaatbezetting en relatief hoge pH kan een outersphere-, monodentaat-, natrium-bicarbonaatcomplex worden gevormd. Maximale adsorptie van carbonaat treedt op tussen pH 7 en pH 9, afhankelijk van de carbonaatbezetting en de ionsterkte.

De modelparameters, afgeleid in de hoofdstukken 2 tot en met 6, omvatten een deel van de belangrijke ioninteracties in een gecompliceerd multicomponent systeem zoals bodem. In *Hoofdstuk 7* is dit concept toegepast op een grond om de totaal extraheerbare fosfaatvoorraad te berekenen op grond van extracties met een natrium-bicarbonaat oplossing bij pH 8.5. Er wordt aangetoond dat het geparameteriseerde CD model voor inner- en outersphere oppervlaktecomplexering in staat is het effect te beschrijven van de variatie in de $NaHCO_3$ concentratie en de grond/vloeistofverhouding op de P gehalte in het extract. Deze benadering leidt tot een schatting van het effectieve oppervlak van de metaal (hydr)oxidefractie in de bodem en ook een schatting van de totale hoeveelheid reversibel gebonden fosfaat.

Acknowledgement

This thesis is by far the most significant scientific accomplishment in my life and it would be impossible without people who supported me and believed in me. I would like to express my gratitude to all those who gave me the possibility to complete this thesis. Thanks to Ministry of Science, Research, and Technology of Iran for providing me a four years scholarship which enabled me to begin my PhD program at the Department of Soil Quality, Wageningen UR, The Netherlands.

I am deeply indebted to my supervisor Tjisse Hiemstra, who his ideas, stimulating suggestions and encouragement, enthusiastic, and critical atmosphere during our discussions helped me in all the time of laboratory experiments, modeling of the data, and writing of the thesis.

With a deep sense of gratitude, I wish to express my sincere thanks to Willem van Riemsdijk for his immense help in planning the research, interpreting the results, and writing the articles. It is a great pleasure to me to conduct this thesis under his supervision.

The cooperation I received from other scientific members of the department is gratefully acknowledged, especially thanks to Meindert Keizer for some additions to ECOSAT which provided me some new flexibility for data handling.

I will be failing in my duty if I do not mention the administrative staff (Winne, Minke, Esther, Riette, Gerda, Lucie) and laboratory staff (Rein, Kees, Arie, Monique, Gerlinde, Andre, Carry, Peter, Wim, …) of this department for their timely help, thanks a lot.

I also want to thank my parents, who taught me the value of hard work by their own examples. I wish I could meet my father after coming back home. I would like to share this moment of happiness with my mother, brothers and sisters and my brother-in-law Reza Shahaeeyan. They rendered me enormous support during the whole tenure of my research. The encouragement and motivation that was given to me to carry out my research by my father- and mother-in-law is also appreciated.

I am grateful to my wife, Setareh Oveisi, for her unrelenting support provided throughout my research work and her patience was tested to the utmost by a long period of separation. Without her loving support and understanding I would never have completed my present work.

During more than four years working in this department along many other PhD students, I received a lot of valuable supports from them. Particularly, I would never forget the company I had from Nicole, Ram, Thomas, and Liping. I want also to thank Romulo, Eduardo, Maria, Laura, Monika, Bert, Erwin, Walter, Gijs, Ellen, Debby,

Odair, Franciska, … and my Iranian friends, Reza Khorasani and Hassan Sayyari, for the friendship and nice moments we had together.

I would also like to acknowledge with much appreciation my Iranian friends, in particular Mahmoud Otroshy, Behbood Mohebby, Hadi Peighambardoust, Akbar Arabhosseini, Mohammad J. Ardeh, Mohammad A. Hejazi, Abbas Pakdel, Merdad Madani and many others for their help and support and also making a nice atmosphere during the time we gathered together in Wageningen.

As always it is impossible to mention everybody, finally I would like to thank all whose direct and indirect support helped me during the time being in Wageningen and completing my thesis.

About the Author

Rasoul Rahnemaie was born on March 25, 1968 in Neiriz, Fars, Iran. After completing high school in biology science in June 1986, he began his studies in Tehran University and received a BSc degree in soil science. After a short time working in a soil and water consulting company, he started his MSc at the Tarbiat Modares University, Tehran, Iran. He worked on the “kinetics and transformations of soil micronutrients in calcareous soils” as his master thesis. In 1997, he was appointed as an instructor at the Department of Soil Science, Guilan University, Rasht, Iran. He worked there for almost 3.5 years. In 1997, he received a 4-years scholarship from the Ministry of Science, Research, and Technology (MSRT) of Iran to continue his study. In October 2000, he started his research in soil chemistry group at the Department of Soil Quality, Wageningen University, The Netherlands. This book presents the main results of his research as a PhD student.

Netherlands Research School for the
Socio-Economic and Natural Sciences of the Environment

CERTIFICATE

The Netherlands Research School for the
Socio-Economic and Natural Sciences of the Environment
(SENSE), declares that

Rasoul Rahnemaie

Born on: 25 March 1968 at: Neyriz, Iran

has successfully fulfilled all requirements of the
Educational Programme of SENSE.

Place: Wageningen Date: 18 May 2005

the Chairman of the SENSE board	the SENSE Director of Education
Prof. H.A. Udo de Haes	Dr. C.Kroeze

Educational Programme of:
R. Rahnemaie

SENSE PhD courses:

- Environmental Research in Context (2002; 2 ECTS)
- Understanding Soil Reactivity for Environmental and Economic Purposes (2004; 6 ECTS)
- Basic Statistics (2003; 1 ECTS)
- Uncertainty Modelling and Analysis (2003; 1 ECTS)
- Speciation and Bioavailability (2003; 1 ECTS)
- Modelling Techniques and Systems Engineering (2002; 3 ECTS)

Selected other PhD courses and activities :

- Techniques for Writing and Presenting Scientific Papers (2002; 1 ECTS)
- Time Planning and Project Management (2003; 1 ECTS)
- Presenting in English (2003; 1 ECTS)
- Training on ECOSAT &ORCHESTRA softwares for modeling of adsorption data

Oral presentations at:

- 4th European Meeting on Environmental Chemistry (December 10-13, 2003, Plymouth, England)
- 14th Annual Goldsmidt Conference (June 5-11, 2004, Copenhagen, Denmark)
- Workshop on Phosphorus and Metals in Soils and Surface Waters, (March 5-8, 2004, Wageningen, The Netherlands)
- SENSE PhD Colloqium (April 16, 2004, Groningen, The Netherlands)

Publications:

- One accepted and two submitted articles in refereed scientific journals

Deputy director SENSE

Dr. A. van Dommelen

This research was financially supported by the Ministry of Science, Research, and Technology (MSRT) of Iran.

Printed by: Ponsen & Looijen BV, Post bus 68, 6700 AB Wageningen